Production, functionalization and application of carbon materials.

Doctoral Dissertation
Doctoral Program in Chemical Engineering (30th Cycle)

Production, functionalization and application of carbon materials.

By

Aamer Abbas Khan

******

Supervisor(s):
Prof. Alberto. Tagliaferro, Supervisor

Doctoral Examination Committee:
Prof. Jesper de Claville Christiansen, Referee, University of Aalborg.
Prof. Hanshan Dong, Referee, University of Birmingham.
Prof. Antonio Domenico Veca, Referee, Centro Ricerche Fiat.
Prof. Tatjana Haramina, Referee, University of Zagreb.
Prof. Marco Sangermano, Referee, University of Politecnico di Torino.

Politecnico di Torino
2017

Declaration

I hereby declare that, the contents and organization of this dissertation constitute my own original work and does not compromise in any way the rights of third parties, including those relating to the security of personal data.

Aamer Abbas Khan

2017

* This dissertation is presented in partial fulfillment of the requirements for **Ph.D. degree** in the Graduate School of Politecnico di Torino (ScuDo).

I would like to dedicate this thesis to my loving parents

Acknowledgment

And I would like to acknowledge Prof. Alberto Tagliaferro for his guidance, support and trust in my capabilities over the course my PhD work. I would like to thank Dr Pietro Mandracci for ensuring continuous availability of the PlasmaFab508. I am great full to Prof. Carlo Rosso for his guidance and arrangments for the composite characterizations. I extend my gratitude towards Prof. Faranco Gaspari (UOIT, Canada) and Dr Simone Quaranta (UOIT, Canada) for a learing experience at UOIT, Canada and exposure to the Candaian research community. I am thankful to Dr Pravin Jagdale and Dr Mauro Giorcelli for their help and support in my research work. Last but the not least I am indebted to my family specially my mother and wife who kept me going with continuous love and comfort.

Abstract

The work of this thesis was structured into 2 main activities: (1) to devise a surface functionalization technique for commercial carbon fibres (CFs) based on lignin precursor developed under the European Union FP7 Project "Functionalized Innovative Carbon Fibres Developed from Novel Precursors with Cost Efficiency and Tailored Properties" (FIBRALSPEC), grant agreement No. 604248. (2) To perform the exploration of low cost carbon fillers for application to polymer composites.

1st chapter presents a general introduction of the different carbon materials and their applications. 2nd chapter is concerned with the existing commercial carbon fibre manufacturing techniques and precursors. A small portion on the surface modification techniques is also added in this chapter. The 3rd chapter deals with the production techniques and limitations of Carbon nano tubes as a filler for the application to composites. A brief introduction on biochar materials has been added as well. The 4th chapter deals with functionalization study of commercial carbon fibres and lignin based carbon fibres. Commercial carbon fibres T700 were purchased from Toray, Japan to study the surface modification through low pressure oxygen plasma at Polito. Treatment parameters in an oxygen environment such as holding time (1~10 minutes), plasma power (100~200 W), flow rate (250 Standard Cubic Centimeters) and plasma chamber pressure (53 Pa) were set. Morphology of the carbon fibres before and after plasma treatment was studied through Field Emission Scanning Electron Microscopy (FESEM).

Chemical nature of the functional groups formed on the carbon fibres surface after the treatment was studied through Fourier Transform Infrared (FTIR) spectroscopy and atomic percent was quantified through X-Ray Photoelectron Spectroscopy (XPS). Raman spectroscopy was carried out to study the structural changes in the carbon fibres. Wettability test was carried out to study the interaction of the surface functional groups with epoxy matrix. Tensile strength of the CFs was determined after the plasma treatment to ensure optimum mechanical performances of the treated fibres in the subsequent composites. In order to ensure the effectiveness of the plasma treatment the same samples were studied after six months of storage in ambient conditions. On the basis of the obtained results from the activities above, optimum plasma treatment parameters such as treatment time, plasma power, oxygen flow rate, plasma chamber pressure were singled out and applied on the lignin based carbon fibres. The lignin based CFs were plasma treated for 5 minutes at 100 W and 200W at a flow rate of 250 SCCM and 53 Pa plasma chamber pressure. Surface morphology was studied through FESEM. Plasma treated fibres showed canals and pits on the surface. The fibre started to damage at a plasma power of 200W. Also the oxygen pickup reduced at this treatment power as depicted by the XPS analysis. The 200 W, 5 minutes treatment was identified as an upper limit for the treatment parameter. The treated fibres were shredded finely and dispersed in epoxy resin using an overhead mixer to produce composites. Mechanical and tribological analysis was carried out and compared with the neat epoxy and untreated CFs composites. The plasma treated carbon fibre composites outperformed their counterparts. Based on the observations we recommended low pressure oxygen plasma treatment for the surface modification of the lignin based carbon fibres intended for commercial use.

To further support our recommendations we produced carbon fibers from waste cotton clothes in Polito and applied the same treatment to them. The temperature profile for the thermal treatment was deduced from

thermogravimetric analysis of cotton fibres in argon environment. XPS and FTIR analysis was carried out to ensure the absence of any impurity in the cotton fabrics. Carbonization process was carried out in a Carbolite furnace (TZF12/65/550) at the temperatures of 400^{o} C, 600^{o} C and 800^{o} C for one hour in nitrogen environment at a ramp rate of 15^{o} C/minute. The sample prepared at 800^{o} C was selected to study the plasma treatment due to its more ordered structure and high carbon content as depicted by the Raman and XPS analysis respectively. The carbon fibres were treated with oxygen plasma at 100 W and 200 W for 5 minutes. Surface morphology and structure of the treated CFs were studied via FESEM and Raman spectroscopy. Surface of the treated fibres showed pits and canals confirming the action of the plasma elements while a degradation of the I_D/I_G ratio in the Raman spectra evidenced the effects of the plasma elements on the structure of the CFs. The functional groups on the surface of the plasma treated CFs were studied through X-Ray Photoelectron Spectroscopy and Fourier Transform Infrared spectroscopy. Chemical groups like alcohols, carboxyl and carbonyl were found on the surface of the treated CFs. BET analysis showed that surface area of the fibers increased after treatment. The plasma treated CFs retained higher amount of the epoxy resin in the wettability test. The plasma treated fibres were applied in composites. Epoxy based composites were fabricated with the pristine and treated CFs in 1% and 3% by weight. Mechanical and tribological analysis was carried out on all composites. The composites of the plasma treated fibres showed superior mechanical and tribological properties when compared to their untreated CFs counterparts. Morphology of the mechanical and tribological specimen were studied with FESEM to investigate the interaction of the filler with the matrix. Above results supported our earlier argument and low pressure oxygen plasma was recommended as a suitable treatment for the modification of the carbon fibres.

The 2nd part of the thesis emphasizes the application of cheap precursor based carbon materials for the tailoring of composites properties. In recent years, low-

cost carbons derived from recycled materials have gained a lot of attention for their potentials as filler in composites and in other applications. The electrical, frictional and mechanical properties of polymer composites can be tailored using different percentages of these fillers. In the Carbon lab at Polito we synthesized carbon nano materials (CNMs) from waste polyethylene bags in two different morphologies namely carbon nano beads (CNBs) (P1) and a mix of carbon nano tubes (CNTs) and carbon nano beads (P2) using chemical vapour deposition (CVD) technique by varying the carrier gas pressure. Morphology of the CNMs were studied through FESEM and their purity through Thermogravimetric Analysis (TGA) and Raman spectroscopy. Epoxy based composites were fabricated using these CNMs as filler in 1% and 3 % by weight. Mechanical properties and tribological properties were compared with the epoxy composites of commercial Multi Walled Carbon Nano Tubes (MWCNT). It is observed that the in house generated CNMs composites show overall better mechanical and tribology properties compared to the neat epoxy and the commercial MWCNTs based composites. Morphology of the composites was analysed through FESEM to study the interaction of the filler with the matrix that lead to improved performances. A model on the fracture behaviour was proposed on basis of FESEM analysis. Chapter 6 is concerned with this activity.

In chapter 7, the maple based biochar has been explored as a cheap alternative filler to enhance the polymer properties. In this regard, the mechanical, tribological and electrical behavior of composites with two types of biochar based on maple wood namely biochar and biochar HT were investigated and compared with those of a composite containing multiwall carbon nanotubes. HT is heat treated at 900^{o} C in nitrogen at 1 hour. Superior mechanical properties (ultimate tensile strength, Young modulus and tensile toughness) were noticed at low biochar concentrations 2~4 wt. %). Biochar based composites showed equivalent tribology properties to the composites fabricated with MWCNTs. Furthermore, dielectric properties in the microwave range comparable to low carbon nanotubes

loadings can be achieved by employing larger but manageable amounts of biochar (20 wt. %) rending the production of composites for structural and functional application cost-effective.

Conclusive remarks and future plans are compiled in chapter 8.

Contents

List of Figures

List of Tables

Chapter 1

Carbon materials: An overview.

Carbon is derived from the Latin word "carbo" meaning charcoal or ember. In the modern era the word carbon means much more than mere charcoal. Carbon is the back bone of strongest known fibres i.e. carbon fibres, one of the best known lubricant i.e. graphite, and the hardest known crystal i.e. diamond. In non-crystalline form it is the best gas adsorber, activated charcoal and one of the best helium gas barriers (vitreous carbon) [1]. Carbon possesses a unique property called catenation. Due to this property carbon can form bonds between its atoms and create stable compounds for instance chains, rings and branched chains. There are six million compounds of carbon known today. Due to this vast range carbon compounds present, the whole field of organic chemistry is based on the investigation of carbon and hydrogen containing compounds only [2]. Carbon is a common element in all living organisms. Carbon is crucial for the life on earth as pure carbon compounds comes in various personifications with diverse effective dimensionalities. Still there is a lot of room to learn about carbon and its forms or allotropes. Most commonly known allotropes of carbon are graphite, diamond, lonsdalite, fullerene, carbon nano tubes and recently bio-chars[3]. The various allotropes of carbon are applied in diverse fields ranging from electronics to aerospace industry due to their superior electrical, mechanical and thermal properties.

1.1. Historical Perspective

Carbon and its allotropes have played a significant role in the technological progress in the history of science and technology. The discovery of diverse novel materials in the field of nanotechnology has made carbon the king of elements [4]. Very first report was published in 1889 reporting the possibility of producing carbon based filaments from thermal breakdown of gaseous methane [5]. Thomas Edison used the carbon filaments in light bulbs at Paris Universal Exposition. These discoveries made a classified scheme to recognize all the carbon forms and to predict new ones. Hollow fibers in the nanometer dimension were 1st reported by the Swedish scientists Hillert and Lange in the year 1958 [6].

However, amorphous carbon, diamond and graphite were the only known allotropes of carbon till 1980s. Kroto et al. 1985, [7] and Richard Smalley discovered fullerenes in 1985. Fullerenes are a large family of hexagonal carbon rings, mostly in spherically closed cage arrangement. The contributors won the Nobel Prize in Chemistry 1996. The field of carbon materials research found a renewed interest after the report of Carbon Nano Tubes (CNTs) by Ijima in 1991 [8].CNTs were termed as rolled sheets of graphene. Single rolled sheet was termed as Single Wall Carbon Nano Tube (SWCNT) while CNT made by multiple layers were termed as Multi Wall Carbon nano Tubes (MWCNTs). The tubular nature of carbon filaments in nano dimension was reported in Physical Chemistry Journal of Russia in 1952 but these articles are not well known and cited [9] .The latest breakthrough is the formation of stable single layer of Graphite called graphene discovered in 2004[10] though the word ‘graphene’ was mentioned by Mouras in 1987 [11]. The biochar history dates back some 2,000 years ago in the Amazon Basin. The regions of dark, highly fertile soil were called terra preta, in Portuguese language meaning ‘black earth’ were discovered and analyzed. High concentrations of charcoal and organic matter was found in these samples and given the name biochar [12].

1.2. Structure of Carbon

Carbon is the 4th most abundant element by mass after Hydrogen, Helium and Oxygen. It is a very interesting element due to its properties as a solid material and its wide range of applications. Carbon has an atomic number of 6 and is represented by the symbol C [13]. Carbon possesses an exceptional characteristic with the diversity of structures that can be formed when two or more atoms bond

together. The six electrons of carbon atom are represented in figure 1.1. The arrows head corresponds towards the electron spin. Two of the six electrons occupy the 1s orbital close to the nucleus, the next two in 2s orbital and the last two reside in two different 2p orbitals. All p orbitals have equal energy the electrons reside in separate orbitals.

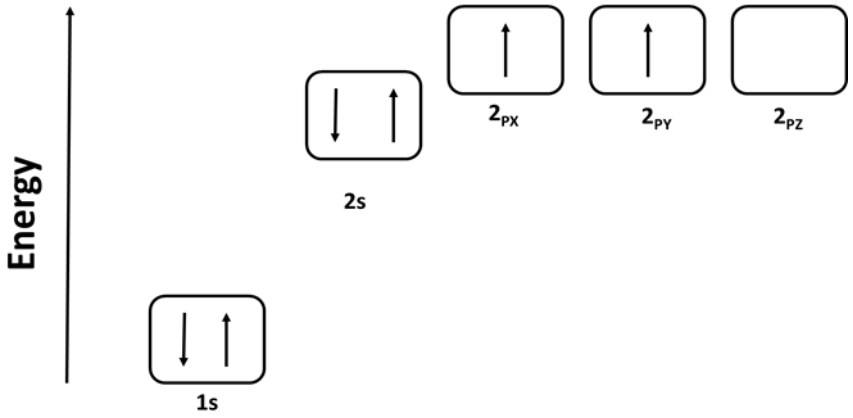

Figure 1.1: Energy levels of carbon atom.

The introduction of quantum mechanics in the 20th century provided the novel frame for understanding the chemical bond between the atoms. The 4 electrons of carbon atom resides in the valence shell. The electronic configuration of carbon atom is $1s^2$ $2s^2$ $2p^2$. This configuration results in a variety of crystalline and amorphous forms of carbon. The molecular orbitals formed by a carbon atom can have three different types of hybridizations namely sp, sp2 and sp3. The combination of s and p orbitals leads to σ-type orbitals while the combination of off-axis p orbitals to π-type bonds. This mechanism of electronic orbital hybridization as shown in the figure 1.2 leads to different types of covalent bonding.

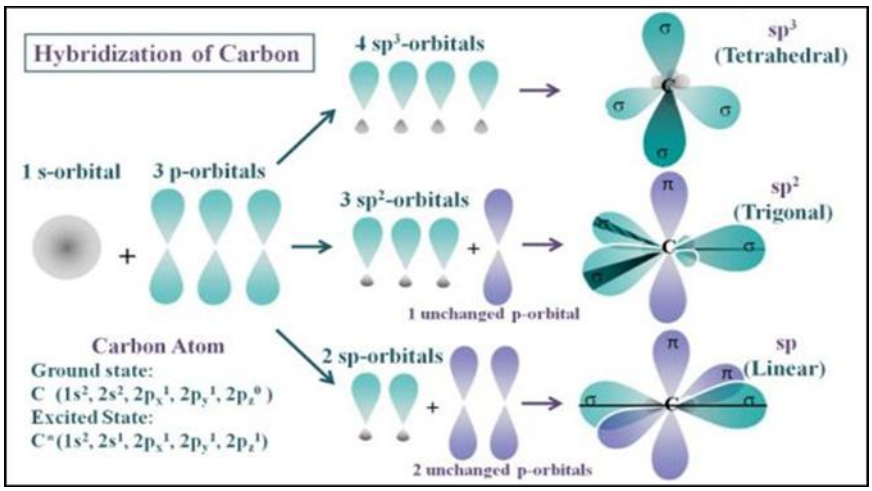

Figure 1.2: The sp, sp2, sp3 hybridization Model of Carbon.

1.3. Allotropes of carbon

Carbon possesses several allotropic forms with two main forms amorphous and crystalline. Bundy et. al. 1996, [14] reported the phase diagram for carbon as shown in figure 1.3. Hexagonal graphite is the stable thermodynamic phase which exists at the ambient temperature and pressure conditions. Graphite exist with a continuation of rhombohedral and polytype variety under metastable conditions. The cubic diamond phase is metastable under the ambient conditions of temperature pressure and stable under high pressures. Lonsdaleite (L), i.e. hexagonal diamond is found under specific conditions of temperature and pressure as shown in the figure 1.3. The carbyne phase exist at high temperature, below the graphite melting line. These phase transformations of the carbon are hypothetically reversible. The new carbon phases e.g. fullerenes and CNTs etc. are not included in the same diagram because they are non-classical forms.

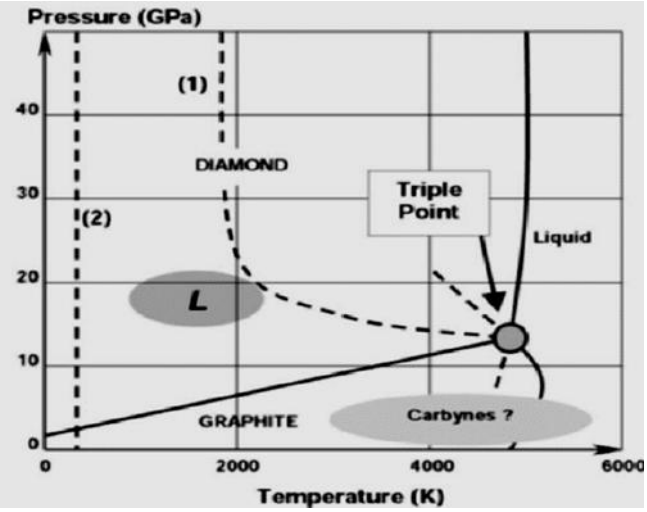

Figure 1.3: Phase diagram of carbon, Equilibrium phase boundaries represented by solid lines and kinetic transformations represented by dotted lines; L stands for Lonsdaleite Phase [14].

1.3.1. Crystalline Allotropes of Carbon

Carbon can exist in three crystalline forms. Two of the well-known and oldest allotropes of carbon are Diamond and graphite based on sp3 and sp2 hybridization respectively [15]. These two allotropes have different structures and textures compared to the conventional materials e.g. carbon black and activated carbon. Carbyne is another allotrope of carbon with sp hybridization.

a. Diamond

Diamond is an allotrope of carbon possessing crystalline structure due to its sp3 hybridization. The 4 sp3 orbitals organize in a tetrahedral configuration which promotes strong σ bonds with the neighboring atoms and are arranged in a three-dimensional tetrahedral structure with a bond length of 0.154 nm. The closely packed rigid structure of carbon atoms accounts for the hardness properties of diamonds and very high melting points [16]. The structural properties of diamond arise due to formation of σ bonds. Diamond possesses the highest atom density, thermal conductivity (2000–2500 W/(m·K)) and smallest thermal expansion coefficient at room temperature compared to other crystals[1].

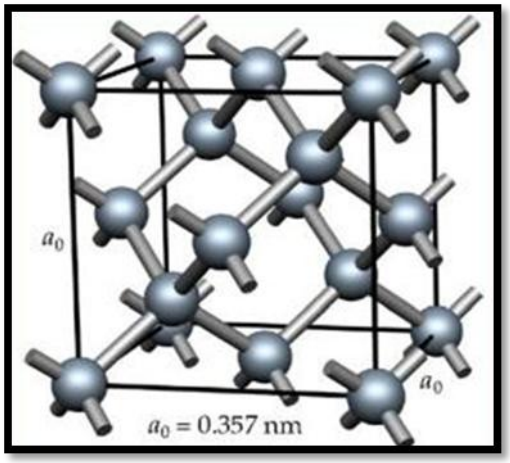

Figure 1.4: Structure of diamond.

b. Graphite

Graphite is an allotrope of carbon with a layered, planar structure. The individual layers are called graphene sheets. The carbon atoms in each layer are arranged in a honeycomb formation with a separation of 0.142 nm. The distance between the planes is 0.335 nm [17]. Graphite possesses sp2 hybridization. The three out of the four valence electrons reside into trigonally organized sp2 orbitals, making three σ bonds in a plane. The 4th electron resides in the p orbital and forms π bonds with the neighboring atoms at right angle to the σ bonding plane. The electrical conductivity of graphite comes due to the π- π bonds. Graphite is stronger in-plane than diamond but only weak Van der Waals forces exists between the layers. This makes graphite a good lubricant. Graphite exists in two forms namely Alphaά and Beta (ß).These 2 forms are physically alike but differ in crystal structure where alpha is hexagonal while beta is rhombohedral. In nature, graphite possesses 30% beta and 70% alpha from, while lab synthesized graphite is almost 100% alpha form.

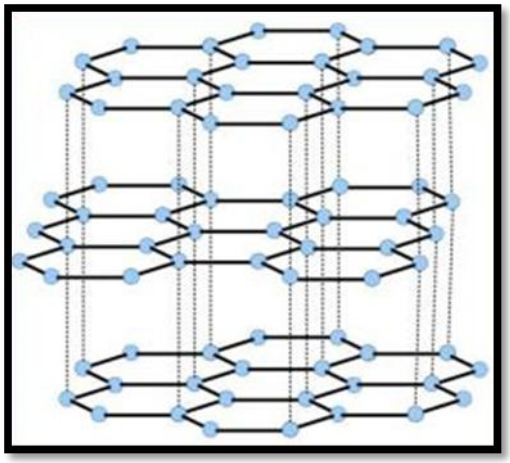

Figure 1.5: Structure of graphite.

c. Carbynes (Linear Acetylene carbon)

Carbyne is an allotrope of carbon with sp hybridization. Carbyne was reported in 1995 by the American chemists. Carbynes consist of long chains of carbon atoms with alternate carbon-carbon triple and single bonds [18]. Carbyne is semiconductor in character, sensitive to light and can be used in photodiodes and other electronic devices. Carbynes have gained substantial attention in nanotechnology as they are believed to have Young's modulus forty times higher than that of diamond, the hardest known crystal . One dimensional sp hybridized carbyne with alternate single and triple bond and some other proposed allotropes of this family are shown in figure 1.6 [19].

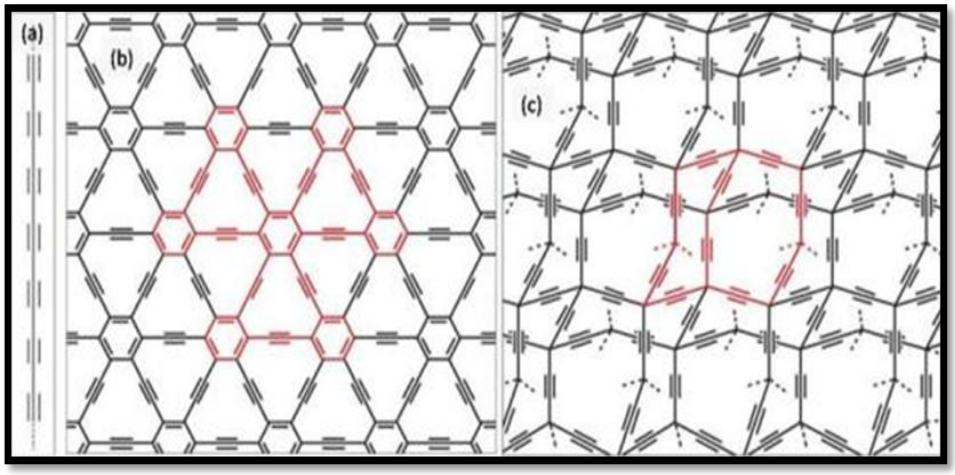

Figure 1.6: (a) 1-D Carbyne, (b) 2-D graphyne, (c) 3-D diamond [19].

1.3.2. Amorphous Carbon

Amorphous carbon does not possess any medium or long range crystalline structure. The localized π electrons in amorphous carbon cause variation in the inter-atomic spacing and in the bond angle. In mineralogy, the term amorphous carbon is associated with the derivatives of soot, coal and carbides. These materials are impure carbon and differ from graphite and diamond. Amorphous carbons can be treated a polycrystalline material with forms of diamond or graphite incorporated in the bulk of amorphous matrix of carbon. Amorphous carbon can be fabricated by the advanced techniques like sputtering deposition and chemical vapor deposition (CVD) etc. Fast quenching of liquid carbon is the simplest and rapid technique to produce amorphous carbon. The sp3 to sp2 ratio determines the properties amorphous carbon. Graphite is sp2 hybridized, on the other hand diamond possess only sp3 hybridized bonds. The carbon material with high ratio of sp3 to sp2 bonds is known as diamond like carbon owing to their resemblance with diamond in different physical properties.

1.4. Carbon Nanomaterials

The discovery of carbon nanomaterials e.g. carbon nano tubes, carbon nano beads, Bucky balls, graphene etc. have opened a wide range of research opportunities in various applications. The fabrication of carbon nanostructures enabled the production of novel devices with extraordinary properties and functionalities due to their superior electrical, mechanical and transport properties compared to other materials. Due to the ability to forge nano devices the carbon nano materials have opened new horizons for research in the fields of nano-electronics, nano-chemistry, nano-biomedicine, nano-photonics and nano-biology. Some of the extensively investigated carbon nanomaterials are briefly below to create more interest for the readers.

1.4.1. Fullerene

Fullerene was discovered In 1985 by Robert Curl and co. by the pulsed laser ablation of graphite [7]. Fullerenes were named as Buckminsterfullerene or simply fullerene to honor R. Buckminster Fuller who first developed a geodesic architecture that resembles to that of fullerene structure [18]. A Fullerene C60 consist of twenty hexagonal and twelve pentagonal faces that form a closed cage structure, similar to a soccer ball in which carbon atoms are sp2 hybridized and readily react with electron rich species as shown in figure 1.7. Because of their

structural, physical and chemical properties, fullerenes have been extensively studied for biological, medical, optical, chemical, electronic and magnetic applications.

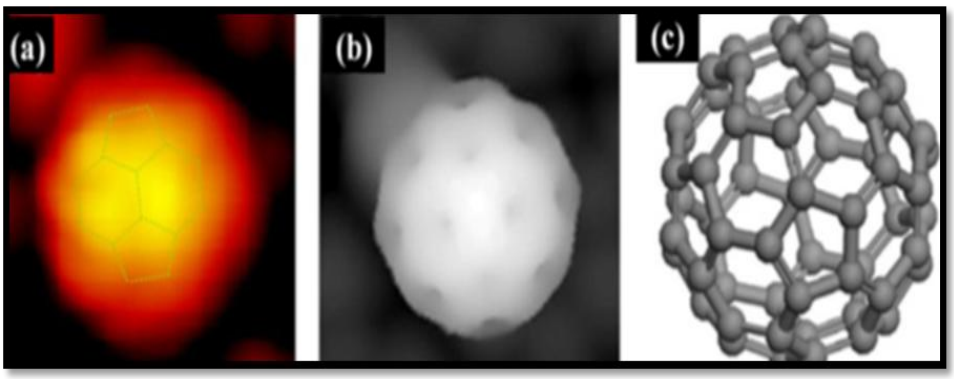

Figure 1.7: (a) STM Image of fullerene, (b) Simulated image, (c) Fullerene geometry [21].

1.4.2. Carbon Nanotubes

The deposition of graphite on cathode by arc discharge technique can deposit many different carbon nano structures under different experimental conditions. Filaments like structures were deposited on one of the electrode when the DC power of the arc was changed to alternating current. The deposited filaments first caught the attention of the world after S. Iijima observed these structures in high-resolution transmission electron microscope in 1991 [8]. These circular structures were named carbon nanotubes (CNTs), due to their tubular structures with diameters in nanometer range as shown in figure 1.8. CNTs can also be assumed as a cylindrical component of the fullerene family, with at least one end capped with a hemisphere. CNTs have a diameter 50000 times smaller than a human hair and a length of a few millimeters. CNTs have highest strength at a given size when compared other materials. Their exception strength to weight ratio makes them ideal for structural application in polymer composites. Limitations in cost and scalability as well as in reproducibilty curb their full exploitation in composites. Further discussions on cost and scalability is done in chapter 6. In CNTs the re-hybridization process occurs due to which a definite σ character can be found in π –type orbitals changing their chemical and physical characteristics[19].

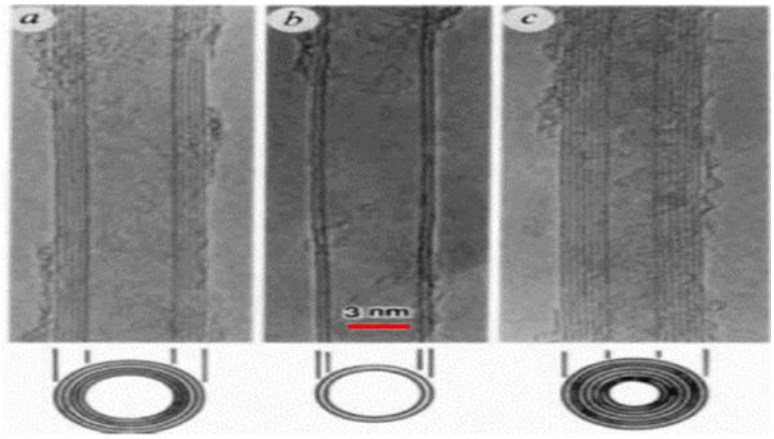

Figure 1.8: HRTEM image of MWCNTs. Dark lines correspond to the walls of MWCNTs. (a). 5 walls, (b). 2 walls, (c) seven walls [8].

1.4.3. Graphene

Graphene is a crystalline form of carbon nano materials along with CNTs and fullerenes. Graphene has two dimensional structures with single layer of carbon atoms arranged in hexagonal honeycomb as shown in figure 1.9. Graphene is the strongest and the thinnest material known till to date [1]. Graphene sheets are almost transparent but owing to their high density even the smallest atoms of Helium gas rarely diffuse through it. Commercial graphene can be applied in many applications because of its two dimensional structure and interaction with light. Graphene possesses outstanding properties of high strength, light weight, transparency, electric and heat conductance that are 2nd to none. Major techniques for the synthesis of graphene includes exfoliation of graphite, reduction of graphite oxide, by melting of metal carbon, cutting of CNTs, reduction of carbon dioxide and Sonication of graphite etc.[20]

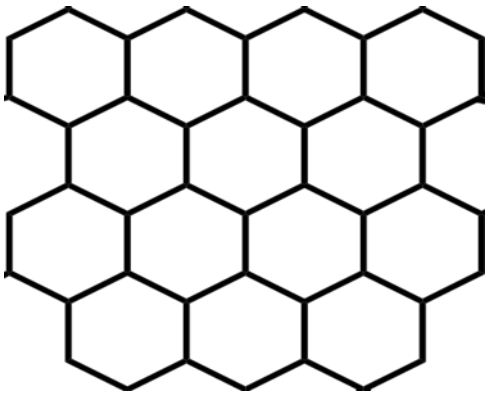

Figure 1.9: Structure of graphene.

1.4.4. Carbon Nano Spheres

Carbon nano spheres (CNSs) can be synthesized in the presence of polyoxometalates (POMs) as catalyst under hydrothermal conditions. The POMs apart from their catalyst role also support the glucose dehydration process. POMs also plays it role as a preservative to stop the aggregation of CNSs. The CNSs can be potentially applied as electrodes for biosensors and catalysis. CNSs are different from C60 and carbon onions and less investigated than fullerenes, CNTs and nanofibers. The properties of CNSs are similar to graphite but a scalable economical method for their synthesis is not available till to date [24].

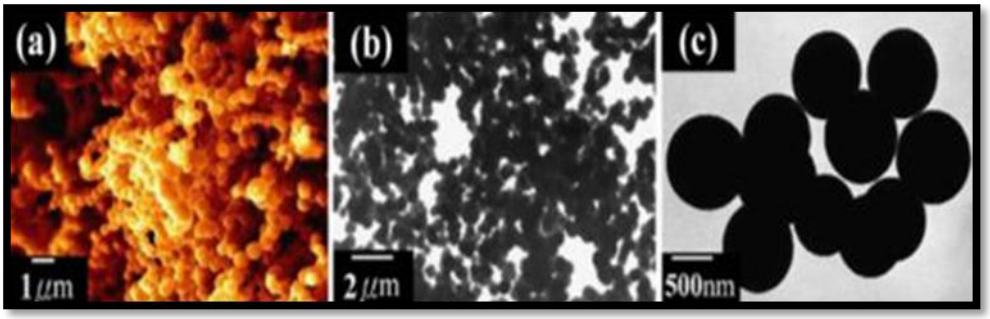

Figure 1.10: (a) SEM image of CNSs, (b) & (c) TEM Image of CNSs [24].

1.5. Carbon fibres

Carbon fibres (CF), also known as graphite fibres, are composed of more than 90% by weight of carbon atoms. The carbon atoms are bonded together in a hexagonal form and aligned parallel to the fibre axis [21]. The high tensile strength of carbon fibres arise due to this alignment pattern. Commercial carbon fibres are available in from of tows containing some thousands of filaments for instance 3000 up to 24000. Each filament has an average diameter of 5 to 10 μm, which is roughly one tenth the size of human hair. A carbon fibres tow can be used as it is or in woven form in composites application. The CF tow or fabric wound or molded into shapes and joined together with the help a polymer matrix forms a composite material that is light in weight and possesses high strength. Carbon Fibre Reinforced Polymer (CFRP) components are used in aircraft industry and spacecraft parts, racing car bodies, golf club shafts, bicycles frames, fishing rods, automobile springs, sailboat masts, and many other applications where light weight and high strength is sought[22].

Figure 1.11: Applications of carbon fibres composites.

1.6. Bio char

Biofuels and biomaterials have gained a lot of attention due their availability in abundunce in nature and eco friendly characteristics. The residue materials obtained after pyrolysing biomass and biogenic wastes under controlled environment is termed as a biochar[3]. Biochar mostly contains stable aromatic forms of carbon and thus cannot be readily returned to the atmosphere as CO2 even under favorable environmental conditions. Biochars can be used in various applications in diverse areas because they possess versatile physio-chemical properties. Some important area of applications are char gasification,energy production via combustion, activated carbon, soil remediation, carbon sequestration, catalysis, and in biomedical industry.[12]. Pyrolysis temperature and heating rates are the key factors that determine the biochar properties such as carbon yield, mineral phases, surface area, porosity, electrical conductivity etc. Biomass conversion technologies include thermochemical processes like torre-faction, pyrolysis, gasification,liquefaction and supercritical fluid etc.An example of olive based bio char is shown in the figure 1.12.

Figure 1.12: Bio char from wood.

1.7. Summary

Carbon has always been a key element for humans and nature. The industrial applications of carbon based materials has developed exponentially in last three decades. The number of publications reported per year in the field of carbon materials continues to increase exponentially, and it is likely that real life applications and devices will soon become an important part of international markets. However, the bulk synthesis processes of the nano-carbons still need to be devised to realize the dream of industrial scale products based on carbon nano materials. The high price of carbon fibres and dependence on the petroleum precursors undermine their full industrial application potential. Carbon fibres based on renewable sources with low price is still a vast area of research. Biochar is new to the family of carbon and is finding its applications in various dimensions. The remarkable characteristics of carbon in its various forms has always attracted the scientists and is expected to continue and motivate further investigations and findings.

1.8. References.

1. Pierson, H.O. Handbook of carbon, graphite, diamond, and fullerenes : Properties, processing, and applications. http://public.eblib.com/choice/publicfullrecord.aspx?p=631930
2. The forms of carbon. In *Carbon fibers and their composites*, CRC Press: 2005; pp 15-63.
3. Nanda, S.; Dalai, A.K.; Berruti, F.; Kozinski, J.A. Biochar as an exceptional bioresource for energy, agronomy, carbon sequestration, activated carbon and specialty materials. *Waste and Biomass Valorization* **2016**, *7*, 201-235.
4. Demming, A. King of the elements? *Nanotechnology* **2010**, *21*, 300201.

5. Sami, A.; Hussein, A. Growth of carbon nanofibers synthesised from decomposition of liquid organic waste on a ni/al2o3 catalyst: Thermodynamic and kinetic analyses. *Energy Procedia* **2015**, *74*, 32-43.

6. Hillert, M.; Lange, N. The structure of graphite filaments. *Zeitschrift für Kristallographie-Crystalline Materials* **1959**, *111*, 24-34.

7. Kroto, H.W.; Heath, J.R.; O'Brien, S.C.; Curl, R.F.; Smalley, R.E. C60: Buckminsterfullerene. *Nature* **1985**, *318*, 162-163.

8. Iijima, S. Helical microtubules of graphitic carbon. *Nature* **1991**, *354*, 56-58.

9. Monthioux, M.; Kuznetsov, V.L. Who should be given the credit for the discovery of carbon nanotubes? *Carbon* **2006**, *44*, 1621-1623.

10. Geim, A.K.; Novoselov, K.S. The rise of graphene. *Nat Mater* **2007**, *6*, 183-191.

11. Mouras, S.; Hamm, A.; Djurado, D.; Cousseins, J.-C. Synthesis of first stage graphite intercalation compounds with fluorides. *Revue de chimie minérale* **1987**, *24*, 572-582.

12. Lehmann, J. Bio-energy in the black. *Frontiers in Ecology and the Environment* **2007**, *5*, 381-387.

13. Crick, F. Face to face. *Resonance* **2011**.

14. Bundy, F.P.; Bassett, W.A.; Weathers, M.S.; Hemley, R.J.; Mao, H.U.; Goncharov, A.F. The pressure-temperature phase and transformation diagram for carbon; updated through 1994. *Carbon* **1996**, *34*, 141-153.

15. Grady, B.P. *Carbon nanotube-polymer composites: Manufacture, properties, and applications*. John Wiley & Sons: 2011.

16. ZHU, Z. Detonation of molecular precursors as a tool for the assembly of nano-sized materials. *Modern Physics Letters B* **2003**, *17*, 1477-1493.

17. DIR, Z. Graphene nanoelectromechanics (nems). *Graphene: Properties, Preparation, Characterisation and Devices* **2014**, 341.

18. Lagow, R.J.; Kampa, J.J.; Wei, H.-C.; Battle, S.L.; Genge, J.W.; Laude, D.A.; Harper, C.J.; Bau, R.; Stevens, R.C.; Haw, J.F. Synthesis of linear acetylenic carbon: The" sp" carbon allotrope. *Science* **1995**, *267*, 362-368.

19. Hirsch, A. The era of carbon allotropes. *Nature materials* **2010**, *9*, 868.

20. Richard, B.F. Self-strutted geodesic plydome. Google Patents: 1959.

21. Chen, X.; Chen, F.; Du, X.; Yu, S.; Cai, Y.; Liu, X.; Wang, L. Controlling adsorption status of individual fullerene at room-temperature. *Surface Science* **2012**, *606*, 1308-1312.

22. Niyogi, S.; Hamon, M.A.; Hu, H.; Zhao, B.; Bhowmik, P.; Sen, R.; Itkis, M.E.; Haddon, R.C. Chemistry of single-walled carbon nanotubes. *Accounts of Chemical Research* **2002**, *35*, 1105-1113.

23. Sun, Z.; Yan, Z.; Yao, J.; Beitler, E.; Zhu, Y.; Tour, J.M. Growth of graphene from solid carbon sources. *Nature* **2010**, *468*, 549-552.

24. Miao, J.-Y.; Hwang, D.W.; Narasimhulu, K.V.; Lin, P.-I.; Chen, Y.-T.; Lin, S.-H.; Hwang, L.-P. Synthesis and properties of carbon nanospheres grown by cvd using kaolin supported transition metal catalysts. *Carbon* **2004**, *42*, 813-822.

Chapter 2

Overview of carbon fibres production and surface modification processes.

2.1. Introduction

Carbon fibres (CFs) are defined as fibres containing at least 92 wt. % of carbon and are polycrystalline in the non-graphitic stage. They manifest a long range two dimensional order. The carbon atoms are arranged in a planar hexagonal network as shown in the figure 2.1 with no crystallographic order in the third dimension [23]. Carbon fibres can be distinguished on the basis of the structure of the fibre and degree of orientation of the crystallites. Different varieties of commercial carbon fibres are available in the market with the intended end use sought for instance Ultra High Modulus (UHM), High Modulus (HM), Intermediate Modulus (IM), High Tensile strength (HT) and isotropic as shown in the table 2.1. The Ultra High Modulus and High Modulus carbon fibres are graphitized at a high temperature and manifest a tensile modulus of 300 GPa and 500 GPa respectively. The IM and HT carbon fibres are known for their high tensile strength and low modulus. Heat treatment at low temperatures is the cause of this low modulus. The Intermediate Modulus CFs manifest a 300 Gpa modulus with a strength /modulus ratio of 0.01. On the other hand the HT CFs possess a tensile strength of more than 3 GPa and a strength /modulus ratio between 1.5 and

0.02. The isotropic CFs doesn't possess and ordered strucuture due to the random orientation of the crystallites.They manifest a modulus of 100 Gpa and thier cost is low due to the low modulus.

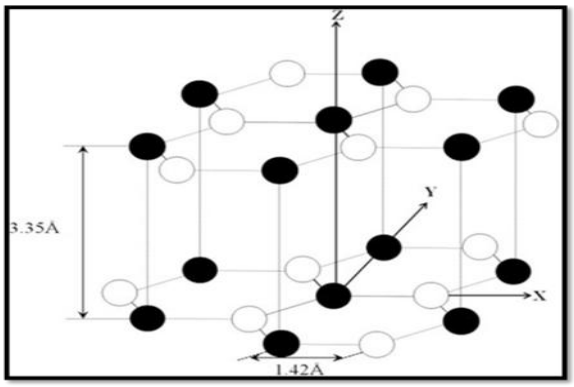

Figure 2.1: Crystallographic structure of carbon fibres[2].

Table 2.1: Categorization of carbon fibres.

Type of CFs	Temperature of heat treatment (°C)	Orientation of the crystallites	Long distance crystallite order	
Type I **High Modulus**	2000+	Parallel to the axis of CFs	Highly ordered	UHM, HM
Type II **High Strength**	≈1500	Parallel to the axis of CFs	Low order	IM, HT
Type III **Isotropic**	<1000	Indiscriminate	Very low	Isotropic

2.2. History of carbon fibres.

The earliest carbon fibres are believed to have reported by Thomas Edison who applied cotton and bamboo fibres char for incandescent lamp filaments [24]. Carbon fibres were commercially used in the late 1950s for the applications to composites. The main aim at that time was improve the ablative properties of the

materials used to manufacture rocket components. In early 1960s, Union Carbide introduced a carbonized rayon based fabric aiming for such functionality. During the time period of 1960s and 1970s a lot of research was carried out to optimize the performance to price ratio of CFs. Research focus was to look for precursors yielding large amounts of commercial grade carbon fibres. A variety precursors such as poly acrylonitrile (PAN), pitch, rayon, phenols, lignin, imides, vinyl polymers, and naturally occurring renewable cellulosic materials have been evaluated over the years for the production of CFs with desired properties at the commercial scale [25]. During the 1970s, the search for alternative precursor led to the introduction of petroleum pitch based carbon fibres. Pitch based CFs are about 85% by weight carbon and possess excellent flexural strength but a low compressive strength limitation led to their demise in the race towards the top. 1980s the carbon fibre demand rose to a 1000 metric tons per annum. Major consumers were the aerospace and sporting goods industry. PAN based carbon fibre surpassed all other precursors based CFs. This fact may be surprising to some as dominant belief was that low raw material cost with higher yield of char from pitch would be win win situation but, a spin-able pitch production process was expensive and time consuming. Consequently, PAN fibres emerged as the dominant precursor for commercial carbon fibres production and are still reigning today. Rayon precursor stands at the third postion. Despite of lower raw material cost the carbon fibres produced by rayaon fibres are inferior in properties and a low yield of 20 to 25% carbon fibres made the overall conversion process economically unviable. By the ’90s, companies like Zoltek and Fortafil introduced a new cost effective PAN based carbon fibre. A goal of reducing the carbon fibre price to 5$/lb was set by the year 2000. This policy brought a lot of attention to the accelerated development of the carbon fibre industry [26]. The report “Carbon Fibres & Carbon Fibre Reinforced Plastic (CFRP) – A Global Market Overview.” was released 2013 by the Research and Markets Company (Dublin, Ireland) predicting the global carbon fibre demand will reach 141,000 metric tons annually in the year 2020 as the composites market reaches 210,000 metric tons in the same year. The United States, Japan, and Western Europe are the leading producers of carbon fibres.

2.3. Structures and Properties of Carbon fibres

The atomic structure of the carbon fibre resembles to the graphite structure with layers of carbon atoms arranged in a regular hexagonal pattern as shown in

figure 2.2. These layer planes in CFs can either be turbostratic or graphitic or a hybrid structure of both depending on the precursors and the heat treatment process. The carbon atoms layers are stacked parallel to one another in a regular fashion in the graphitic structure and the atoms are covalently bonded through sp2 bonding in the in-plane while weak Van der Waals forces exists between the planes. The d-spacing between two graphene layers (d002) is about 0.335 nm [27]. However the structure of commercially available carbon fibres consists of a stack of turbostratically arranged (irregularly or haphazardly folded, tilted, or split) layers of graphene. The turbostratic structure and the sp3 bonds increase the d-spacing to 0.344 nm [28].

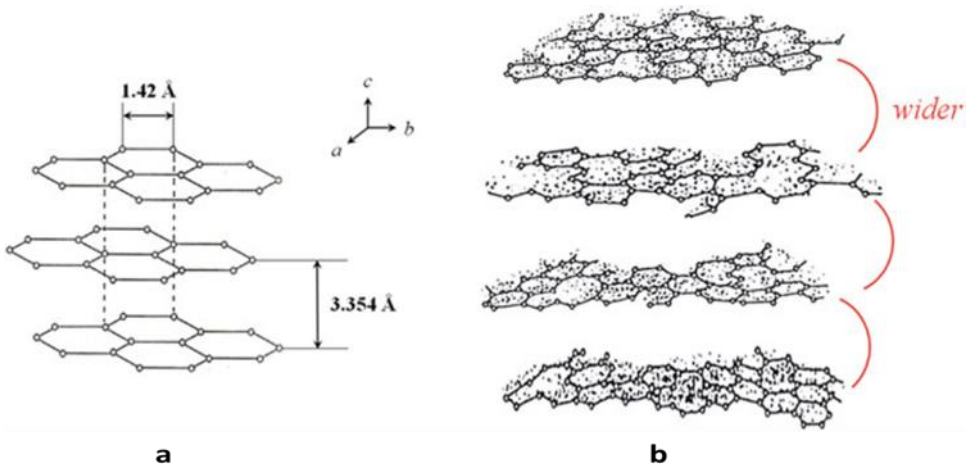

Figure 2.2: (a) Crystal structure of a graphite crystal, (b) structure of turbostratic carbon [2].

2.4. Precursors for carbon fibres

On the commercial scale four types of precusrors are employed to manufacture the CFs [29-31].

2.4.1. Acrylic precursors

PAN precursor has been the most widely used precursor to manufacture commercial grade CFs by the majority of industrial manufacturers. The quality of the material produced is still 2nd to none.

2.4.2. Cellulosic precursors

Cellulose molecule constitutes of 44.4 % carbon by weight but, the practical yield of carbon is not more than 25~30 wt. % due to the complications in the conversion process and the heat treatment behavior of cellulosic materials.

2.4.3. Pitch-based precursors

Pitch is characterized by its high yield of carbon material, roughly 85%. The resulting carbon fibres are characterized by a highly graphitic structure and high modili.On the other hand pitch based CFs display low compression and transverse properties when compared to the PAN based CFs.

2.4.4. Other forms of precursors

Phenolic resins and vinylidene chloride have been investigated as a potential precursor to manufacture commercial grade carbon fibres but the conversion process has proved to be economically unviable.

2.5. PAN precursor

PAN-based polymers can be classified into homo-polymer and co-monomers. The co-monomers are largely used to synthesize PAN-based polymers. The PAN precursors are used to produce commercial grade CFs. The manufacturing process to produce carbon fibres from PAN is elaborated in the figure 2.3.

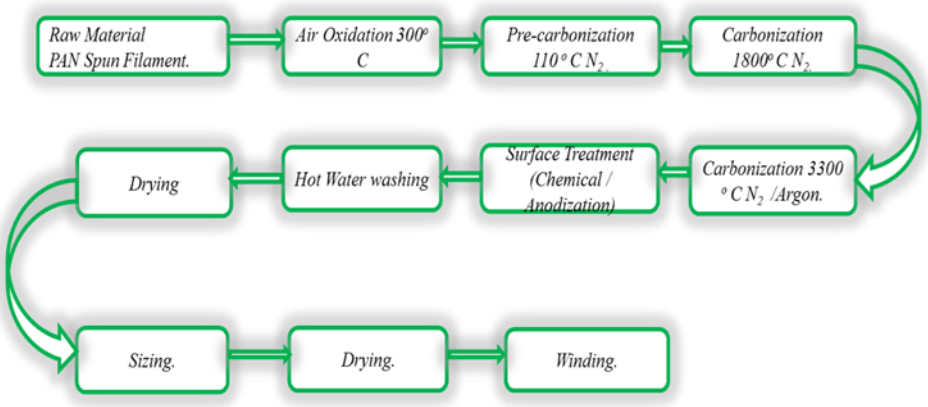

Figure 2.3 : Manufacturing process carbon fibres from PAN based precursor.

The whole conversion process can be categorized in following sections.

1. PAN precursor polymerization,
2. Filament spinning,
3. Oxidation,
4. Carbonization, and graphitization.

The poly acrylonitrile copolymer contains around 2~15 wt. % of acrylic acid, methacrylic acid and /or itaconic acid. The molecular alignment and oxidation conditions depend upon the type of co-monomers. An approximate yield of 50–60 % by weight carbon fibers can be obtained by carbonizing PAN precursor [32].

2.5.1. Polymerization and spinning of PAN precursors

The PAN filaments are are most widely used precursor to produce commercial grade carbon fibres. The chemical structure of PAN polymer is shown in the fig. 2.4. Commercial PAN fibres contain approximately between 2 to 10 % by weight of co-monomers like Methyl Methacrylate (MMA) or Itacon acids (ITA). Most of the commercial manufacturers synthesize in-house PAN precursors so the chemcial composition of the polymer is still a secret. The PAN polymer comprises of polar nitrile groups which promote a strong intermolecular interactions between the fibres chains. For this reason PAN fibres manifest a high melting temperature. PAN fibres in the carbon fibre industry are spun with traditional spinning techniques for acrylic fibres. PAN fibres are produced generally through the wet spinning technique but the dry jet wet spinning of PAN fibre is capturing more attention [33]. Commercial PAN fibres production through melt spinning technique is obsolete now.

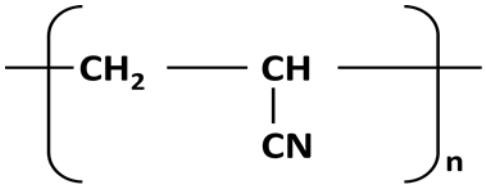

Figure 2.4: Basic structure of PAN polymer.

2.5.2. Thermal stabilization (oxidation)

Oxidation of the PAN precursor is critical to obtain high-quality carbon fibres. This oxidation process may last for several hours. This process depends upon the final heat treatment temperature, diameter of the PAN fibres, and

precursor fibre properties [34-36]. Process parameters such as heating ramp rate, treatment time, and temperature of heating affect the quality of the final carbon fibres. The PAN fibres are oxidized in a controlled environment with a temperature range between 200 and 300° C. The oxidation process converts the fibres into an intermediate form that can be heat treated at elevated temperatures without melting or fusing the fibres within each other [37]. In the stabilization process the linear PAN molecules are converted into cyclic structures. However, this cyclization mechanism is quite complicated and requires further investigations. The mechanism of the oxidation reaction is depicted in the figure 2.5.

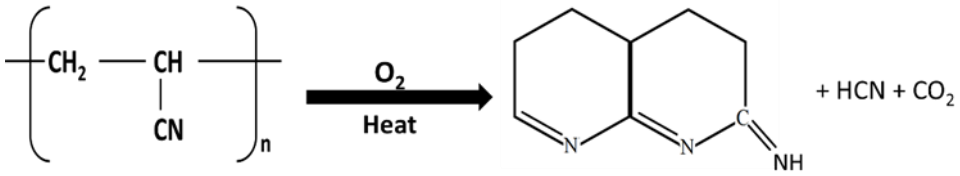

Figure 2.5: Cyclization mechanism of PAN.

2.5.3. Carbonization and graphitization

The oxidized PAN fibres are carbonized and subsequently graphitized in an inert atmosphere (N_2 or Ar gas) [38]. Argon is generally preferred over nitrogen regardless of its high price compared to the nitrogen but argon confer superior mechanical properties to the carbon fibres owing to its high density and viscosity. The carbonization temperature usually depends upon the intended final application. For high-strength applications the carbon fibres are treated in the range of 1500~1600° C. Above this temperature the tensile strength decreases. For high modulus carbon fibres the treatment temperature is set between 1800° C and 3000° C. This process is called graphitization [39, 40]. Nitrogen environment cannot be used at temperatures above 2000° C due cyanogen formation which happens when carbon react with nitrogen. Type of precursor and oxidation conditions dictate the carbonization process parameters like heating ramp rate and housing time. Carbonization at a low temperature range of 200~1000° C evolves gases and volatiles from the PAN precursor. This effect was confirmed by Bromley et al.[41], 1992. Removal of hydrogen from the PAN joins the molecule chains in a graphite like ribbon strucutre while the removal of the nitrogen from these ribbons cause them to from a sheet-like structure. The heat treatment assist the formed structure to grow in the thickness and area dimension.This phenomena

orientates the crystallite along the fibre axis and reduces the void content. Consequently, interlayer spacing reduces. Highly graphite structures can further be obtained by treatment at high temperatures of 1500° C. Heat treatment above this temperature ensures the complete elimination of N_2. Schematic diagram of the carbonization and graphitization process is depicted below.

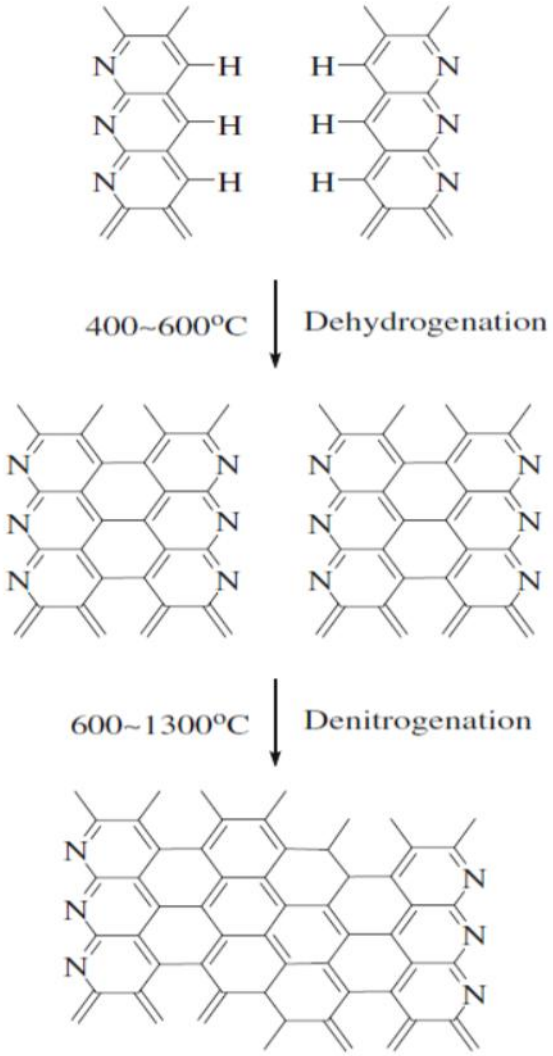

Figure 2.6: Schematic structure of Graphite sheets[2].

2.5.4. Surface treatment and washing.

The surface of the carbon fibres is modified in order to improve adhesion with the matrix. Higher adhesion leads to superior mechanical behavior in the composite application. The treatment technique to modify the carbon fibres

surface is still kept confidential by many manufactures. Liquid and gaseous oxidation treatments are commonly employed to alter the surface of commercial CFs. The liquid oxidation treatment are very effective in surface modification of CFs and can double the shear strength of the composites with a slight reduction, roughly 4–6 % in the fibre tensile strength [42]. Anodic oxidation treatment method is widely utilized in the surface treatment of commercial carbon fibres due to intriguing benefits like low cost, low treatment time and high efficiency. Commercial carbon fibres are electrically conductive and play the role of anode in the electrolysis of an acid solution e.g. nitric acid (HNO_3) and sulfuric acid (H_2SO_4) or a salt solution like ammonium sulfate ($(NH_4)_2SO_4$) and ammonium bicarbonate (NH_4HCO_3)[43]. Washing with warm water after the surface treatment removes the excess electrolyte. The surface treated CFs are subsequently supplied to the next process after drying. The demand of the surface treated carbon fibres has been significantly elevated due the increased demand for high-performance carbon fibre composites.

2.5.5. Sizing

Carbon fibres are brittle in nature and require surface protection and lubrication for the ease of handling during processing. The carbon fibres are dried prior to the sizing treatment. The sizing material is chosen to preserve the physical properties of carbon fibres. The sizing material is required to provide consistent handling and not to build up residue on the processing equipment. The sizing material should also be compatible with the matrix. Solubility of the sizing agent in the matrix or its reactivity with the formulated resin are important considerations before the application of the sizing agent. In this way the resin can penetrate the fibre bundle and interact with the fibre surface. Epoxy resins based sizing is usually applied on the surface of CFs. Ideally the sizing materials do not alter the chemical and physical state of the CFs during the storage. Size coating can be washed after the weaving or the braiding process [23].

2.5.6. Winding.

The carbon fibres are dried after the application of the size coating and wound into 12 kg spools by automatic winding machines.

2.6. Cellulose based precursors

Thomas Edison in 1880s used the cellulose based carbon fibres in his revolutionary electric lamp filament. Union Carbide (National Carbon Company) synthesized carbon fabric from the rayon precursor fabric in 1959, in 1961, a carbon yarn was introduced [44]. In 1965 carbon fibres with tensile strength of 1.25 GPa and Young's modulus of 170 GPa were introduced. The improved properties of carbon fibres were attributed to the post-carbonization treatment inculpating stretching at 2500° C but, the carbon fibres production halted for more than a decade due unviable parameters like the cost of the hot drawing process, low yield of carbon and faliure to achieve the desired properties of the cellulosic precursor. A heat treatment process for monofilaments based on Rayon precursor, cellulose based yarns and pre-woven rayon textile material was proposed by Ford & Mitchell [45]. The fibres were heat treated under a controlled environment at a ramp rate of 10° C/hour for tepmeratures upto 100° C, 50 °C/hour the temparatures range of 100 to 400° C. A ramp rate of 100 °C/h was set for heat treatment up to the temperature of 900 °C. If graphitization is sought the heat treated fibres can be subsequently treated up to 3000° C. Heat treatment at a temperature range of 900~3000° C was performed in an inert atmosphere of N_2 or Ar gas. Carbon fibres obtained after the heat treatmnet manifest superior tensile strength when compared to their untreated counterparts. X-ray patterns confirmed the presence of highly ordered graphitic structure[46]. Cellulose can be converted into carbon by following a simplified 4 steps process proposed by Tang and Bacon[47].

- *Step 1*. Heat treatment of cellulose at a temperature range of 25~150° C results in the physical desorption of the adsorbed moisture. A small degree of change in the lateral order is also observed due to the water desorption.
- *Step 2*. Heating at a temperature range of 150~240° C dehydrates the C–H and C–OH fragments of the cellulose unit. Infrared spectroscopy confirms the presence of carbon carbon bond and carbonyl groups which shows that the dehydration occurs with in the molecules.
- *Step 3*. Heat treatment between higher temperature range of 240~400° C causes cleavage of the glycosidic linkage and C=O and some C–C bonds scission by means of a free radical reaction. This reaction leads to the formation of large amounts of tar, H_2O, CO and CO_2.
- *Step 4*. Aromatization begins at 400° C or more. During the aromatization the cellulose unit breaks down forming a residue structure comprising of 4 carbon atoms. These carbon strucutures further polymerize into polymer of

carbon having a graphite like structure through condensation reactions, accompanied by the removal of hydrogen.

A lab scale heat treatment for stress graphitization of rayon based precursor was proposed by Strong et.al [48]. This phenomena occurs at approximately 2800° C and any non-uniformity in the filament leads to either a non-uniform stretch or breakage during the stretching process. It is imperative that the filament is supported and transported by rollers. The textile finish on the Rayon filament was removed by the boiling water. Pyrolysis of the Rayon can be carried out in in two ways (i) heat treatment continuously for seven minutes between temperature range of 260~280 ℃ in oxygen environment, (ii) Heat treating a batch at 225 ℃ for 20h in air. A 40 % weight loss occures during this treatnment.The treated fibres are further heat treated for 7 minutes in oxygen with a total yield of carbon upto 45~ 50%. The final carbon structure can be developed with sufficient strength to endure stress-carbonization by heat treatment in nitrogen enviorment for a minute and a half at 350 ℃. The material was carbonized over the range 900~2000° C and graphitized over the range 2800~2900° C. X-ray diffraction studies showed that the starting material Cellulose II was converted to the Cellulose IV structure before degradation started. It was observed that during pyrolysis in air, shrinkage occurred at approximately 25~45 % weight loss, associated with a tendency to kink if the yarn was not under tension. So, the pyrolysis stage was deliberately limited to postpone the second weight loss stage to the carbonization step, during which sufficient tension could be applied to prevent kinking.

2.6.1. Carbonization of Rayon fibres to attain carbon fibres

Rayon fibres with the cellulosic background can be converted into carbon fibres with carbonization process. During the stabilization and carbonization processes carbon fibres experience physical, chemical and mechanical changes as well as their microstructure exhibit an alteration. In light of changes in mechanical and chemical properties, the stabilization process is very important to synthesis of stable carbon fibres. Thermal shrinkage occur in the cellulose fibres as a reuslt of the weight loss during the stabilization process [49]. The conversion processes like stabilization, carbonization, and graphitization cellulose precursor to carbon fibres are explained below. Subsequent processes after conversion like surface treatment, sizing, and winding are similiar to that of the PAN based process.

a. Oxidation / Stabilization

Cellulose is a linear polymer based on glucose molecule.The glucose molecules are connected by β-(1-4) glycosidic linkages to form the cellulose strucutre as shown in the figure 2.7. The -OH fucntional groups in the clullose structure are responsible for the intramolecular and intermolecular hydrogen bonds. This type of bond formation governs different ordered crystalline strucutre. The stoichiometric amount of carbon in the cellulose is about 44.4% as shown in the chemical formula of cellulose $(C_6H_{10}O_5)_{n.}$ But, the actual carbon yield obtained is only between 10 % to 30 % by weight. The reason for the low yield is that macromolecular chains depolymerize during heat treatment and carbon content also reduces due to the explusion of carbon containing gases like carbon monoxide (CO), carbon dioxide (CO_2), aldehydes, organic acids, and tars etc. Therefore it is imperative to carefully choose the stabilizer materials for improved carbon yield and consequently the properties of carbon fibres [50-52]. The cellulose fibres start degrading at around 200° C and complete degradation at 380° C in an inert environment. The thermal stability of the cellulose precursor is dependant upon on the manufacturing process. Complex physicochemical changes occur in the cellulose fibres during the conversion process and a variety of oxygenated compounds are produced during the heating process. Formation of the volatile substances and solid residue causes the major mass loss. The yield of carbon material can be improved by reducing the burning loss. Cellulose precursors can be modified to improve the yield and properties of the carbon fibres. These attributes can be achieved by either slowly heating the cellulose precursor with a heating rate of a few °C/h or treating with compatible impregnators [53, 54]. Two predominant reactions control the pyrolysis of cellulose precursors namely dehydration and depolymerization or cleavage as shown in the figure 2.7. At 300^o C dehaydration occurs in the cellulose and its structure is stabilized. Conjugated double bonds are formed due to the dehydration reaction. As a concequence the conjugated ring is more resistant to cleavage when compared to the original cellulose structure. Major mass loss at high temperature is caused by the depolymerization in the early stages of pyrolysis with the incomplete dehydration of the cellulose structure. Slow heating rate during the carbonization process improve the carbon yield and also influence positively the properties like density, porosity and microstructure etc. [55].

b. Carbonization and graphitization

The 1st dehydration of the cellulose occurs at 25~150° C. At a temparture range of 150~240° C cellulose molecules dehydrates and water desorps

physically. Dehydration causes the formation of intermediate conjugate bonds [56]. During the carbonization process the depolymerize strucutre of cellulose repolymerizes to form a graphitic structure. The repolymerization process starts at a temperature of 300 ℃ and continues till 900 ℃ temperature. The basic microstructure of the carbon is formed during the Stage III [44]. The cleavage of glycosidic linkages and the ether bonds occur between 240~400° C. Further more the monosaccharide derivatives depolymerize at this stage. The release of non carbon (O & H) gases from the intermediates causes the formation of aromatic structures [57]. Heat treatment at 400 ~ 900° C in an inert atmosphere fascilitates the formation of ordered carbon structures. The full mechanism of aromatization to graphitic structure is yet to be known due to the complex decomposition of the cellulose and reactions during the various stages of the carbonization process. Semi-ordered carbon structure is formed at around 900^{o} C. Graphitization can be carried out under stress in a temperature range of 900~3000° C to obtain high-modulus fibres due to the enhanced order of the graphene stacks, both laterally between the layers (crystallographic register) and in terms of the preferred orientation along the fibre axis. The Young's modulus is dependent on the treatment temperature with the graphitization conducted under tension. The carbon content of the fibres increases up to 99 % after the graphitization process with the fibre density increases due to the growth of crystallites [58].

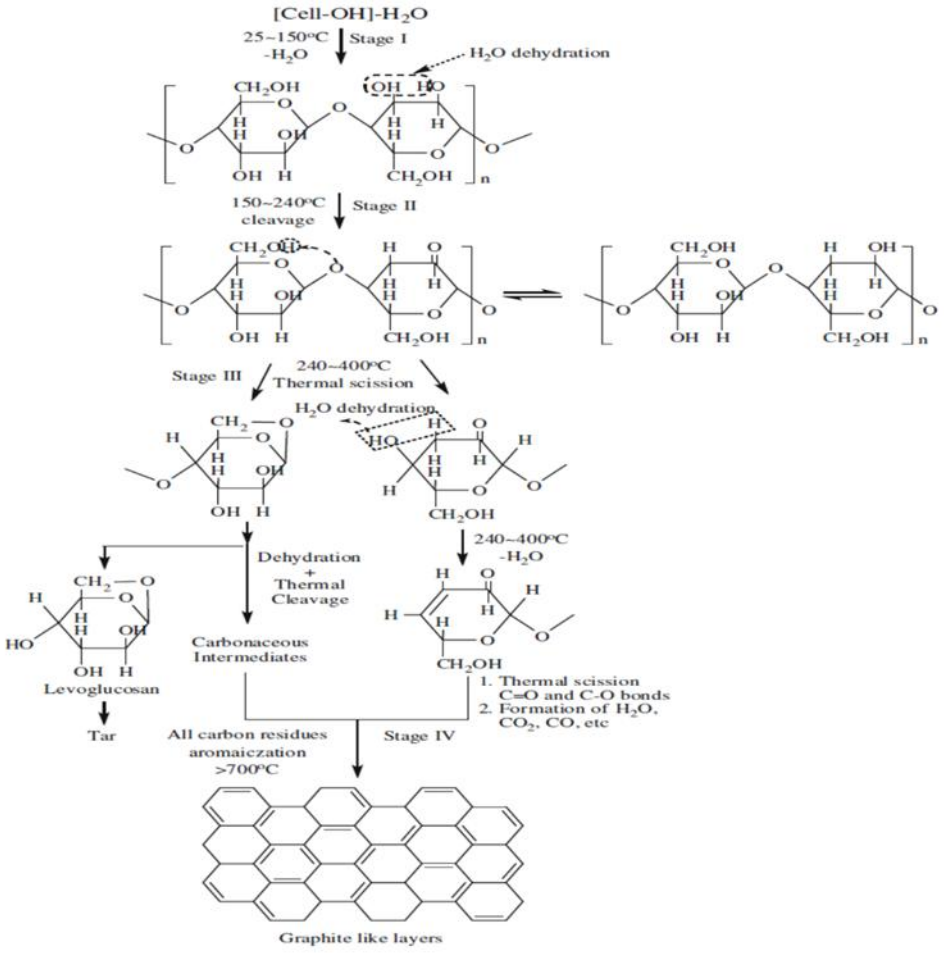

Figure 2.7: Mechanism of CF formation from Cellulose [2]

2.7. Pitch precursors.

Pitch is a complex blend of polyaromatic molecules and heterocyclic compounds. Pitches have been used as precursor to produce commercial grade carbon fibres and also as fillers in carbon composites. Pitch comprises of more than 80 % carbon and this composition is dependent upon tar source and the processing conditions [59]. Pitch is available through various sources as listed below.

(i) Residue after extraction of petroleum also known as bitumen or asphalt,

(ii) Residue obtained after the destructive distillation of coal,

(iii) Natural asphalt,

(iv) Pyrolysis of PVC,

Pitch precursor has several intriguing advantages over the PAN precursor such as low material cost, higher char yield and higher degree of orientation[60]. Pitch-based carbon fibres possess a high elastic modulus, high electrical & thermal conductivity in the fibre direction due to their more graphitic structure [61]. One undermining factor for the pitch precursor is the high processing cost. Petroleum and coal tar based pitch is isotropic in nature. The isotropic pitch is melt-spun into low-cost general purpose carbon fibres after the evaporation of the low molecular weight fractions. Where high performance is desired a hot stretching process is employed that is expensive and adds cost to the final product. High-performance carbon fibres from the pitch precursors are produced by using an anisotropic pitch e.g. mesophase pitch [38]. Various types of pitches are described below.

a. Isotropic pitch

Isotropic pitches are generally used to manufacture only general purpose carbon fibres. The general purpose carbon fibre are characterized for their non-graphitic structure and poor properties as compared to the high performance carbon fibres. High performance CFs are manufactured from mesophase pitch. Isotropic pitch can be converted to mesophase pitch with a special treatment process. Mesophase pitch is optically anisotropic and a graphitic material. The isotropic pitch can be melt spun only after the removal of low molecular weight volatile species and filtration of solid particles. The refining process raise the softening point and avoid the formation of mesophase. GP carbon fibres are generally manfactured from the Ashland Aerocarb 60 and 70 precursors. [62, 63].

b. Mesophase pitch

The high-modulus carbon fibres are manufactured by mesophase pitch precursor. The mesophase pitch is produced by either thermal polymerization of petroleum or coal-tar based pitch or by the catalytic polymerization of pure compounds such as naphthalene. An intermediate phase is formed by thermal the thermal treatment of aromatic hydrocarbons at 400 ~550° C called the messophase. During the mesophase formation, domains of highly parallel, plate-like molecules form and coalesce until 100 % anisotropic material may be obtained in due course. The morphology of the messophase pitch is the deciding

factor in determining the microstructure of the final graphitic material [64]. Mesophase pitch can be produced by the following methods.

(1) Pyrolysis of isotropic pitch,

(2) Solvent extraction,

(3) Hydrogenation,

(4) Catalytic modification.

2.7.1. Carbon fibre production from pitch precursor

CFs can be produced from pitch precursor in different stages. These stages include synthesis of of the fibres, oxidation, carbonization and graphitization. Stabilization of the precursor is the most important stage as in this the thermal oxidation of the precursor takes place. The performance of the final carbon fibres depends greatly on the stabilization of the precursor fibres. The surface treatment, surface coating and winding processes are same as the PAN carbon fibres process. Detailed production process is described below.

a. Fibre production

The melt spinning of the pitch precursor involves three steps namely melting the precursor, extrusion through a spinneret capillary and drawing the fibres as they cool. It is the melt spinning process that governs the structure to the mesophase pitch based CFs and the heat treatment only reinforces this structure. The process variables affect the final structure of the fibres that play the determining factor role in the final graphitic structure of the carbon fibres. Melting temperature is 1st most important factor in this list. Each mesophase possesses a unique melt spinnable temperature. Attmept to spin the fibres below the temperature threshold causes a high viscosity of the presucrsor and brittle fracture occurs while the drawdown. Low viscosity, dripping and precursor degradtion occur for a spin temperature higher than the thershold one. A decrease of 15° C in the temperature can increase the viscosity four folds consequently mechanical strength and young’s modulus decrease significantly [45].

b. Oxidation

The pitch fibres are oxidized in air at elevated temperatures before being exposed to the final high temperature carbonization treatment. The oxidization temperature are always less than the glass transition temperature of the fibre in order to keep the orientation of the fibre intact. The mesophase pitch precursor is stabilized in air at 250~350° C for a time period ranging from 30 min to several hours depending upon the composition of the pitch. Fibres may or may not be stretched in this step. The oxidized pitch molecules contain ketone, carbonyl, and carboxyl groups that lead to the stronger hydrogen bonding between the adjacent molecules. The introduction of oxygen containing groups and formation of hydrogen bonding between the molecules facilitate the three dimensional cross-linking but also limits the crystallites growth. Iodine reportedly reduces the oxidation time and increases the yield of carbon. Sasaki and Sawaki reported the imbibement of 0.05 wt. % of Iodine in the methanol soaked carbon fibres precursor. The fibres were then heated in an oxygen environment to increase their infusibility. The amount of imbibed iodine usually dictates the treatment time. The infusiblilization can be completer in ten minutes. [65, 66].

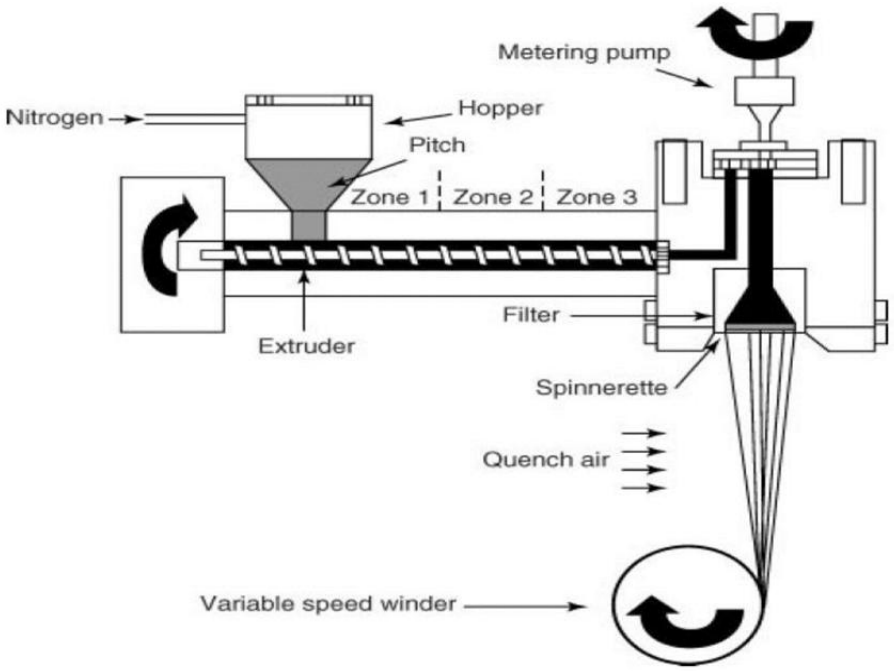

Figure 2.8: Melt spinning of pitch based CF [48].

c. Carbonization and graphitization

Stabilized fibres are then carbonized and graphitized. During the carbonization stage the fibres occur in the maximum weight loss. During carbonization the excessive release of volatiles can cause defects in the fibres. To avoid this problem the fibres are precarbonized for 0.5~5 minutes at a temperature of 700~900 °C. Carbon fibres are produced at a carbonizing temperature range of 1500~1800 °C. Bright and Singer [67] reported a decrease in the modulus at a temperatures of 1000 °C owing to the degradation of structure by the release of volatiles. The modulus increased significantly when heat treated above 1000^{o} C. For high modulus applications the carbon fibres are graphitized at temperatures close to 3000 °C. Barr et al. [68] demonstrated the alignment of the crystalline lamellae at elevated temperatures that lead to high modulus of the resulting CFs.

2.8. Overview of surface treatments on the commercial carbon fibres

Carbon fibres (CFs) composites have been applied in various industries because of their intriguing properties, process ability, and recyclability. However, raw CFs require a surface treatment and sizing for ease of handling in the subsequent process and interaction with the matrix at the interface of the two species [69]. Surface treatment enhances the adhesion between the fibres and matrix. A physical or chemical change in the properties at the interface can be achieved by either treatment of CF surface by suitable surface modifier or by applying surface finish [70]. A suitable surface treatment method increases the surface area of the CFs and creates functional groups on the surface of the CFs to enhance the CF-matrix interactions consequently, mechanical properties of the composites improve. The interfacial shear strength increases due to the chemical bonds formation between the fibres and the matrix. A variety of oxidizing agents and gases are avaialble today to modify the surface of carbon fibres. The most prominent techniques for surface modification are plasma, electrochemical treatment, acid and thermal treatments [71].

2.8.1. Gaseous Oxidants

Dry oxidation is carried out in the presence of air, oxygen (O2) and ozone (O3). This method of surface modifications brings advantages like low cost, ease of operation, lack of pollution and excellent homogeneity [54, 55].

a. Air Oxidation

Carbon fibres oxidize on exposure to high temperature in the ambient conditions. As a result the properties of final composites change but the mechanical properties of the CFs degrade. Tong et al. [56] heat treated PAN based CFs in air at a temperature range of 400~700° C. The crystallite height decreased at the elevated temperatures due to the oxidation of carbon. A significant decrease in the tensile strength was observed with almost identical tensile modulus. The density of the carbon fibres increased after oxidation which suggests that the glass-like carbon is easier to burn off compared to the graphitic carbon in the fibre. After oxidation the graphite size in the fibre decreased while the spacing between the graphite layers increased. This behavior is due to the oxidation of the C atoms of the graphite layers[55]. Wang et al.[57] studied the changes in the surface morphology of the pitch based CFs after oxidation at the temperatures of 300, 400, 500, and 600 °C respectively in air. Li et al. [59] observed that the specific surface area and roughness of the CFs increase after oxidation in air. They further observed the deterioration trend in the fibre mechanical properties with increasing either treatment temperature or time. They witnessed that the flexural strength, flexural modulus, and shear strength of the composites increased by 149, 91, and 29 % respectively after treatment while the impact strength decreased by 23 %.

b. Ozone treatment

Carbon fibre surface can be activated using ozone gas. This treatment modifies the morphology of the CFs. Consequently the flexural and compressive properties of the composites improve [58]. This phenomena can be explained by 2 ways (i) formation of chemical bonds between the resin and fibre (2) high surface and high roughness increases the physical interaction between the matrix and fibre. For optimal composite properties it is recommended to treat carbon fibres at 120 °C rather than at 160 °C as ozone rapidly decomposes at this temperautre.

c. CO_2 oxidation

Carbon fibres can be surface treated using CO_2 gas. Sun et al.[60] reported the activation of PAN based hollow CFs. They observed an enhanced specific surface area of the CFs after treatment. They further observed an increasing trend in the mesopores size with increased treatment time.

2.8.2. Acid Oxidation

Surface treatment of CFs with acids is the most commonly used technique in the wet surface treatments. Park et al. [61] reported the effects of nitric acid treatment on the multi-metal adsorption by basic ACFs from the interfacial and textural points of view. The amounts of the adsorbed metals like copper and nickel increased after the nitric acid treatment. The higher adsorption can be attributed to the higher number of oxygen containing functionalities that shifted the isoelectric point of the ACFs towards the lower pH i.e. more acidic nature of the ACFs. Fathi et al.[62] reported the enhanced performances of the carbon fibre polyester composites after treatment with sulfuric acid. Important properties like flexural strength, modulus and stiffness imporoved due to better fibre-matrix interfacial properties. Tang et al.[63] reported the PA 66 matrix reinforced with arylboronic acid treated CF. The composites fabricated by the treated fibres performed better in the mechanical and tribological analysis. While Xu et al. [64] studied the ILSS (Inter laminar shear strength) of the acrylic acid treated carbon fibre composites. They reported a 15% increase in the ILSS after the surface modification with the acrylic acid due to a higher wettability of the treated fibres.

2.8.3. Electrochemical Oxidation

Electrochemical oxidation is the most commonly used technique to functionalize the surface of carbon fibres. The functional groups improve surface energy, surface roughness of CF and significantly improve fibre-matrix adhesion. Process variables such as type of electrolyte, concentration, treatment time and conditions play a vital role in achieving the optimum surface properties for improved interfacial adhesion [65]. Variety of electrolytes are available today to modify the surface of carbon fibres for instance sodium hydroxide, ammonium hydrogen carbonate, ammonium carbonate, sulfuric acid and nitric acid are the commonly used electrolytes [66]. Electro-oxidative treatment remove the weak boundary layers from the surface of the carbon fibres and enhances the surface activity by forming acidic and basic moieties and enhance the surface area due to the formation of micro pore and crevices on the fibre surface [67]. Cao et al.[68] studied the compressive strength of carbon fibres phenolic resin composites after an electrochemical modification. An increment of 38% was observed in the compressive strength of the composites formed by the electrochemically treated fibres.

2.8.4. Treatment with non-oxidative agents

Carbon fibres can be surface treated with isopropylidene malonate which reacts with the already existing surface defects of the CFs [69]. The terminal malonic esters are grafted and thus creates a carboxyl functional group on the surface. The tensile strength of the CFs was preserved since there were no additional surfaces created by the treatment. The formation of the functional groups can be validated using X-ray photoelectron studies (XPS) and Fourier transform infrared (FTIR) spectroscopy. This method improves the interfacial adhesion with the matrix without compromising the fibre strength. There is potential to open a new paradigm in the carbon fibre composite industry [70].

2.8.5. Radiation method

The radiation affects the crystal lattice in two ways, (i) atoms gets dispalced within the lattice (ii) electronic excitation [71]. The excited electrons cause a topographical change in the CFs and create active sites on the fibre surfaces [72].Gamma ray radiation have been commonly employed to functionalize carbon fibres. Xu et al. [71] reported the surface modification of the CFs with γ-ray radiation from a Co 60 source. Tiwari et al.[70] employed the γ-ray radiation technique on the carbon fabric. They observed and enhanced ILSS and tribology behavior of the polyetherimide (PEI) matrix and γ-ray radiation treated carbon fabrics. Wan et al. [73] also demonstrated the enhanced mechanical behavior nylon matrix composites reinforced with the gamma ray radiation treated PAN-based CFs.

2.8.6. Polymer Coating

Carbon fibre surface can be modified by grafting polymers on the surface. Wei et al. [74] reported the grafting of polyesters onto the surfaces of the vapor grown carbon nanofibres (VGCF) by the anionic ring-opening alternating copolymerization of epoxides with cyclic acid anhydrides initiated by COOK groups introduced onto the VGCF surface. The surface treated VCGFs showed less entanglements.

2.8.7. Plasma treatment

Plasma, also known as the fourth state of matter, is a partially or fully ionized gas that contains electrons, ions, radicals and neutral atoms or molecules [75, 76]. Gas plasma based on a particular gas can be produced by the introduction of the desired gas into a vacuum chamber at low pressure of 0.1~10 Torr and exciting this gas using radiofrequency energy. The free radicals and electrons created in the plasma collide with the exposed surface of the material and ruptures covalent bonds and creates free radicals. Plasma composed of inorganic gases such as argon, helium, hydrogen, nitrogen, and oxygen leads to the implantation of atoms, radical generation, and etching reactions while plasma composed of organic gases such as hydrocarbons and alkylsilanes leads to polymerforming reactions. Schematic of oxygen gas plasma assembly is presented in the figure 2.9. Montes-Morán et al. [77] treated the ultrahigh modulus carbon fibres with oxygen plasma. Scanning Electron Microscope images showed that all the fibres contain scratched areas, crevices and pits formed by the attack of the plasma elements. XPS analysis confirmed the formation of oxygen containing functional groups such as carboxylic, alcohols and aldehydes and ketones.

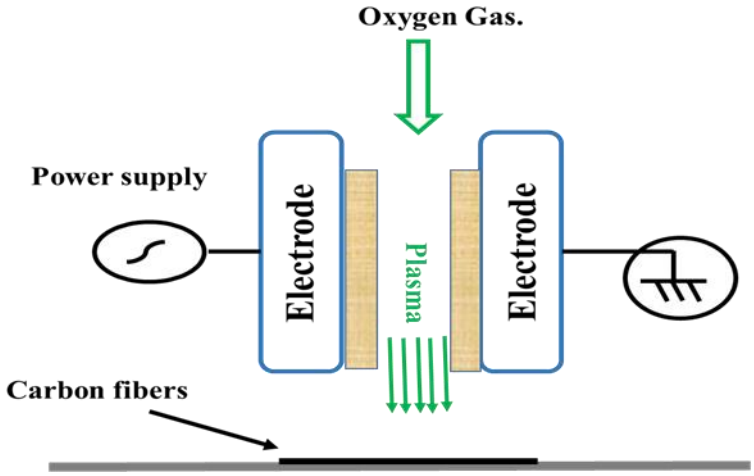

Figure 2.9 : Plasma treatment process of carbon fibres.

Park and Kim [61] carried out the atmospheric pressure plasma treatment in oxygen environment on ACFs. They reported an increase in the functional groups like C-O- and COO- after the plasma treatment. They also found that the HCl removal efficiency of the plasma treated ACFs was higher their untreated counterparts. Plasma treatments hold several intriguing benefits over the other surface modifying techniques such as

- Optimum surface modification in few minutes,
- Ease of operation,
- No hazardous solutions to dispose of,
- Removal of extra processes like washing and drying,
- Possibility to change treatment parameters like gas flow rate, plasma power, treatment time online.

2.9. Surface modification vs. fibre strength

To enhance the adhesion between the single fibre and the matrix the chemical modification and coating techniques require further in-depth analysis. Optimum surface modifications techniques without compromising the fibre strength is an important confront for the advancement of high performance composites materials [78]. Majority of surface treatments distort the fibre surface and increase its roughness by the introduction of specific functional groups in compatibility with the polymer matrix. A comparison of the effects of various surface modifications techniques on the carbon fibre structure and mechanical properties is elaborated in figure 2.10. It seems that plasma treatment and growth of nano particles on the fibre surface seems to be the optimum method to modify the fibre surface.

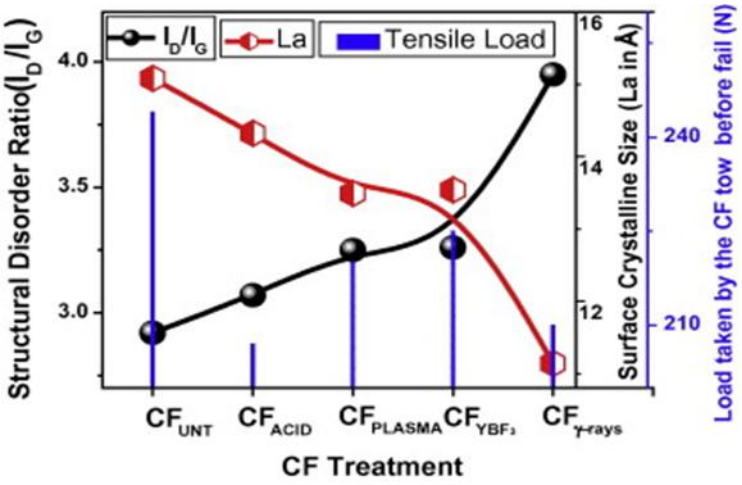

Figure 2.10 : Comparison of various surface treatments on the carbon fibre structure[65].

2.10. Summary

- Carbon fibres are one of the most widely used fibres in the composite industries with applications ranging from sports goods to aerospace industries.

- Commercial grade carbon fibres are manufactured with various precursors such as petroleum sources, bio renewable sources and synthetic fibres.Lignin based precursor is finding its place as a potential precursor to produce commercial grade carbon fibres owing to its abundance in nature and low cost compared to the existing precursors.

- Surface modifications of carbon fibres for optimum fibre-matrix adhesion is a very important front to explore in order to take the composites industry to its maximum potential.

- Plasma treatment is an ideal candidate for further investigation as an effective technique for surface modification of commercial grade carbon fibres.

2.11. References

1. Edie, D.D. The effect of processing on the structure and properties of carbon fibers. *Carbon* **1998**, *36*, 345-362.
2. Lee, S.-J.P.a.S.-Y. Carbon fibers, history and structure of carbon fibers. *Springer Series in Materials Science* **2015**, *210*, 1~30.
3. Edison, T.A. Electric lamp. Google Patents: 1880.
4. Weil, E.D. Carbon fibers, 2nd edition by j. B. Donnet and r. C. Bansal, marcel dekker, new york (1990), isbn 470 pp., price $150.00. *Polymers for Advanced Technologies* **1992**, *3*, 47-47.
5. Corporation, Z. Annual report. 1995, 1995.
6. Park, S.-J.; Lee, S.-Y. History and structure of carbon fibers. In *Carbon fibers*, Springer Netherlands: Dordrecht, 2015; pp 1-30.
7. Chung, D.D.; Chung, D. *Carbon fiber composites*. Butterworth-Heinemann: 2012.

8. Hammel, E.; Tang, X.; Trampert, M.; Schmitt, T.; Mauthner, K.; Eder, A.; Pötschke, P. Carbon nanofibers for composite applications. *Carbon* **2004**, *42*, 1153-1158.

9. Shin, H.K.; Jeun, J.P.; Kang, P.H. The characterization of polyacrylonitrile fibers stabilized by electron beam irradiation. *Fibers and Polymers* **2012**, *13*, 724-728.

10. Yan, B.; Matsushita, S.; Akagi, K. An advanced method for preparation of helical carbon and graphitic films using a carbonization substrate. *Chemistry of Materials* **2016**, *28*, 8781-8791.

11. Chen, J.; Harrison, I. Modification of polyacrylonitrile (pan) carbon fiber precursor via post-spinning plasticization and stretching in dimethyl formamide (dmf). *Carbon* **2002**, *40*, 25-45.

12. Gupta, V.B. Solution-spinning processes. In *Manufactured fibre technology*, Gupta, V.B.; Kothari, V.K., Eds. Springer Netherlands: Dordrecht, 1997; pp 124-138.

13. Bahl, O.P.; Manocha, L.M. Characterization of oxidised pan fibres. *Carbon* **1974**, *12*, 417-423.

14. Shen, W.; Zhang, S.; He, Y.; Li, J.; Fan, W. Hierarchical porous polyacrylonitrile-based activated carbon fibers for co2 capture. *Journal of Materials Chemistry* **2011**, *21*, 14036-14040.

15. Xie, J.L.; Guo, C.X.; Li, C.M. Construction of one-dimensional nanostructures on graphene for efficient energy conversion and storage. *Energy & Environmental Science* **2014**, *7*, 2559-2579.

16. Peebles, L.H. *Carbon fibers: Formation, structure, and properties*. CRC Press: 1995.

17. Rahaman, M.S.A.; Ismail, A.F.; Mustafa, A. A review of heat treatment on polyacrylonitrile fiber. *Polymer Degradation and Stability* **2007**, *92*, 1421-1432.

18. Mittal, J.; Mathur, R.B.; Bahl, O.P.; Inagaki, M. Post spinning treatment of pan fibers using succinic acid to produce high performance carbon fibers. *Carbon* **1998**, *36*, 893-897.

19. Yusof, N.; Ismail, A. Post spinning and pyrolysis processes of polyacrylonitrile (pan)-based carbon fiber and activated carbon fiber: A review. *Journal of Analytical and Applied Pyrolysis* **2012**, *93*, 1-13.

20. Jain, M.K.; Abhiraman, A. Conversion of acrylonitrile-based precursor fibres to carbon fibres. *Journal of materials science* **1987**, *22*, 278-300.

21. Drzal, L.T.; Madhukar, M. Fibre-matrix adhesion and its relationship to composite mechanical properties. *Journal of Materials Science* **1993**, *28*, 569-610.

22. Bismarck, A.; Kumru, M.E.; Springer, J.; Simitzis, J. Surface properties of pan-based carbon fibers tuned by anodic oxidation in different alkaline electrolyte systems. *Applied Surface Science* **1999**, *143*, 45-55.

23. Cheng, T.H.; Zhang, J.; Yumitori, S.; Jones, F.R.; Anderson, C.W. Sizing resin structure and interphase formation in carbon fibre composites. *Composites* **1994**, *25*, 661-670.

24. Bacon, R.; Tang, M.M. Carbonization of cellulose fibers—ii. Physical property study. *Carbon* **1964**, *2*, 221-225.

25. Gibson, D.W.; Mcghee, K.B.; Stroup, R.C. Graphite cloth laminates. Google Patents: 1965.

26. Paris, O.; Zollfrank, C.; Zickler, G.A. Decomposition and carbonisation of wood biopolymers—a microstructural study of softwood pyrolysis. *Carbon* **2005**, *43*, 53-66.

27. Tang, M.M.; Bacon, R. Carbonization of cellulose fibers—i. Low temperature pyrolysis. *Carbon* **1964**, *2*, 211-220.

28. Strong, S.L. Small-scale heat-treatment of rayon precursors for stress-graphitization. *Journal of Materials Science* **1974**, *9*, 993-1003.

29. Chand, S. Review carbon fibers for composites. *Journal of Materials Science* **2000**, *35*, 1303-1313.

30. Kim, D.-Y.; Nishiyama, Y.; Wada, M.; Kuga, S. High-yield carbonization of cellulose by sulfuric acid impregnation. *Cellulose* **2001**, *8*, 29-33.

31. Huang, J.-M.; Wang, I.-J.; Wang, C.-H. Preparation and adsorptive properties of cellulose-based activated carbon tows from cellulose filaments. *Journal of Polymer Research* **2001**, *8*, 201-207.

32. Byrne, N.; Chen, J.; Fox, B. Enhancing the carbon yield of cellulose based carbon fibres with ionic liquid impregnates. *Journal of Materials Chemistry A* **2014**, *2*, 15758-15762.

33. Kilzer, F.J.; Broido, A. Speculations on the nature of cellulose pyrolysis. **1965**.

34. Lee, J.; Lee, B. A simple method to determine the surface energy of graphite. *Carbon letters* **2017**, *21*, 107-110.

35. Nakagawa, K.; Tamon, H.; Suzuki, T.; Nagano, S. Preparation and characterization of activated carbons from refuse derived fuel (rdf). *Journal of Porous Materials* **2002**, *9*, 25-33.

36. Scheirs, J.; Camino, G.; Tumiatti, W. Overview of water evolution during the thermal degradation of cellulose. *European Polymer Journal* **2001**, *37*, 933-942.

37. Trinh, T.T.; Vlugt, T.J.H.; Hägg, M.-B.; Bedeaux, D.; Kjelstrup, S. Simulation of pore width and pore charge effects on selectivities of co2 vs. H2 from a syngas-like mixture in carbon mesopores. *Energy Procedia* **2015**, *64*, 150-159.

38. Huang, X. Fabrication and properties of carbon fibers. *Materials* **2009**, *2*, 2369.

39. Herod, A.A.; Bartle, K.D.; Kandiyoti, R. Characterization of heavy hydrocarbons by chromatographic and mass spectrometric methods: An overview. *Energy & Fuels* **2007**, *21*, 2176-2203.

40. Zhu, J.; Park, S.W.; Joh, H.-I.; Kim, H.C.; Lee, S. Study on the stabilization of isotropic pitch based fibers. *Macromolecular Research* **2015**, *23*, 79-85.

41. Council, N.R. *High performance synthetic fibers for composites*. The National Academies Press: Washington, DC, 1992; p 148.

42. Yang, K.S.; Lee, D.J.; Ryu, S.K.; Korai, Y.; Kim, Y.J.; Mochida, I. Isotropic carbon and graphite fibers from chemically modified coal-tar pitch. *Korean Journal of Chemical Engineering* **1999**, *16*, 518-524.

43. Choi, Y.O.; Yang, K.S. Preparation of carbon fiber from heavy oil residue through bromination. *Fibers and Polymers* **2001**, *2*, 178-183.

44. ÖZEL, M.Z.; Bartle, K.D. Production of mesophase pitch from coal tar and petroleum pitches using supercritical fluid extraction. *Turkish Journal of Chemistry* **2002**, *26*, 417-424.

45. Edie, D.D.; Dunham, M.G. Melt spinning pitch-based carbon fibers. *Carbon* **1989**, *27*, 647-655.

46. Yang, C.Q.; Simms, J.R. Infrared spectroscopy studies of the petroleum pitch carbon fiber—i. The raw materials, the stabilization, and carbonization processes. *Carbon* **1993**, *31*, 451-459.

47. Bright, A.A.; Singer, L.S. The electronic and structural characteristics of carbon fibers from mesophase pitch. *Carbon* **1979**, *17*, 59-69.

48. Matsuhisa, Y.; Bunsell, A.R. 16 - tensile failure of carbon fibers. In *Handbook of tensile properties of textile and technical fibres*, Woodhead Publishing: 2009; pp 574-602.

49. Tang, M.Y.; Rice, G.G.; Fellers, J.F.; Lin, J.S. X-ray scattering studies of graphite fibers. *Journal of Applied Physics* **1986**, *60*, 803-810.

50. Yamada, K.; Fujii, H.; Takayanagi, M. The relationship between structure and viscosity of petroleum pitch in the process of mesophase formation. *Journal of Materials Science* **1986**, *21*, 4067-4070.

51. Park, S.-J.; Meng, L.-Y. Surface treatment and sizing of carbon fibers. In *Carbon fibers*, Springer Netherlands: Dordrecht, 2015; pp 101-133.

52. Wang, L.; Liu, N.; Guo, Z.; Wu, D.; Chen, W.; Chang, Z.; Yuan, Q.; Hui, M.; Wang, J. Nitric acid-treated carbon fibers with enhanced hydrophilicity for candida tropicalis immobilization in xylitol fermentation. *Materials* **2016**, *9*, 206.

53. Lu, Y.; Chen, J.; Cui, H.; Zhou, H. Doping of carbon fiber into polybenzimidazole matrix and mechanical properties of structural carbon fiber-doped polybenzimidazole composites. *Composites Science and Technology* **2008**, *68*, 3278-3284.

54. Zhang, X.; Pei, X.; Jia, Q.; Wang, Q. Effects of carbon fiber surface treatment on the tribological properties of 2d woven carbon fabric/polyimide composites. *Applied Physics A* **2009**, *95*, 793-799.

55. Rong, H.; Ryu, Z.; Zheng, J.; Zhang, Y. Effect of air oxidation of rayon-based activated carbon fibers on the adsorption behavior for formaldehyde. *Carbon* **2002**, *40*, 2291-2300.

56. Tong, Y.; Wang, X.; Su, H.; Xu, L. Oxidation kinetics of polyacrylonitrile-based carbon fibers in air and the effect on their tensile properties. *Corrosion Science* **2011**, *53*, 2484-2488.

57. Wang, Z.M.; Yamashita, N.; Wang, Z.X.; Hoshinoo, K.; Kanoh, H. Air oxidation effects on microporosity, surface property, and ch4 adsorptivity of pitch-based activated carbon fibers. *Journal of colloid and interface science* **2004**, *276*, 143-150.

58. Li, N.; Liu, G.; Wang, Z.; Liang, J.; Zhang, X. Effect of surface treatment on surface characteristics of carbon fibers and interfacial bonding of epoxy resin composites. *Fibers and Polymers* **2014**, *15*, 2395-2403.

59. Li, J. Interfacial studies on the ozone and air-oxidation-modified carbon fiber reinforced peek composites. *Surface and Interface Analysis* **2009**, *41*, 310-315.

60. Sun, J.; He, C.; Zhu, S.; Wang, Q. Effects of oxidation time on the structure and properties of polyacrylonitrile-based activated carbon hollow fiber. *Journal of Applied Polymer Science* **2007**, *106*, 470-474.

61. Park, S.-J.; Shin, J.-S.; Shim, J.-W.; Ryu, S.-K. Effect of acidic treatment on metal adsorptions of pitch-based activated carbon fibers. *Journal of Colloid and Interface Science* **2004**, *275*, 342-344.

62. Fathi, B.; Esfandeh, M.; Soltani, A.K.; Amraei, I.A. Effect of fiber acid treatment on the dynamic mechanical properties of unsaturated polyester/carbon fiber unidirectional composites. *Polymer-Plastics Technology and Engineering* **2011**, *50*, 564-567.

63. Tang, G.; Chang, D.; Wei, G.; Lu, H.; Yan, W.; Liu, B. The effect of arylboronic acid treatment of carbon fiber on the mechanical and tribological properties of pa66 composites. *Polymer-Plastics Technology and Engineering* **2012**, *51*, 329-332.

64. Xu, Z.; Chen, L.; Huang, Y.; Li, J.; Wu, X.; Li, X.; Jiao, Y. Wettability of carbon fibers modified by acrylic acid and interface properties of carbon fiber/epoxy. *European Polymer Journal* **2008**, *44*, 494-503.

65. Sharma, M.; Gao, S.; Mäder, E.; Sharma, H.; Wei, L.Y.; Bijwe, J. Carbon fiber surfaces and composite interphases. *Composites Science and Technology* **2014**, *102*, 35-50.

66. Ma, Y.; Wang, J.; Cai, X. The effect of electrolyte on surface composite and microstructure of carbon fiber by electrochemical treatment. *Journal of Physics & Astronomy* **2012**, *1*.

67. Ishitani, A. Application of x-ray photoelectron spectroscopy to surface analysis of carbon fiber. *Carbon* **1981**, *19*, 269-275.

68. Cao, H.; Huang, Y.; Zhang, Z.; Sun, J. Uniform modification of carbon fibers surface in 3-d fabrics using intermittent electrochemical treatment. *Composites Science and Technology* **2005**, *65*, 1655-1662.

69. G.J. Ehlert, H.A.S. International sampe technical conference *SAMPE Fall Technical Conference and Exhibition* **2010**.

70. Tiwari, S.; Bijwe, J.; Panier, S. Strengthening of a fibre-matrix interface: A novel method using nanoparticles. *Nanomaterials and Nanotechnology* **2013**, *3*, 3.

71. Xu, Z.; Huang, Y.; Min, C.; Chen, L.; Chen, L. Effect of γ-ray radiation on the polyacrylonitrile based carbon fibers. *Radiation Physics and Chemistry* **2010**, *79*, 839-843.

72. Burchell, T.D.; Eatherly, W.P. The effects of radiation damage on the properties of graphnol n3m. *Journal of Nuclear Materials* **1991**, *179*, 205-208.

73. Wan, Y.Z.; Wang, Y.L.; Huang, Y.; Luo, H.L.; Chen, G.C.; Yuan, C.D. Effect of surface treatment of carbon fibers with gamma-ray radiation on mechanical performance of their composites. *Journal of Materials Science* **2005**, *40*, 3355-3359.

74. Wei, G.; Fujiki, K.; Saitoh, H.; Shirai, K.; Tsubokawa, N. Surface grafting of polyesters onto carbon nanofibers and electric properties of conductive composites prepared from polyester-grafted carbon nanofibers. *Polym J* **2004**, *36*, 316-322.

75. Kim, B.-J.; Park, S.-J. A simple method for the preparation of activated carbon fibers coated with graphite nanofibers. *Journal of Colloid and Interface Science* **2007**, *315*, 791-794.

76. Ramanathan, T.; Bismarck, A.; Schulz, E.; Subramanian, K. Investigation of the influence of acidic and basic surface groups on carbon fibres on the interfacial shear strength in an epoxy matrix by means of single-fibre pull-out test. *Composites Science and Technology* **2001**, *61*, 599-605.

77. Montes-Morán, M.A.; Martínez-Alonso, A.; Tascón, J.M.D.; Young, R.J. Effects of plasma oxidation on the surface and interfacial properties of ultra-high modulus carbon fibres. *Composites Part A: Applied Science and Manufacturing* **2001**, *32*, 361-371.

78. Donnet, J.B.; Brendle, M.; Dhami, T.L.; Bahl, O.P. Plasma treatment effect on the surface energy of carbon and carbon fibers. *Carbon* **1986**, *24*, 757-770.

Chapter 3

Carbon nano tubes and Biochar: An overview.

3.1. Introduction

Carbon nanotubes (CNTs) are the most investigated carbon based nanomaterials today due to their exceptional electrical, thermal and mechanical properties. CNTs were first reported in by Sumio Ijima. [1] In literature two scientists Raudushkevish and Lukyanovich in 1952 referred CNTs as "carbon tubes" and in 1976 Oberlin, Endo and Koyama referred carbon nano tubes as 'hollow carbon fibers' and presented the first ever microscopic images of CNTs at a low magnification with a hollow instead of tubular structure of MWCNTs [2]. The term 'nano-tubes' for carbon nano tubes was first used by Wiles and Abrahamson in 1978. Hyperion Catalysis International, USA published a series of patents concerning the production and the use of 'nano-fibrils' in polymers as fillers in 1987 [3]. In the past two decades CNTs have been explored extensively to make use of their unique structural, mechanical, electrical, chemical and electromechanical properties in industrial applications [4-6]. The extraordinary properties of CNTs makes them an ideal material to be explored for a wide range of applications [7]. Particularly CNTs have been used as filler materials in composites to improve their properties and performance. Previously, glass fibre, alumina, boron, carbon fibres, and silicon carbide fibres has been used in composites as pseudo one-dimensional fillers. These fibers have mesoscale dimensions with lengths of order of millimeters and diameters of tens of microns while CNTs possess a diameter range of 1-100 nm and lengths up to millimeters [8] and a density as low as 1.3 g/cm3. These dimensions mean that CNTs have a

much larger surface area compared to that of conventional carbon fibers permitting much better interaction with matrix and very few defects in the final composite. CNTs have a Young's modulus in range of 100~1000 GPa and tensile strength of 2.5~3.5 GPa which further cement their place in the category of filler materials [9]. Marianne Reibold et al. discovered the dispersion of CNTs in the medieval time famous Damascus steel which was extraordinarily strong and flexible [10]. Diverse range of applications of CNTs are listed in the table 3.1 below.

Table 3.1: Application of CNTs .

Property	Applications
Strength, toughness, light weight	Sporting goods, Aviation industry, construction panels,
High dimensional stability, low coefficient of thermal expansion, low abrasion	Circuit boards, brakes, antennas, telescopes and optical benches.
Vibration damping	Audio devices, robotics
Electrical conductivity	Printed circuits, EMI shielding, Microwave adsorption, RFIDs.
Low biological reactivity, permeability with x-rays	Prostheses, medical equipment, tooth implants, ligament supports.
Fatigue resistance, Self-	Automobiles parts, as lubricant in pistons.

lubrication	
Low chemical reactivity, high corrosion resistance	Valves and seals, pump components
Electromagnetic properties	Electronic devices. Motor parts.

3.2. Classification of CNTs

CNTs exist in different structures and morphologies. The three main categories of carbon nano-tubes are single-walled nano-tubes (SWNTs), double-walled nano-tubes (DWNTs) and multi-walled nano-tubes (MWNTs). These three types are defined and described below.

- A single wall carbon nano tube (SWCNT) can be looked at as a rolled-up tubular shell of graphene sheets. SWCNTs are available in different sizes and diameters depending upon the end use and technique of manufacture. SWCNTs are generally available in the range of 0.7–2 nm in diameter and a length of up to 1 micron. They exhibit a tensile strength of approximately 200 ~ 300 GPa and an elastic modulus of 1 TPa.
- Double wall carbon nano tubes (DWCNT) are also known as a sub-class of MWCNT. A DWCNT can be looked at as made up of two concentric tubes of graphene rolled over one another and coupled through Vander Waals interaction between them. DWCNT are available with diameters in the range of 0.7 to 4 nm and 1 micron in length. DWCNT differ from SWCNT in Chirality. If the inner tube possess zigzag orientation the outer tube generally do not possess such orientation.
- In contrast, a multi-wall carbon nano tube (MWCNT) is composed of a set of coaxial SWCNTs of different radii as shown in the figure below. MWCNT always consist of nano-tubes with varying number of concentric cylinders ranging from a few to several tens. The separation between the graphene layers is 0.34 nm. MWCNTs are available in the sizes of 8~50 nm in diameter with lengths up to 12 μm. Their

maximum tensile strength is in the range of 150 GPa and an elastic modulus of 500 GPa.

Figure 3.1 : Types of CNTs.

The atomic structure of CNTs is defined by the chiral indices (n, m). The chiral indices are also used to define the primitive vector also named as the chiral vector of a carbon nano-tube. Diameter and helicity of CNTs are determined by their chiral indices. SWCNT can be classified into three types by taking in account chirality or chiral angle. The *(n, 0)* nanotubes with $\boldsymbol{\theta}=0$ are termed zig-zag nanotubes, *(n, n)* nanotubes with $\boldsymbol{\theta}=30°$ are called armchair and all other types of nanotubes with $(n \neq m \neq 0)$ and $0°<\boldsymbol{\theta}<30°$ are called chiral nanotubes as shown in figure 3.2. Chirality or flavor of the carbon nano-tube is determined by the direction in which the graphene sheet *is* rolled.

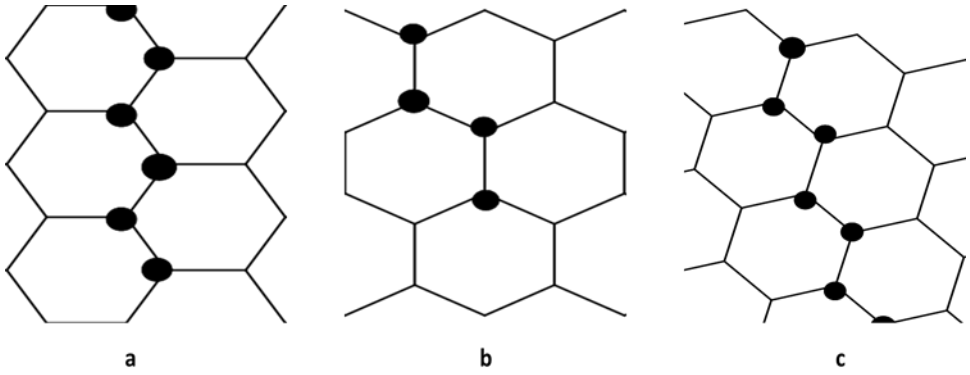

Figure 3.2: Chirality of CNTs, (a) zigzag, (b) armchair, (c) chiral.

3.3. Growth mechanism of CNTs.

A comprehensive understanding of the growth mechanism of CNTs is very important in designing the CNTs growth procedure and process tuning conditions. The way CNTs grow is yet to be precisely conceded. The catalytic growth route

for CNTs resembles to the conventional thin films deposition process on substrates through CVD. There may be more than one mechanism taking place during the CNTs growth [13]. A proposed model of CNT growth is excerpted from Sinnott's work [14]. Spherical or pear shaped metal particles are supported on a substrate or introduced through the gas flow into the reactor. The deposition of carbon takes place on the metal particle surface at the lower curvature spots. The carbon atoms diffuse through the concentration gradient and consequently precipitate on the other half. However, it does not precipitate on the top of the sphere.

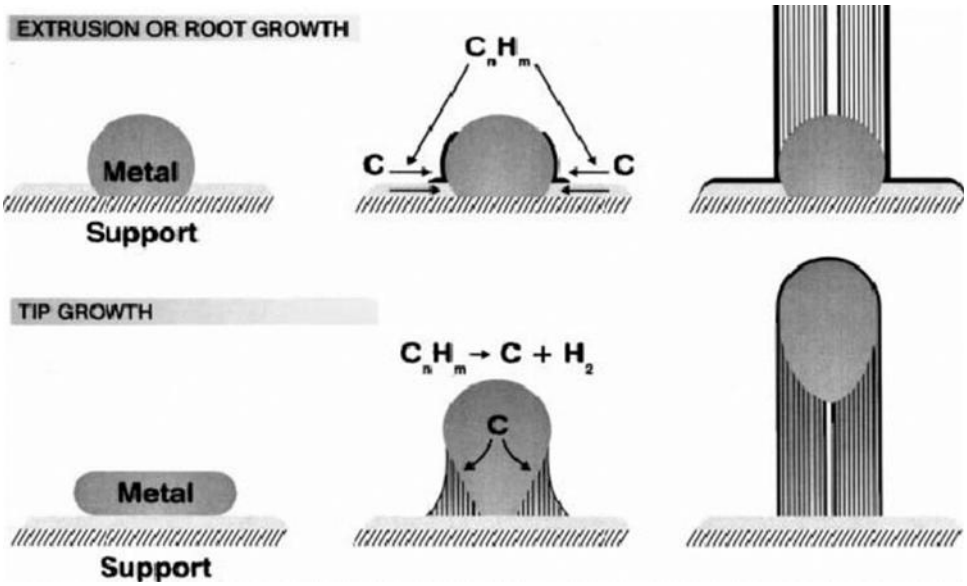

Figure 3.3 13: Mechanism for CNTs growth[14].

3.3.1. Synthesis of carbon nano tubes

Carbon nano-tubes can be synthesized by various processes. The three most widely used methods are visible light vaporization, catalytic chemical vapor deposition or simply chemical vapor deposition (CVD) and arc discharge[15]. The visible light method can be further classified into three separate methods of synthesis namely (1) laser ablation in which a pulsed laser is used to carry out the synthesis of carbon nano tubes, (2) continuous laser vaporization method, while in (3) solar vaporization method a continuous multi wavelength light from a solar furnace source is used to carry out the process. Other methods used to synthesize CNTs are flame synthesis; liquid hydrocarbon synthesis and catalytic plastic pyrolysis. These methods are not used for bulk production so they are of less significance compared to the widely used methods.

a. Arc discharge method

In the arc discharge method two flat sheets of graphite or, more commonly, two graphite rods, are placed under reduced pressure at a prefixed distance. One graphite rod is fixed while the other is movable. The movable graphite rod is fixed on a stage that is used to control the distance between the rods. The synthesis chamber is usually filled with argon, helium or a mixture of gases at a pressure around 500 Torr [16]. A potential of 20 V is set between the rods and the distance between the rods is reduced by moving the stage until an arc between the rods occur. The optimal distance between the rods is in the range of 1–3 mm and the current achieved is between 50~120 Amperes, while the anode surface temperature at this point is around 4000~6000^{o} C. The current achieved depends upon on the size of the electrodes and the pressure of the chamber along with other experimental variables[17]. Carbon sublimates in a temperature range of 2000^{o} C to 3000^{o} C.Current between the rods is a function of distance and the voltage between the rods. Production rate of the CNTs is approximately 50 mg/min which is indepandant of the rod diameter.Schematic diagram of the chamber is shown in the figure 3.4 below.

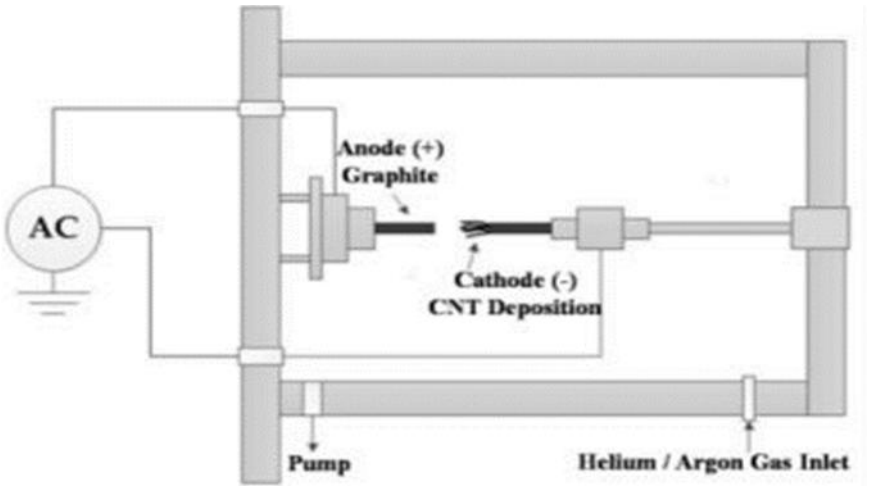

Figure 3.4 : Arc disharge method.

b. Laser ablation method

In laser ablation method a graphite block placed in an atmosphere of reduced pressure around 500 Torr and the temperature of the chamber maintained at around 1200^{o}C. The reaction chamber is illuminated by a high-intensity light source in the presence of Helium or Argon gas. Solid graphite is sublimated to

small particulates of carbon vapors and combine to form nano-tubes. A gentle flow of gas maintains the temperature gradient in the reaction chamber as well as carries the carbon particles in form of vapors [18]. The CNTs obtained by this technique have scalability problem along with high process cost and complicated set up of the system. The advantages of this technique are high quality of CNTs with low defects and high purity along with around 50% yield of carbon nano-tubes [19, 20].

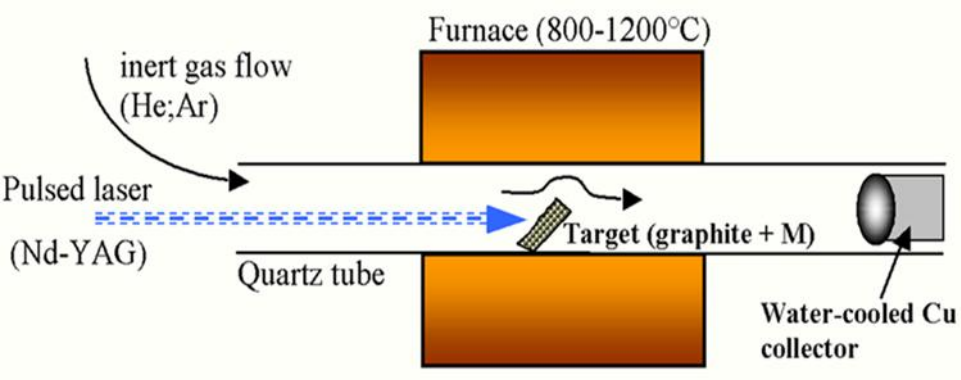

Figure 3.5 : Laser ablation technique.

c. Chemical Vapor deposition (CVD) method

In this technique gaseous hydrocarbon material are cracked thermally into carbon and other constituents like oxygen and hydrogen at a lower temperature in the presence of a catalyst belonging to transition metals group of the periodic table for example cobalt, iron or nickel and deposited on a support. The main difference in this technique is formation of carbon atom via the decomposition of carbon mono oxide or any carbon containing species rather than sublimation of graphite as done in the previous two techniques. The reaction is aided by a catalyst. In any of the cases mentioned above the metal catalyst particles are either carried on the surface by any non-reactive substrate such as alumina or silica or floating catalyst method is used to aid the synthesis. In floating catalyst method the metal particles are carried by a gas[21]. The main difference between this process and the processes used for the growth of vapor-grown carbon fibers is that much smaller metal clusters are used for the manufacture of carbon nano-tubes. Floating catalyst is used for the synthesis of single wall CNTs employing High-Pressure Carbon monoxide (HiPCO) method. In the HiPCO method, CO is decomposed using Iron particles catalyst clusters which are generated in situ by the decomposition of $Fe(CO)_5$ in continuously flowing CO at high pressure and

elevated temperatures [22]. Composition, morphology and preparation technique of the catalyst affect the quality of the final product. CVD method has been employed to synthesize carbon nano-tubes from a wide range of carbon containing species. Carbon monoxide is most commonly used because of the cost and simplicity. Cracking of CO should be at low temperature and this is a critical factor in this method because at high temperatures the metal clusters coalesce and as a result of coalescence carbon fibers are obtained instead of carbon nano-tubes. Other sources of carbon are methane, alcohols, benzene and acetylene. The carbon containing species is mixed with an inert gas either helium or argon for the better control of the reaction. The temperature of the reactor is always adjusted in a way that allows only the cracking of the carbon source instead of pyrolysis of the carbon containing species. For a given combination of the catalyst and gas mixture that is effective at producing carbon nano-tubes, MWCNT formation is favored at a lower temperature range of 700~800^{o} C and at a high temperatures range of 850 ~950^{o} C formation of SWCNTs is favored[23].

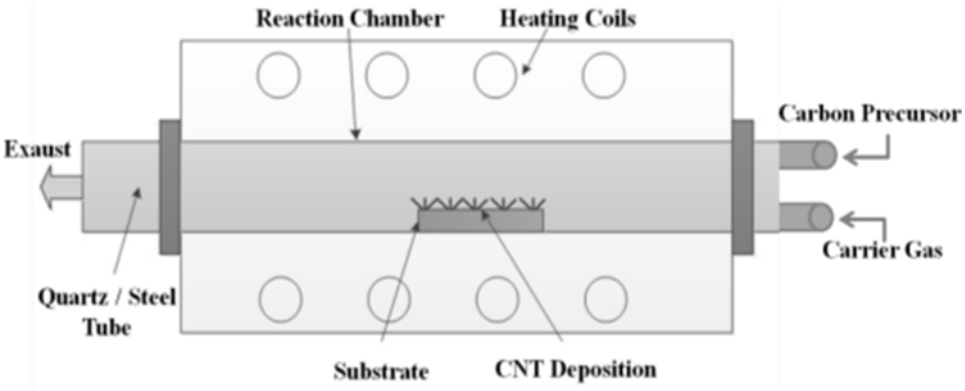

Figure3.6 : Chemical vapor deposition method.

3.4. Problems regarding CNTs.

Problems like anisotropy, defects in CNTs structure, high precursor and catalyst cost, low yield of CNTs, lack of standards and impact on health and safety undermine the full scale industrial applications of CNTs. In the coming chapter we propose a cheap precursor for the synthesis of carbon nano materials through CVD process and their applications in composites. A comparison will be made with commercial CNTs composites.

3.5. Biochar.

Biofuels and biomaterials have gained a lot of attention due their availability in abundunce in nature and eco friendly characteristics. The residue materials obtained after pyrolysing biomass and biogenic wastes under controlled environment is termed as a biochar [24]. Biochars can be used in various applications in diverse areas because they possess versatile physio-chemical properties. Some important area of applications are char gasification,energy production via combustion, activated carbon, soil remediation, carbon sequestration, catalysis, and in biomedical industry. Pyrolysis temperature and heating rates are the key factors that determine the biochar properties such as carbon yield, mineral phases, surface area, porosity, electrical conductivity etc. Biomass conversion technologies include thermochemical processes like torre-faction, pyrolysis, gasification,liquefaction and supercritical fluid etc. While the biochemical processes are also considered as methods to produce biochards. Some exemples of biochemical processes are anaerobic digestion and fermentation[25]. Biochar produced at low pyrolysis temperatures show high carbon yield, relatively higher levels of volatile left, good electrical conductivity and cation-exchange capacity as compared to biochar prepared at high temperatures. On the other hand high temperatures of pyrolysis confer a large surface area, micro porosity and high amount of aromatic carbon. Heating rate during the pyrolysis process determine the amount of char, gas and bio oil. Slow pyrolysis meaning heating for a few seconds or minutes at moderate to low temperatures and can be considered as a continuous process, while the fast pyrolysis refers to the heating of fine biomass particles blown through hot gases in confined oxygen-free chamber at elevated temperature for a very low residense time [26]. The rate of exhaustion of volatiles and gases from the furnace dictates the vapor residence time. Long residence time harvests secondary reactions with the notable reaction of tar on char surfaces, charring of the tar. Low char production has been sought traditionally as char was considered as a problematic low-value waste fraction. For this reason a research focus on fast pyrolysis which maximizes oil and also gasification. Slow pyrolysis is also known as conventional carbonization. It is carried out at a temperature range of 300~700^{o} C with a heating ramp rate of 0.1~1^{o} C/s.The residence time is set in the range of 10~100 minutes. On the other hand fast pyrolysis is carried out at a temperature range of 400~500^{o} C.The heating ramp rate is set at 10~200^{o} C/s with a very low residence time of the order of 30~1500 milliseconds [27].

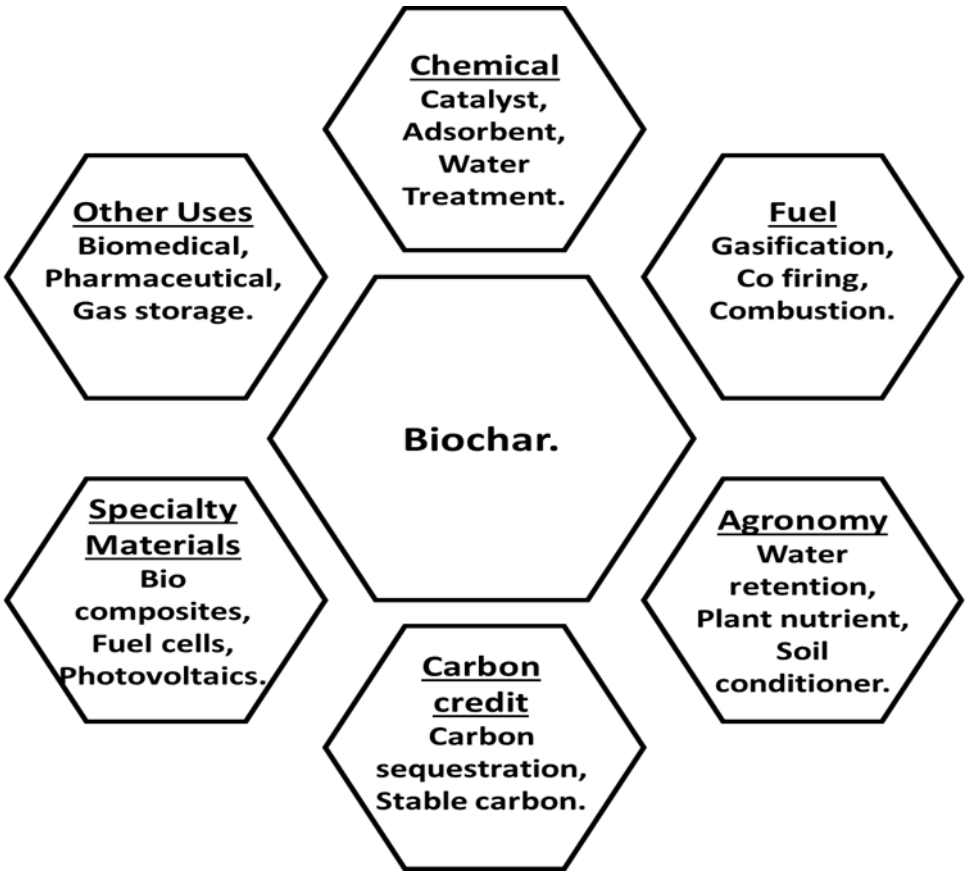

Figure 3.7 : Applications of biochar.

Biochar comprises of mainly carbon with traces of elements like lithium, Sodium, Potassium, Calcium, Magnesium and Barium [28]. The presence of metal particles give biochar the advantage over conventional coke derived from fossil fuel, in metallurgical processes [29]. Biochar may possess meso or micro pores.The type of porrosity depends upon the condtion of pyrolysis and the feedstock. In the thermochemical cracking of bio-oil, biochar is an effective catalyst [30]. Biochars possess high thermal stability and carbon yield the outcome of which is carbon sequestration [31]. These characteristics make the process eligible for carbon credits. Biochar possesses a versatile structure, elemental composition and reactivity.The characterisitcs make them eligbile for various applications in pharmaceutical and chemical industry and in agronomy as well. Biochar obtained after pyrolysis cannot be directly used for the fabrication of devices and structural parts. However they can be used in polymer composites. Das et al.[32] reported the use waste pine wood biochar to reinforce polypropylene matrix. A 24 wt. % of biochar filling was found suitable for improved mechanical properties. DeVallance et al. [33] also reported the use

hardwood biochar in polypropylene (PP) composites and reported the tailoring of different properties of matrix using different weight percentage of biochar. Ho et al.[34] demonstrated that the thermal, optical and mechanical properties of poly lactic acid (PLA) matrix can be improved by reinforcing with bamboo char. While Ayrilmis et al. [35] depicted the improved dimensional and bending properties of PP matrix using a mixture of two different biochars. Ahmetli et al. [36] reported the potential use of three different types of biochars to reinforce epoxy matrix. The reported studies above highlight the use of biochar as a cheap filler to reinforce polymer composites. Lehman et al. reported a schematic of biochar conversion process and application of the obtained char, bio-oil and gas in different areas [37].

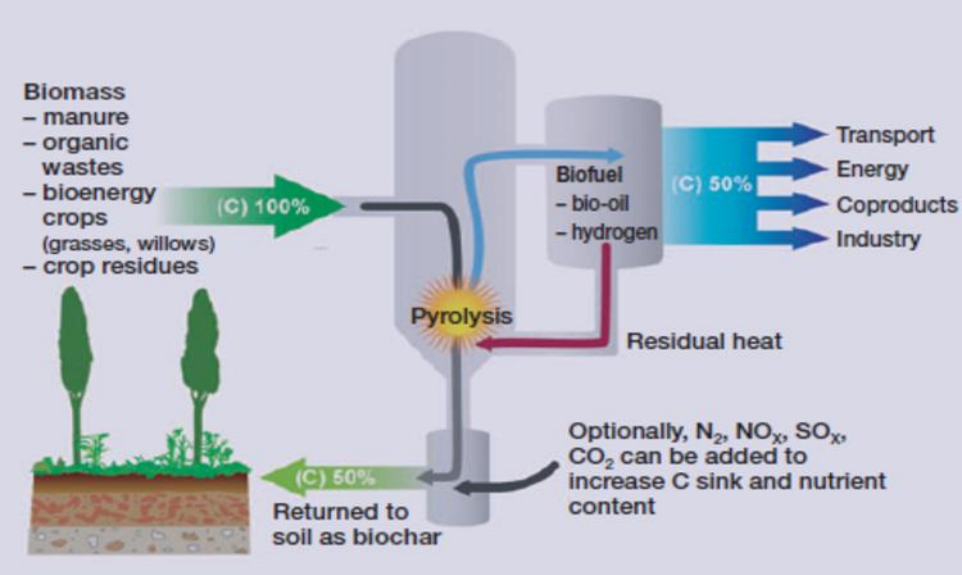

Figure 3.8 : Schematic of biochar production and application[37].

3.6. Summary

- The main aim of this chapter was to provide an overview of the techniques used to synthesize CNTs and highlight the issue of high cost of production of CNTs. In the coming chapter we will discuss the synthesis of CNTs with waste polyethylene precursor to reduce cost of production. We will also demonstrate the use of these CNTs to reinforce epoxy resin and compare with composites of commercial MWCNTs.

- Biochars are the material of the new age. The main advantage is the origin of the precursor from nature that is renewable and available in multi million tons. We will demonstrate the use of wood based biochar to improve the properties of various polymer properties.

3.7. References

1. Iijima, S. Helical microtubules of graphitic carbon. *Nature* **1991**, *354*, 56-58.
2. Oberlin, A.; Endo, M.; Koyama, T. Filamentous growth of carbon through benzene decomposition. *Journal of Crystal Growth* **1976**, *32*, 335-349.
3. Grady, B.P. *Carbon nanotube-polymer composites: Manufacture, properties, and applications*. John Wiley & Sons: 2011.
4. Pierson, H.O. *Handbook of carbon , graphite , diamond and fullerenes: Properties, processing and applications*. NOYES Publications: New Jersy, USA, 1993.
5. Meyyappan, M. *Carbon nanotubes science and applications*. CRC PRESS: London, 2005.
6. Dai, H. Carbon nanotubes: Opportunities and challenges. *Surface Science* **2002**, *500*, 218-241.
7. Loiseau; Launois, P.; Petit, P.; Roche, S.; Salvetat, J.P. *Understanding carbon nanotubes from basics to applications*. Springer: Berlin, 2006.
8. Saito, R.; Dresselhaus, G.; Dresselhaus, M.S. *Physical properties if carbon nanotubes*. Imperial College Press: London, 1998.
9. Salvetat, J.P.; Bonard, J.M.; Thomson, N.H.; Kulik, A.J.; Forr, L.; Benoit, W.; Zuppiroli, L. Mechanical properties of carbon nanotubes. *Applied Physics A* **1999**, *69*.
10. Reibold, M.; Paufler, P.; Levin, A.A.; Kochmann, W.; Patzke, N.; Meyer, D.C. Materials: Carbon nanotubes in an ancient damascus sabre. *Nature* **2006**, *444*, 286.
11. Pravin, J.; Khan, A.; Massimo, R.; Carlo, R.; Alberto, T. Multiwalled carbon nanotube–strength to polymer composite. *Physical Sciences Reviews* **2016**, *1*.
12. Qin, L.-C. Determination of the chiral indices (n,m) of carbon nanotubes by electron diffraction. *Physical Chemistry Chemical Physics* **2007**, *9*, 31-48.

13. Shewale, S.P.; Samdani, S.R.; Rane, N.M.; Deshpande, M.D. An overview on carbon nanotubes. *International Journal of Chemical Sciences and Applications* **2012**, *3*.

14. Sinnott, S.B.; Andrews, R.; Qian, D.; Rao, A.M.; Derbyshire, F. Model of carbon nanotube growth through chemical vapor deposition. *Chemical Physics Letters* **1999**, *315*

15. Catherine, J.; Matthieu, P.; Vincent, J. Carbon nanotube synthesis: From large-scale production to atom-by-atom growth. *Nanotechnology* **2012**, *23*, 142001.

16. Haufler, R.; Chai, Y.; Chibante, L.; Conceicao, J.; Jin, C.; Wang, L.-S.; Maruyama, S.; Smalley, R. Carbon arc generation of c 60. *MRS Online Proceedings Library Archive* **1990**, *206*.

17. Bethune, D.S.; Klang, C.H.; de Vries, M.S.; Gorman, G.; Savoy, R.; Vazquez, J.; Beyers, R. Cobalt-catalysed growth of carbon nanotubes with single-atomic-layer walls. *Nature* **1993**, *363*, 605-607.

18. Guo, T.; Nikolaev, P.; Thess, A.; Colbert, D.T.; Smalley, R.E. Catalytic growth of single-walled manotubes by laser vaporization. *Chemical physics letters* **1995**, *243*, 49-54.

19. Wang, X.; Li, Q.; Xie, J.; Jin, Z.; Wang, J.; Li, Y.; Jiang, K.; Fan, S. Fabrication of ultralong and electrically uniform single-walled carbon nanotubes on clean substrates. *Nano letters* **2009**, *9*, 3137-3141.

20. Guo, T.; Nikolaev, P.; Rinzler, A.G.; Tomanek, D.; Colbert, D.T.; Smalley, R.E. Self-assembly of tubular fullerenes. *The Journal of Physical Chemistry* **1995**, *99*, 10694-10697.

21. Cassell, A.M.; Raymakers, J.A.; Kong, J.; Dai, H. Large scale cvd synthesis of single-walled carbon nanotubes. *The Journal of Physical Chemistry B* **1999**, *103*, 6484-6492.

22. Kind, H.; Bonard, J.-M.; Forró, L.; Kern, K.; Hernadi, K.; Nilsson, L.-O.; Schlapbach, L. Printing gel-like catalysts for the directed growth of multiwall carbon nanotubes. *Langmuir* **2000**, *16*, 6877-6883.

23. Musso, S.; Fanchini, G.; Tagliaferro, A. Growth of vertically aligned carbon nanotubes by cvd by evaporation of carbon precursors. *Diamond and Related Materials* **2005**, *14*, 784-789.

24. Nanda, S.; Dalai, A.K.; Berruti, F.; Kozinski, J.A. Biochar as an exceptional bioresource for energy, agronomy, carbon sequestration, activated carbon and specialty materials. *Waste and Biomass Valorization* **2016**, *7*, 201-235.

25. Nanda, S.; Mohammad, J.; Reddy, S.N.; Kozinski, J.A.; Dalai, A.K. Pathways of lignocellulosic biomass conversion to renewable fuels. *Biomass Conversion and Biorefinery* **2014**, *4*, 157-191.

26. Sohi, S.P.; Krull, E.; Lopez-Capel, E.; Bol, R. Chapter 2 - a review of biochar and its use and function in soil. In *Advances in agronomy*, Academic Press: 2010; Vol. 105, pp 47-82.

27. Bridgwater, A.V. Principles and practice of biomass fast pyrolysis processes for liquids. *Journal of Analytical and Applied Pyrolysis* **1999**, *51*, 3-22.

28. Azargohar, R.; Nanda, S.; Kozinski, J.A.; Dalai, A.K.; Sutarto, R. Effects of temperature on the physicochemical characteristics of fast pyrolysis bio-chars derived from canadian waste biomass. *Fuel* **2014**, *125*, 90-100.

29. Briens, C.; Piskorz, J.; Berruti, F. Biomass valorization for fuel and chemicals production -- a review. In *International Journal of Chemical Reactor Engineering*, 2008; Vol. 6.

30. Majerski, P.; Piskorz, J.; Radlein, D. Energy efficient liquefaction of biomaterials by thermolysis. Google Patents: 2001.

31. Ekström, C.; Lindman, N.; Pettersson, R. Catalytic conversion of tars, carbon black and methane from pyrolysis/gasification of biomass. In *Fundamentals of thermochemical biomass conversion*, Overend, R.P.; Milne, T.A.; Mudge, L.K., Eds. Springer Netherlands: Dordrecht, 1985; pp 601-618.

32. Das, O.; Sarmah, A.K.; Bhattacharyya, D. Biocomposites from waste derived biochars: Mechanical, thermal, chemical, and morphological properties. *Waste Management* **2016**, *49*, 560-570.

33. DeVallance, D.B.; Oporto, G.S.; Quigley, P. Investigation of hardwood biochar as a replacement for wood flour in wood–polypropylene composites. *Journal of Elastomers & Plastics* **2016**, *48*, 510-522.

34. Ho, M.-p.; Lau, K.-t.; Wang, H.; Hui, D. Improvement on the properties of polylactic acid (pla) using bamboo charcoal particles. *Composites Part B: Engineering* **2015**, *81*, 14-25.

35. Ayrilmis, N.; Kwon, J.H.; Han, T.H.; Durmus, A. Effect of wood-derived charcoal content on properties of wood plastic composites. *Materials Research* **2015**, *18*, 654-659.

36. Ahmetli, G.; Kocaman, S.; Ozaytekin, I.; Bozkurt, P. Epoxy composites based on inexpensive char filler obtained from plastic waste and natural resources. *Polymer Composites* **2013**, *34*, 500-509.

37. Lehmann, J. Bio-energy in the black. *Frontiers in Ecology and the Environment* **2007**, *5*, 381-387.

Chapter 4

Functionalization of commercial carbon fibres

4.1. Introduction

Carbon fibres (CF) are important for a wide range of applications. Among them, composites with CF have a great impact on industrial applications. Aircraft, automotive, civil applications, sporting equipment industries are some of the important industries. Low weight, thermal stability, and better mechanical properties of CF make it an ideal material in composites [1-3].

The link between CF surface and polymer plays a key role for achieving the high performances of the composites. A good adhesion between CF and polymer need to achieve a good chemical bonding with better load transfer. A good CF surface adhesion in composite is difficult to achieve by using untreated CF. It shows weak surface link in composite. This limits the performances of CF filled composites [4, 5]. Commercially, various surface treatments are in use to vary the CF surface. These include sizing, heat treatments, nano-structure decoration, chemical functionalization, and surface alteration by plasma radicals [6-9]. The sizing involves the deposition of protective layer on CF surface. Polymer thin films, such as epoxy, urethane, or polyester use a sizing agent to coat the CF surface [10]. The deposition of polymer layer usually has a thickness of a few nanometres. The thickness is obtained by wet processes where the CF is dipped in organic solutions. The CF gains about 1 % in weight. Literature study explains the effect of sizing in increasing the CF adhesion in composite [11, 12]. The other types of surface treatments are able to modify the physio-chemical properties of

CF without adding new material on the surface. Surface treatments may produce morphological changes on the CF surface. It reflects by increasing the surface roughness, or producing some physical patterns. They may change surface chemical properties by introducing new chemical groups on the topmost atomic layer of surface. These effects provide with a single or sequence of treatments [9].

The surface modification techniques of CF are classified in two categories, oxidising and non-oxidising treatments. Common air, oxygen (O2), and carbon dioxide (CO2) are using extensively for CF surface oxidation. These treatments are applied at various temperatures ranging from room temperature to several hundreds of °C. High temperature surface treatments are usually characterised by a noticeable weight loss of the treated CF.

Another widely used oxidising surface treatment is anodic oxidation. The treatment is based on the use of an electrochemical bath where the CF acts as anode. Some examples of electrolytes are sulphuric acid, nitric acid, potassium nitride, sodium chloride [9, 10]. Non-oxidising surface treatments include the growth of carbon-based layer on the CF surface. Plasma aided polymerisation, polymer grafting on CF surface are some examples. Whiskerization method for growth of inorganic crystalline thin films has been tested to improve surface characteristics. Silicon nitrides (Si3N4), titanium dioxide (TiO2), silicon carbide (SiC) were studied for the deposition [13].

Recently plasma treatments are found to be effective in improving the surface activity of carbon fibres. Apart from that plasma surface modification techniques have several advantages. Firstly, Plasma assisted surface modification is strongly limited to alteration of the 1st few atomic layers. It exerts limited influence on the bulk structure of the fibres. This feature is very important, since it prevents the risk to alter the mechanical properties of fibres that may degrade its performance. Moreover, the changes on the CF surface by plasma can be applied at low or even room temperature, thus reducing the process time, the energy required, and the cost of the process. Also the chemicals needed to perform the plasma assisted surface modification are mostly inert gases like argon, helium, nitrogen, or oxygen. This not only reduces the safety concerns but also the cost concerned with the disposal of dangerous chemicals [14-16].

Plasmas are divided in thermal and non-thermal (cold) plasmas[17]. The former are characterized by the fact that kinetic energies of all the plasma components, electrons, ions and neutral particles, are very similar. These plasmas

typically show a high overall temperature. They are rarely used for surface modification processes. A very high electron kinetic energy characterizes cold plasmas [18]. The energy of ions and neutrals is typically lower by several orders of magnitude. This is possible since only a small fraction of the gas molecules are ionized, typically 10^{-6} to 10^{-4}, and since the huge mass difference between the electrons and the molecules makes the energy transfer between them very inefficient. Cold plasmas are thus characterized by the presence of high-energy electrons that are able to activate chemical reactions, which normally could happen only at high temperatures. In fact, electrons provide the dissociation of the gas molecules, thus producing the chemically active radicals that are needed to exert a chemical action on the surface to be treated. Plasma assisted processes are usually divided in two main types. It is depending on if the plasma is produced at low pressure or at atmospheric pressure. In the former case, the processes are referred to as vacuum plasma, or Reduced or Low Pressure Plasma (RPP. LPP), while in the latter case they are called Atmospheric Pressure Plasma (APP). Vacuum plasma processes are more versatile. Use of vacuum technology allows the complete removal of air from the vacuum chamber before the process starts. It avoids contamination of the plasma by the atmospheric molecules. This feature allows the use of a wide range of gases and a very precise control of the chemical reactions involved in the process. Moreover, the process pressure varies in a considerable range, usually from a few Pa to a few kPa. This feature is relevant, since the plasma pressure has a strong impact on the effects that are exerted on the surface in contact with the plasma [19]. Reducing the gas pressure allows the use of lower electric bias to light the plasma, thus reduced electrical power required. This advantage is compensate by the energy require to create the vacuum. Atmospheric pressure plasma, on the other hand, is more limited as for the types of gas that can be used. Since it is practically impossible to avoid their interaction with the oxygen in air. They also require much intense electrical bias to obtain the plasma, typically several kilovolts, thus requiring more expansive electric power generators. The main advantage of APP processes, that often overcomes their intrinsic limitations, is that they can be applied in open air in industrial production lines, while reduced pressure processes can only be applied as batch processes in industrial applications. This is a great advantage, since the application to industrial production lines drastically reduces both process time and cost. APP processes are thus usually preferred for the industrial application. While reduced pressure processes are often used when a more strict control on the process condition is required, as in research.

In the framework of the FIBRALSPEC project, RF plasma processes at reduced pressure was employed to study surface functionalization of commercial carbon fibres at Politecnico di Torino and suggest it as a surface modifying treatment for the in house generated lignin based CF.

4.2. Selection of suitable substrates for functionalization studies

To study the effects of plasma treatments on CFs the following types of carbon fibres were used.

4.2.1. T700 commercial carbon fibres

T700SC-12K-50C were purchased from Toray Corporation, Japan. The details of the CF is as described on the website of Toray are as displayed in figure 4.1.

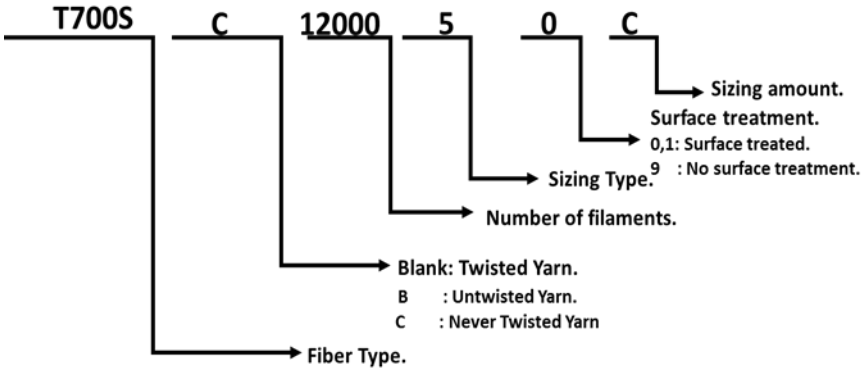

Figure 4.1 : Détails of T700 commercial carbon fibres.

T700S is a carbon fibre that contains 0 twist, tow comprises of 12000 filaments, it is surface treated and contains 1% of epoxy/ phenolic/ polyester/vinyl ester sizing agent by weight.

4.2.2. Lignin based in house prepared CF.

Lignin based carbon fibres were obtained from NTUA, Greece. These fibres were designated as in house generated carbon fibres.

4.3. Characteristics of Low pressure plasma system

In the framework of FIBRALSPEC project, the reduced pressure plasma treatments were applied on carbon fibres at Politecnico di Torino using a commercial barrel reactor laboratory plasma system (Plasmafab 508). The system is suitable for the application of plasma treatments based on inert gases, such as argon (Ar.), nitrogen (N2) or helium (He.).The plasma treatments also based on oxidizing gases, such as oxygen (O2). Both planar and tri dimensional samples can be treated. The system, shown in the figure 4.2, is composed by a steel vacuum chamber, electrically grounded, and a barrel grid electrode, coaxial with one of the horizontal axis of the chamber. The RF bias at 13.56 MHz is applied between the electrode and the grounded chamber walls. The vacuum chamber is pumped by a rotary vane pump, able to provide a minimum base pressure of about 1 Pa (10-2 mbar), while the plasma treatment is applied at a pressure of about 10-50 Pa (1-5 10-1 mbar). Two separated mass flow controllers allow to generate Ar or O2 plasma discharges.

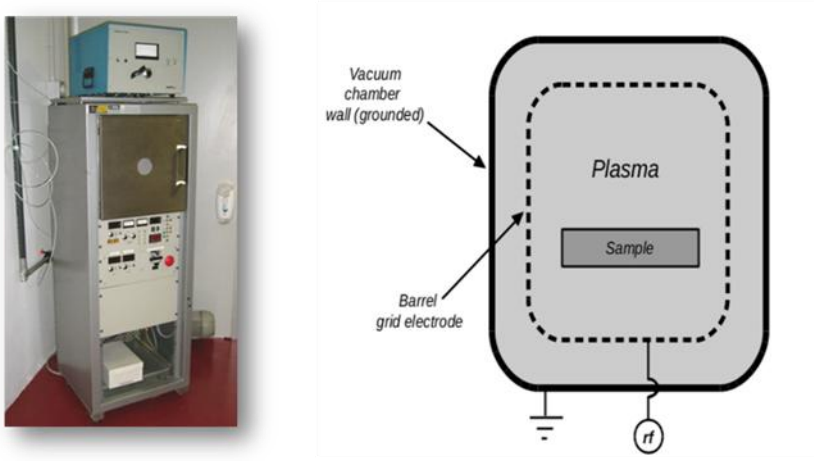

Figure 4.2 : Plasma Fab 508.

The barrel configuration is designed to minimize the ion bombardment on the samples, while enhancing the chemical action provided by the radicals, thus producing an isotropic etching effect. In fact, the discharge is activated between the inner electrode (RF biased) and the chamber walls (grounded), so the acceleration of ions is directed mainly on the electrode and on the walls, on which they are absorbed. The neutral radicals produced by the dissociation of gas molecules are free to move in the inner region of the reactor, thanks to the grid

structure of the barrel electrode. Thus, they can reach the sample, on which they produce their chemical etching effect.

The following process parameters can be tuned by the operator in order to optimize the results.

- Mass flow rate of the gases injected in the vacuum chamber;
- RF power applied by the generator to the grid electrode;
- Duration of the treatment.

The process pressure is not independently controllable, but depends on the mass flow rates of the gases injected in the reactor, following this relation.

$p=Q/S$

Where

- p is the total pressure in the chamber,
- Q is the throughput of the gas mixture injected in the vacuum chamber,
- S is the effective pumping speed provided by the pumping system.

4.4. Design of experiments.

After careful literature survey we decided to functionalize the different carbon fibres in O2 environment for a time in the range 1 ~ 10 minutes at a constant gas flow rate of 250 SCCM at a power of 100 and 200 W at 40 Pa chamber pressure. Surface morphology, amount of oxygen on the surface of the carbon fibres and mechanical properties of the fibres after treatment are the important parameters to be taken into considerations before selecting any treatment. Summary of the design of the experiment is shown in table 4.1.

Table 4.1: Design of experiments.

S/no.	Material	Reagent	Treatment time (min)	Power (W)	Gas flow rate (SCCM)
1	T700 Pristine	O_2	1, 3, 5, 10	100 , 200	250
2	Thermally cleaned T700	O_2	1, 3, 5, 10	100 , 200	250
3	Chemically cleaned T700	O_2	1, 3, 5, 10	100 , 200	250
4	Lignin based Carbon fibres	O_2	1, 3, 5, 10	100 , 200	250

4.5. Procedure for the treatment of carbon fibres by RF Reduced Pressure Plasma.

Sample preparation was carried out using the following standard operating procedure to ensure reproducibility.

1. Clean the working table and the tools (for example tweezers, tongs, scissors, glass slides etc.).
2. Use Nitrile gloves to keep hands safe and the tools and sample free from contamination.
3. Take out the carbon fibres from the container with the help of tweezers under the standard air blowing hood with care.
4. Cut a small piece of carbon fibres of suitable length and place them on the glass slide. Make sure the fibres are and remain in a flat and stretched position on the glass slide.
5. Switch on the power of the Plasma Fab 508 machine and open the gas supplies. Make sure all the valves are opened and functioning properly as shown in figure 4.3.
6. Run the plasma operation for 5 minutes with oxygen gas at low plasma power without any specimen in the plasma chamber to clean the lines and the plasma chamber.

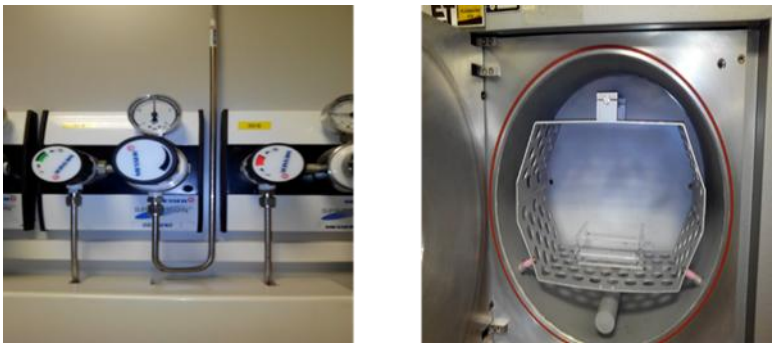

Figure 4.3 : Gas controls and plasma chamber.

7. Place the samples in the plasma chamber as shown in figure 4.4a and close the door of the chamber.
8. Tune the plasma power, gas flow rate and treatment time from the controls of the machine as shown in figure 4.4b.

Figure4.4 : (a) Sample placement, (b) controls of Plasma Fab 508.

9. Push the "start" button and then wait until machine finishes the treatment and gives the "time out" signal.
10. Push the "stop" button and then push the "vent" button as shown in figure 4.5. After treatment keep the samples in a clean and air tight containers.

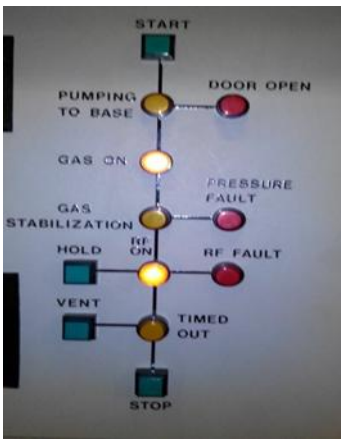

Figure 4.5 : Process controls interface.

11. Repeat the process for next samples.
12. Avoid unnecessarily handling of the fibres.

4.6. Characterizations after plasma treatments

4.6.1. Morphology of T700 commercial carbon fibres.

Morphology of the pristine and plasma treated CFs was studied through Field emission scanning electron microscopy (FESEM) with the following technical specification.

1. Nominal resolution: 1.5 nm at an applied voltage of 10KV and WD= 2mm.
2. Acceleration voltage: 0.1 ~30 KV.
3. Probe current: 4 p Amp ~10 n Amp.
4. Magnification: 12 ~900,000 X.
5. Sample holder: 9 slots.
6. Sample dimensions: $1cm^2$.
7. Working distance: 1~50 mm.

Figure 4.6 : FESEM MERLIN.

Layer of the sizing agent can be clearly seen on the surface of the pristine carbon fibres. Upon plasma treatment the surface layers get etched by the plasma elements. Sample treated at 100 W, 5 min (see fig.4.7b) shows very little signs of plasma etching. The top surface layer formed by the sizing agent remain intact with few marks and scratches. Increasing the time to 10 minutes at 100 W plasma power scrape the polymer layer further. Pits and grooves can be seen on the surface of the CF. At 200 W for 5 minutes we see well-formed pits on the surface of CF destroying the top sizing layer and exposing the carbon fibre surface. The chemical groups formed on the surface of the CF were studied with X-Ray photoelectron microscope.

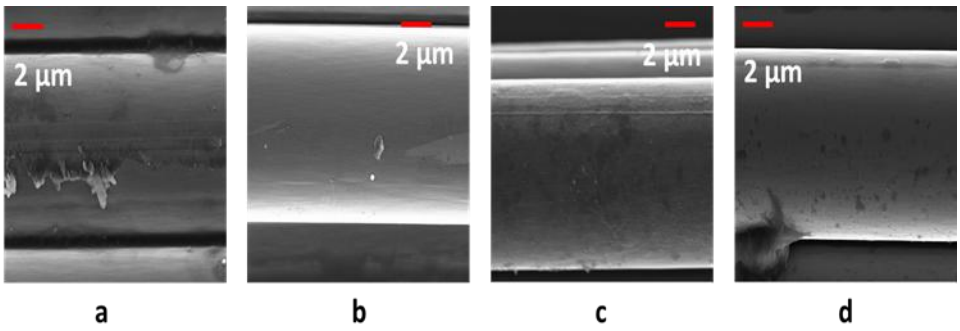

Figure 4.7 : (a) Pristine T700, (b) 100 W; 5min, (c) 100 W; 10min, (d) 200W; 5 min

4.6.2. X-Ray Photoelectron microscopy.

X-Ray Photoelectron Spectroscopy (XPS) was carried out using a PHI 5000 Versa Probe (Physical Electronics) system. The X-ray source was a monochromatic Al Kα radiation (1486.6 eV). A spot size of 100 µm was used in order to collect the photoelectron signal for both the high resolution (HR) and the survey spectra. Different pass energy values were exploited: 187.85 eV for survey spectra and 23.5 eV for HR peaks. The semi-quantitative atomic compositions and deconvolution procedures were obtained using Multipack 9.6 dedicated software. All core level peak energies were referenced to C1s peak at 284.5 eV (C-C) and the background contribution has been subtracted by means of a Shirley function.

Figure 4.8 : PHI 5000VersaProbe instrument.

Survey spectra after 20 scans, for pristine carbon fibres and plasma treated CF is shown in figure 4.9. All the specimen possess relative C1s, O1s, N1s peaks and impurities like Ca2p and Si2p peaks. Relative atomic concentration was evaluated after subtracting the background with a Shirley function, and the O/C ratio was calculated. Atomic percentage of all the elements with 5% error bar is reported in table 4.2.

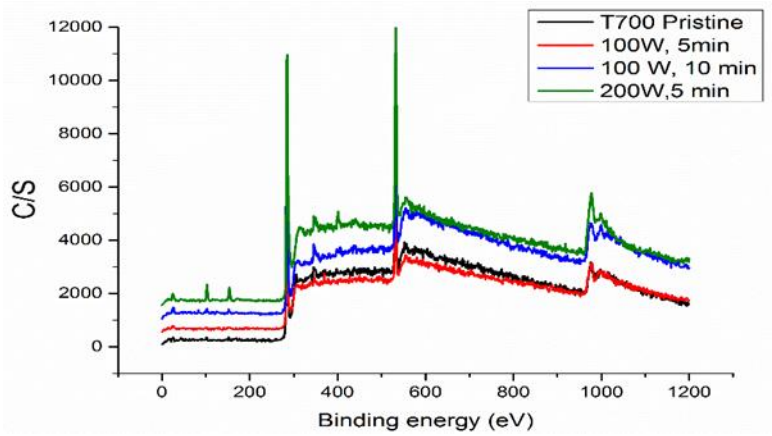

Figure 4.9 : Survey spectra of pristine and plasma treated CFs.

Table 2.2: Survey spectra comparison of pristine and plasma treated carbon fibres with 5% error bar in atomic %age.

Survey spectra.						
Sample Id.	**C1s**	**O1s**	**Si2p**	**N1s**	**Ca2p**	**O1s/C1s**
Pristine CF	80.3	17.7	0.7	0.6	0.8	0.22
5 min, 100 W	76.4	22.5	0.6	0.5	0	0.29
10 min, 100 W	72.5	25.6	1.2	0	0.7	0.35
5 min, 200 W	71.5	26.6	1.5	0	0	0.37

From table 4.2 we see that after plasma treatment the amount of oxygen on the carbon fibres surface increases and so do the O/C ratio. Highest oxygen take up was shown by the sample treated at 200 W for 5 minutes. The nature of the functional groups formed was further studied by high resolution spectra C1s with 50 scans on each specimen and then fitting the obtained data in multi pack software. A typical example of high resolution spectra and fitting with Gaussian-Lorentzian sum function is shown in figure 4.10. Assignation to each chemical shift has been done according to Briggs chemical shift table [20].The atomic percentage of C-C bonds on the surface of carbon fibres decreases while the oxygen containing functional groups at their relative binding energies of 286 eV and 288 eV increases. The atomic percentage of all the functional groups calculated from fitting the H.R spectra is reported in table 4.3 with 5% error bars in the calculated values. At higher power of 200 W the amount of C-C bonds again increases probably due to the sizing layer being peeled off by the plasma

elements and exposing top layer of carbon fibres. This effect can further be seen in the SEM images (fig. 4.7 d).

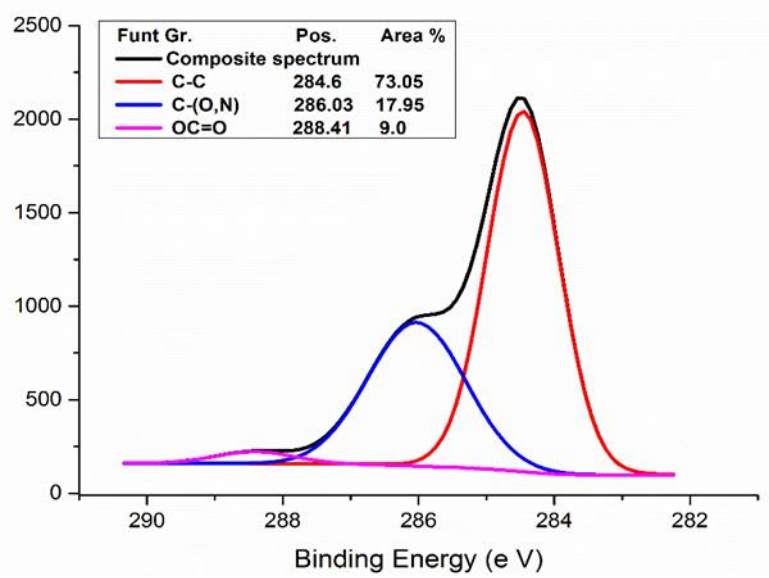

Figure 4.10 : H.R spectra of pristine carbon fibres fitted with Gaussian-Lorentzian sum function.

Table 4.3: Functional groups comparison of pristine and plasma treated CF with 5% error bars.

HR Spectra C1s					
S/no.	**Bond type**	**Pristine CF**	**5 min, 100 W**	**10 min, 100 W**	**5 min, 200 W**
1	C-C	73.05	65.5	52.6	59.0
2	C-O	17.95	32.3	47.4	36.1
3	O=C-O	9.0	2.2	Weak signal	4.9

4.7. Cleaning of the fibre surface and study of the plasma treatment effects.

In order to remove the sizing agent these carbon fibres were heat treated at 300^{o} C in nitrogen environment for 1 hour in a furnace. We can see from the SEM images that most of the sizing agent is decomposed due to heat treatment and a small amount is still clinging to the fibre surface. Heat treatment of the carbon fibres provide enough bare surface to be studied through plasma treatment. Also

the commercial carbon fibres were cleaned by washing with acetone bath for 5 cycles in soxhlet extraction method. The fibres obtained after surface cleaning in both the processes were then treated with low pressure oxygen plasma following the same design of experiment as mentioned in table 4.1. A comparative study was made as elaborated below.

4.7.1. Morphology before and after treatment.

After plasma treatment the top surface of the CF is abraded due to the action of the plasma radicals, forming pits, holes and canals on the surface of the fibres. Sample treated at 100 W, 5 minutes show little surface damage for both techniques of cleaning the fibres. The SEM images clearly shows the impact of plasma elements on the fibre surface. 10 minutes at 100 W and 5 minutes at 200 W of plasma treatment modifies greatly the surface of the CF. The surface of fibres show scratches and small pits caused by the plasma radicals and etching of the few surface layer as well as shown in the SEM images (fig. 4.11 c & d). The change in the fibre surface is in conformance to the literature reported on the plasma treatment of the carbon fibres. The change in morphology contributes to enhanced surface adhesion with the matrix that leads to improved mechanical properties [14, 21, 22].

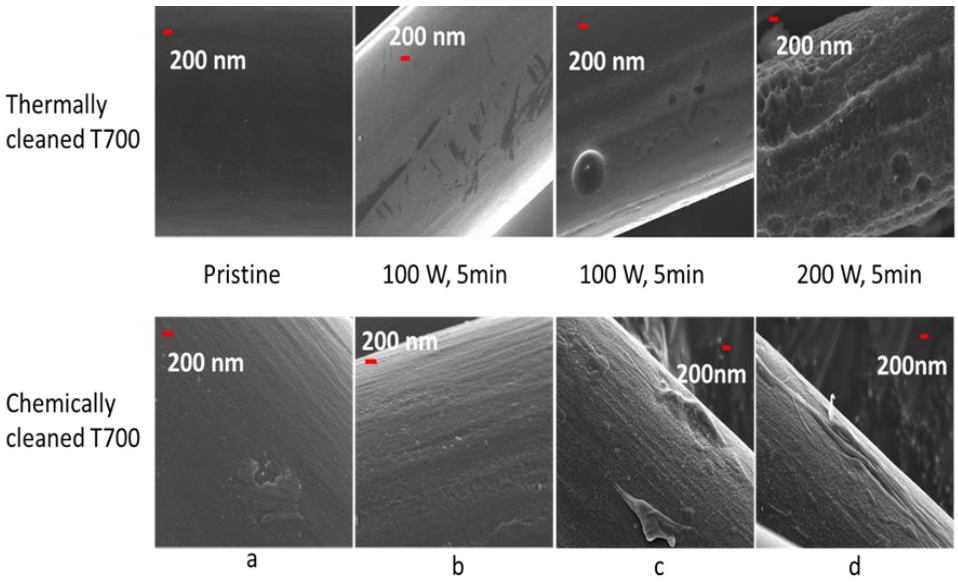

Figure 4.11 : Morphology analysis before and after plasma treatment.

4.7.2. X-ray Photo electron Spectroscopy (XPS).

The plasma treated carbon fibres were characterized with X-ray photo electron spectroscopy to study the chemical nature of the oxygen containing functional groups formed on the surface. Atomic percentage of the different elements calculated from the survey spectra of the pristine and plasma treated carbon fibres is reported in table 4.4 below with a 5 % error bar in the atomic content. The amount of oxygen varies in the pristine, cleaned and plasma treated fibres. The as received carbon fibres contain 17.7 % of oxygen which may arise from the sizing agent and the surface treatments carried out on the fibre during manufacturing. Thermal cleaning reduces the amount of oxygen on the surface of the carbon fibres. Chemical cleaning further decreases the amount of oxygen on the surface of carbon fibres probably by cleaning the sizing agent and the oxygen containing functional groups. After plasma treatment the amount of oxygen on the surface of the carbon fibres increases as reported in table 4.4. The thermally cleaned carbon fibres pick up around 42% oxygen while the chemically cleaned CF pick up around 77% oxygen compared to their respective counterparts. When the treatment power was doubled the amount of oxygen decreases on the surface of the fibres probably due to etching reaction of the plasma radicals on the fibre surface which destroys the functional groups along with the top surface layers of the carbon fibres as shown in figure 4.11.

Table 4.4: Elemental composition from survey spectra of cleaned and plasma treated CFs with 5% error bar in atomic %age.

Sample id	C1s	O1s	N1s	O/C	N/C
T700	81.5	17.7	0.8	0.21	0.01
T700 thermally cleaned.	83.5	16.1	0.4	0.19	0.005
100 W,5 min	74.6	22.9	2.5	0.30	0.03
200 W, 5min	74.9	22.8	2.3	0.30	0.03

T700 chemically cleaned	87.4	11.5	1.1	0.13	0.01
100 W,5 min	75.7	20.4	3.9	0.26	0.05
200 W, 5min	80.6	16.7	2.7	0.20	0.03

The atomic content of the different functional groups inferrered from the high resolution spectra C1s with a 5% error bar after 50 scans is reported in table 4.5. After functionalization with low pressure oxygen plasma the carbon fibres show the presence of functional groups like alcohols, carboxyl and carboxylic acid on the surface. The amount of C-C bonds decreases at 100 W treatment and then remains almost unchanged on increasing the power to 200 W in the thermally cleaned carbon fibres. The chemically cleaned carbon fibres show a different trend where the amount of C-C bonds 1st decreases and then increases at higher plasma powers. This effect is probably due to the ablation of the top surface layers of the CF due to the action of plasma elements which can be seen clearly in the SEM images (see figure 4.11). The oxygen containing functional groups like alcohols and carboxylic acid continue to increase at higher plasma powers. The π–π^* (HOMO–LUMO) component which is a characteristic shake-up line (satellite peak located at ~6 eV from sp2 peak) for carbon in aromatic compounds (e.g. aromatic rings) is generated by the ring excited by the exiting photoelectrons. This feature is the fingerprint of extended delocalized electrons in the material and it is present in graphitic material such as HOPG (Highly Oriented Pyrolytic Graphite) [23] , rGO (reduced Graphene Oxide) [24], CNT (Carbon Nano Tube) [25]. The π–π^* bonds amount increase with increase in the plasma power as reported in table 4.5. This increase is probably due to the exposure of the core layers of carbon fibres after plasma treatment. Similar studies have been reported by Park S.J et.al 2005 & 2015 [8, 10]. These functional groups formed on the fibre surface improved interaction with matrix and enhance the composite properties [9, 26-28]. The interaction of the functional groups with the matrix is further explained in the wettability test section.

Table 4.5: High resolution spectra C1s of cleaned and plasma treated CFs.

sample id	C-C	C-O/O-C-N	C=O	-O-C=O	π–π*
T700 thermally cleaned.	81.19	15.62	Weak signal	3.19	Weak signal
100 W,5 min	66.09	14.57	Weak signal	9.51	3.29
200 W, 5min	65.70	19.42	Weak signal	10.40	4.74
T700 chemically cleaned	62.07	25.10	4.30	4.64	3.89
100 W,5 min	65.60	11.63	10.26	9.04	3.48
200 W, 5min	68.34	13.51	7.88	6.31	3.96

Since the thermal cleaning method can affect the quality of the carbon rings on the surface layers of the CF, so only chemically cleaned CF were chosen for further analysis.

4.7.3. Raman spectroscopy.

The structural quality of the carbon fibres and the effects of the plasma treatment were studied with Raman spectroscopy using a Renishaw ® Ramanscope InVia H43662 model equipped with a green laser source (λ=514 nm). Raman spectra of the pristine and plasma treated CF are reported in figure 4.12b. The pristine and treated CF show the characteristic D and G peaks of carbon fibres [29]. The D and G bands were fitted with Gaussian-shaped functions to estimate the ID/IG ratio between the areas of the peaks. The positions of D and G peaks of the various carbon fibres samples along with the ID/IG ratios are reported in table 4.6. The ID/IG ratio is a measure of the degree of disorder in the material [16], we find that the plasma treated fibres show a larger degree of disorder because of their higher ID/IG ratio. The degree of disorder decreases slightly as we increase the power of the plasma treatment. This effect can be understood by the FESEM images and the XPS analysis where the introduction of functional groups and change in morphology in the crystalline structure of carbon fibres governs a higher degree of disorder [30]. Our findings in this study are in conformance with the one reported in literature. Montes et.al, 2002 and Wen et.al, 2006 reported the same trend in the degree of disorder of commercial carbon fibres after plasma treatment [31, 32].

Table 4.6: Raman spectra and I_D/I_G comparision of pristine and plasma treated CFs.

S/no.	Sample Id.	Position (cm^{-1})		I_D/I_G
		D-peak	G-Peak	
1	Pristine CF	1357	1604	0.73
2	100 W, 5 min	1350	1597	0.77
3	200W, 5 min	1351	1596	0.76

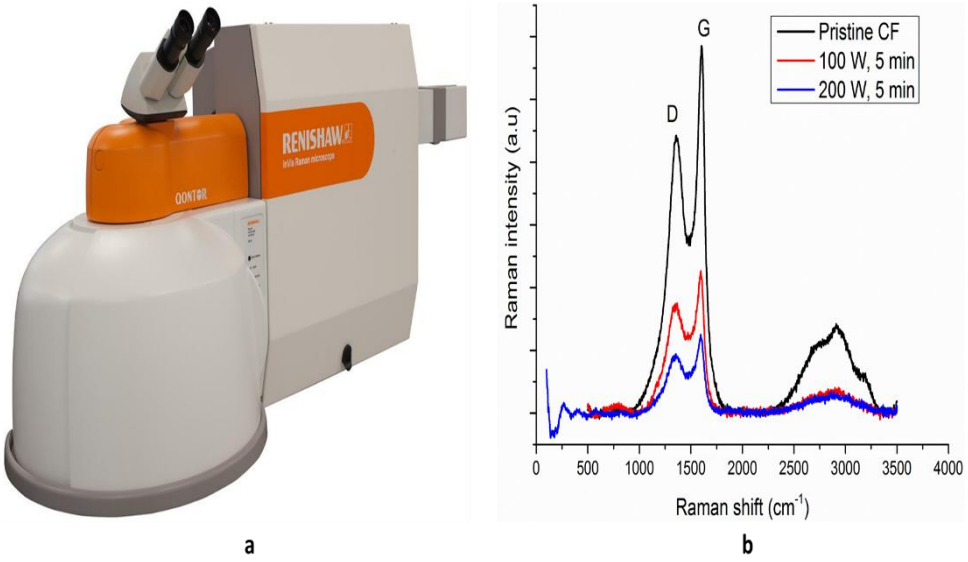

Figure 4.12: (a) Reinshaw Raman, (b) Raman spectra of pristine and plasma treated carbon fibres.

4.7.4. Fourier Transform Infrared Spectroscopy analysis.

FTIR analysis was performed on the untreated and the treated CF, diluted in KBr pallet, using Equinox, Bruker instrument with a resolution of 2 cm^{-1} in the frequency wavenumber range of 400 to 4500 cm^{-1} as shown in figure 4.13.The functional groups at their respective wave numbers were identified referring to ref. 33 [33]. The oxygen containing functional groups at the wave number 1650 cm^{-1} is assigned to the C=O bonds from unsaturated Ketones/Aldehydes. The

weak band in the spectra of the plasma treated CF at 1460 cm^{-1} is attributed to the C-O stretching and/or the O-H deformation of the carboxylic acid group. The peak in the 3440 cm^{-1} region is associated with the carboxylic acid and alcohol functional groups. Two peaks at 2850 cm^{-1} and 3440 cm^{-1} are associated to the OH stretching of the carboxylic acid. The C-O, O=C and O-C=O functional groups are formed due to plasma treatment [34]. XPS analysis (see XPS section) of the plasma treated CF confirms the presence of C-O, C=O and O-C=O bonds. These functional groups contributed to enhance the adhesion between the fibre (see wettability test section) and the matrix that may contribute to improved mechanical and tribology properties in the composites.

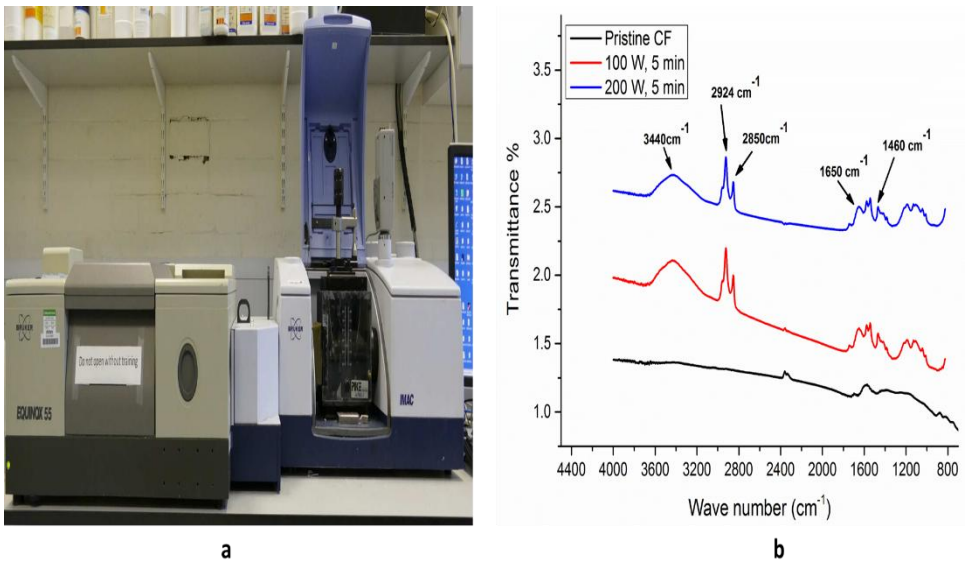

Figure 4.13: (a) Equinox, bruker instrument, (b) FTIR spectra of pristine and plasma treated carbon fibres.

4.7.5. Single fibre and micro-plastic strength study

Mechanical analysis was carried out on the single fibre and micro-plastic samples to study the effect of plasma treatments on the mechanical properties of the carbon fibres. Diameter measurements of single fibres were performed using the Phenom Pro desktop scanning electron microscope (SEM). The carbon fibres have an average diameter of 6.86 + 0.50 microns. Results for 20 samples for each category of pristine and plasma treated CF are displayed in figure 4.14a. The specimens of micro-plastic (unidirectional fibres) based on pristine and plasma treated T700 CF bundle (100W, 5 min). The impregnation of CF was performed

on MAW 20 FB 5/1 winding machine. Huntsman three-component epoxy resin was used to impregnate the CF tow.

The plasma treated CF lose strength after the treatment due to etching of the surface layers and rupture of crystalline chains due to the action of the plasma radicals as evident from the FESEM images(fig.4.11). The 100 W, 5 min sample shows a decline of 8% in the tensile strenght while the 200 W samples losses slightly more tensile strength at around 12% when compared to the untreated carbon fibres tensile strenght. These values are in conformance with the threshold set for the application of surface modified CFs in composites. Generally the fibre should not lose more than 15~20% of the original tensile strength after any surface treatment for better performance in the composites [27, 35]. The slightly higher loss in the 200W sample is probably due to the severe action of the plasma radicals as evident in the FESEM images as well.

Figure 4.14: (a) MAW 20 FB 5/1winding machine, (b) Micro-plastic specimen.

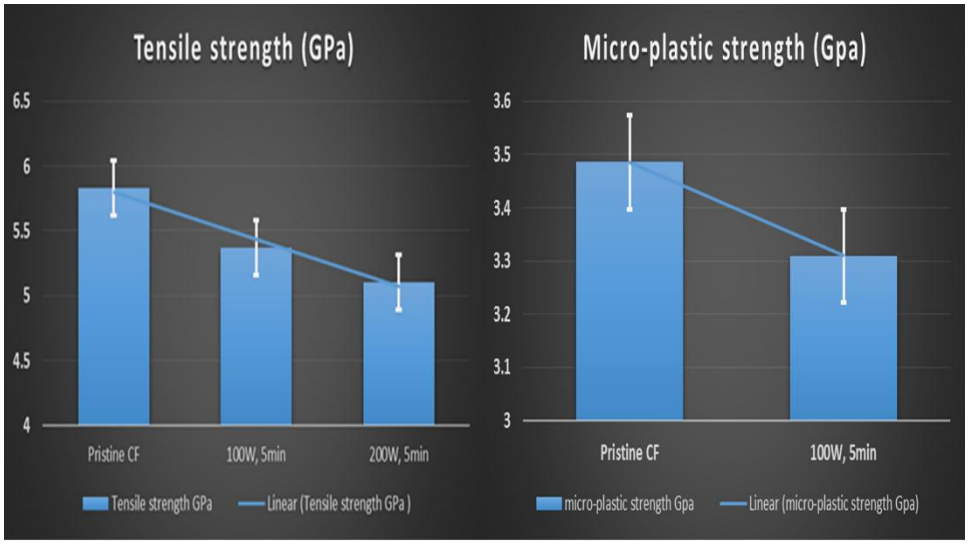

Figure 4.15: (a) Single fibre strength, (b) micro-plastic strength comparison of pristine and plasma treated CFs.

In the micro-plastic analysis the 100 W, 5 min sample shows a strength of 3.3 GPa compared to 3.48 Gpa for the pristine sample. The 5 % loss is probably due to the damage caused by the plasma elements during the treatment. Since the carbon fibres retain their tensile strength within 90% after the plasma treatment, we can recommend the same treatments for the in house generated lignin based carbon fibres under the FIBRALSPEC project.

4.7.6. Wettability test

A simple technique was employed to study the effects of plasma treatment on the adhesion between the matrix and the carbon fibres. Carbon fibres in dimensions 7.5 cm were cut, weighed and dipped in epoxy resin (HEXION. EPIKOTE TM Resin MGS® RIM 135) for 5 minutes and then hanged under the fume hood as shown in the figure 4.16. The samples were weighed after 1 hour and 24 hours to study the amount of the resin retained by the pristine and the treated carbon fibers. 5 samples for each category were tested.

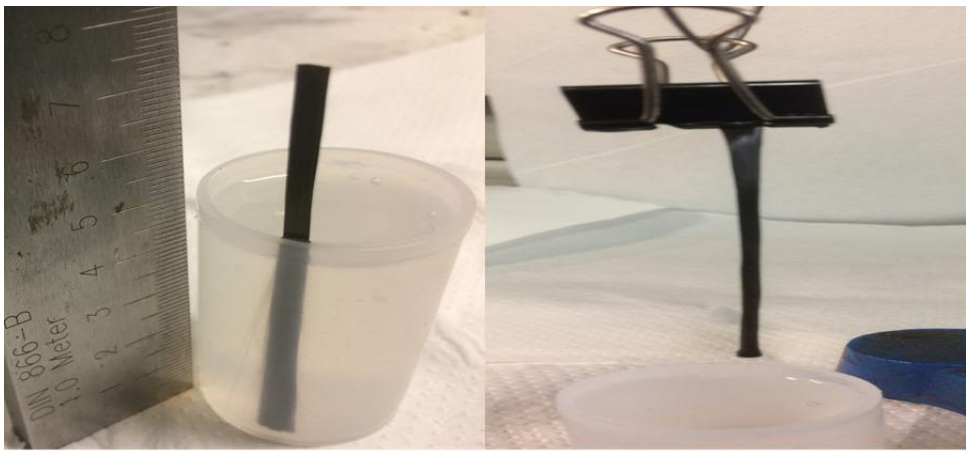

Figure 4.146: Wettability test.

The plasma treated CF showed better adhesion to the matrix. Taking as a reference the retention of epoxy resin by the pristine CF after 1 hour, the specimen treated at 100 W showed 21% more resin retention while the 200W treated specimen showed a marginally low resin retention of 18%. After 24 hours, the analysis shows that the resin retention was 14% for 100W sample and 15 % for 200W sample respectively as shown in figure 4.17. The higher adhesion of CF to the matrix can be attributed to the surface morphology and functional groups induced after the plasma treatment. Tiwari et.al [7] reported similar results for the enhanced adhesion of carbon fibre with the Polyetherimide matrix after surface functionalization with Ytterbium fluoride nano particles.

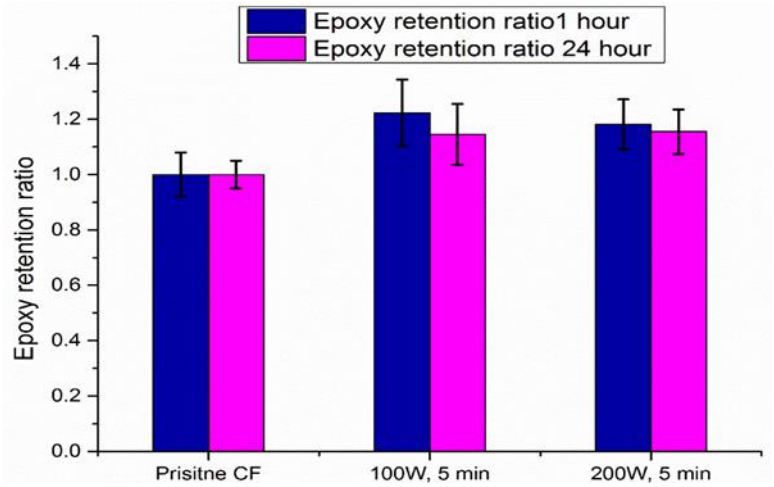

Figure 4.157: Wettability test comparison.

4.7.7. Decay of the functionalization after 6 months storage in ambient

The plasma treated carbon fibres were stored in ambient for 6 months and then characterized with XPS to study any decay in the oxygen picked up after the plasma treatment. Detailed analysis is reported in the table 4.7 below.

Table 3.7: Elemental and fucntional groups comparison by XPS analysis after 6 months.

Survey spectra.					
Sample id.	**C1s**	**O1s**	**N1s**	**O/C**	**N/C**
Chemically cleaned CF	87.4	11.5	1.1	0.13	0.01
100 W,5 min	75.7	20.4	3.9	0.26	0.05
After 6 months, 100W,5 min	79.6	17.1	3.3	0.21	0.04
High resolution spectra C1s					
	C-C	**C-O/O-C-N**	**C=O**	**-O-C=O**	**pi-pi***
Chemically cleaned CF	62.07	25.10	4.30	4.64	3.89
100 W,5 min	65.60	11.63	10.26	9.04	3.48
After 6 months, 100W,5 min	70.80	11.30	9.40	4.55	3.95

From the survey spectra we can see a decrease in the amount of the oxygen. Carbon fibres lost around 16% of the oxygen from it surface. From the high resolution spectra C1s we can observe a loss in the C=O and O-C=O bonds while C-C bonds observe an increase in their relative amount. Further investigation in this dimension is being carried out currently to know the exact cause of the oxygen contents loss.

Taking into account that fibers are functionalized with the prupose of improve the binding to a matrix and hence they are not expected to be operating in contact with open air, we can conclude that oxygen plasma treatment is not only effective in functionalization of the carbon fibres but also quite stable. Based on the discussion above we applied similar treatments for the in-house generated carbon fibres based on the lignin precursor.

4.8. Functionalization of lignin based CF and application to composites

Lignin precursor based carbon fibres were provided by our project partners at National Technical University of Athens. The in house generated CF were plasma treated for 5 minutes at 100 W and 200 W in oxygen environment. The results of the plasma treatment and subsequent application to the composites is reported as follow.

4.8.1. Morphology analysis

The morphology of the pristine and the plasma treated CF is reported in figure 4.18. Pristine CF possess a smooth surface. After plasma treatment we can see the peeling of the surface layers along with pits, crevices and cuts on the surface formed due to plasma treatment.

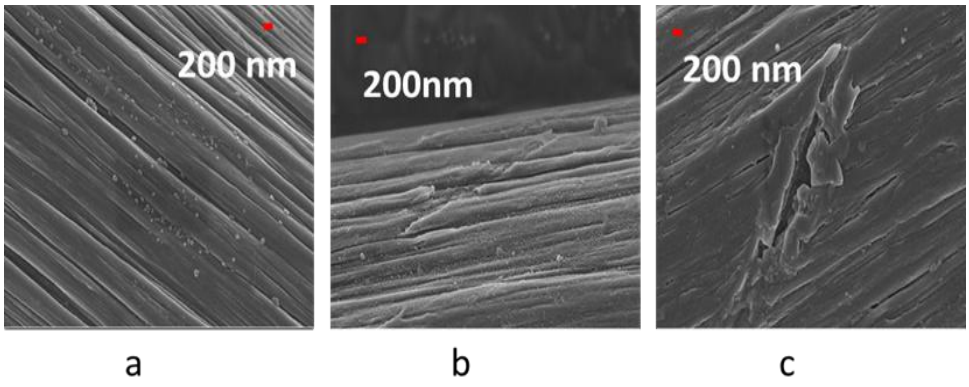

Figure 4.168: Morphology analysis of the (a) inhouse , plasma treated CFs (b) 100 W, (c) 200W.

4.8.2. XPS analysis.

From the survey spectra we find that the pristine CF contain about 19% oxygen on their surface. This oxygen is the chemically attached oxygen to lignin and remains their after the carbonization process. The carbonization conditions need further tuning which is under investigation these days. Survey spectra of the various CFs is displayed in the figure 4.19. C1s and O1s spectra are highlighted while the impurities are not mentioned for the sake of simplicity. After plasma treatment the amount of oxygen 1st increases on the surface of the CF and then slightly decreases as we doubled the plasma power for the same time for treatment. Similar trends were noted in the O/C ratios which decreased as the

plasma power increases. The conversion of carbon-carbon bonds to carbon oxygen bonds as result of plasma treatment is reported in table 4.8 along with their relative atomic percentages.

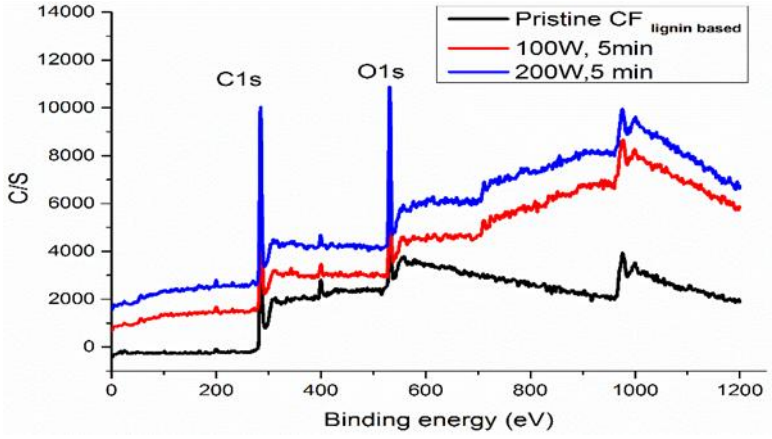

Figure 4.179: XPS analysis on Lignin based pristine and plasma treated CFs.

XPS analysis confirms the presence of C-O, C=O, O-C=O and acid anhydride groups on the surface of the CF after plasma treatment. The interaction of the functional groups with the epoxy matrix and their role in enhancing the mechanical properties of the CF-epoxy composites is discussed in the section below.

Table 4.8: Elemental composition from survey spectra on lignin based pristine and plasma treated CFs with 5% error bar in atomic %age.

Sample id	C1s	O1s	N1s	O/C	N/C
Pristine CF	74.2	19.5	5.1	0.26	0.07
100 W, 5min	59.1	25.1	15.8	0.42	0.27
200 W, 5min	61.9	22.8	15.3	0.37	0.25

Table 4.9: Functional groups comparison from H.R C1s spectra on lignin based pristine and plasma treated CFs with 5% error bar in atomic %.

Sample id	C-C	C-O	C=O	-O-C=O	O=C-O-C=O
Pristine CF	54.12	40.48	2.21	3.19	Weak signal
100 W, 5min	34.61	45.07	2.86	12.29	Weak signal
200 W, 5min	40.62	38.18	6.19	11.32	3.69

4.9. Application to epoxy composites

4.9.1. Composite preparation

Carbon fibres were shredded to short fibrous form using an industrial pulveriser (Savatec BB90E) and dispersed in epoxy resin (HEXION. EPIKOTE TM Resin MGS® RIM 135) using an overhead mixer (Ultra-Turrax T18) at a speed of 20,000 rpm for 2 minutes. Subsequently cross linker (EPIKURE TM Curing Agent MGS ® RIM H 137) was added. The composite mixture was then sonicated (Elma sonic S15H) for 15 minutes and degassed in a vacuum chamber (50 mbar) for 20 minutes. The composites were subsequently cured at 60 °C for 4 hours in the oven [36, 37] and molded into dog-bone shape (ASTM D 638-04) for mechanical analysis and 25 mm X 25 mm X 5 mm specimen for the tribology analysis. Five samples for each concentration were prepared for statistical purposes.

4.9.2. Tensile analysis.

The tensile behavior of the untreated and treated CF composites was studied using mechanical tester (MTS Q-test 10). All the samples were analyzed using a load cell of 10 kN and a strain rate of 1 mm/min. Stress vs strain curves were plotted and results were compared with the blank epoxy resin and with untreated and treated CF composites (Fig. 4.20). The composites fabricated with the plasma treated CF show higher tensile properties compared to blank epoxy and pristine CF based composites. Blank epoxy shows a maximum load bearing capacity of 51 MPa. Reinforcement with CF enhances the load bearing capacity and induces

plasticity in the epoxy matrix. The ultimate tensile strength of 61 MPa, 70 MPa and 72 MPa are shown by composites of pristine CF, 100W and 200W respectively. The 200 W sample depicts an increase of 41% compared to blank epoxy and 18% when compared to the pristine CF based composites.

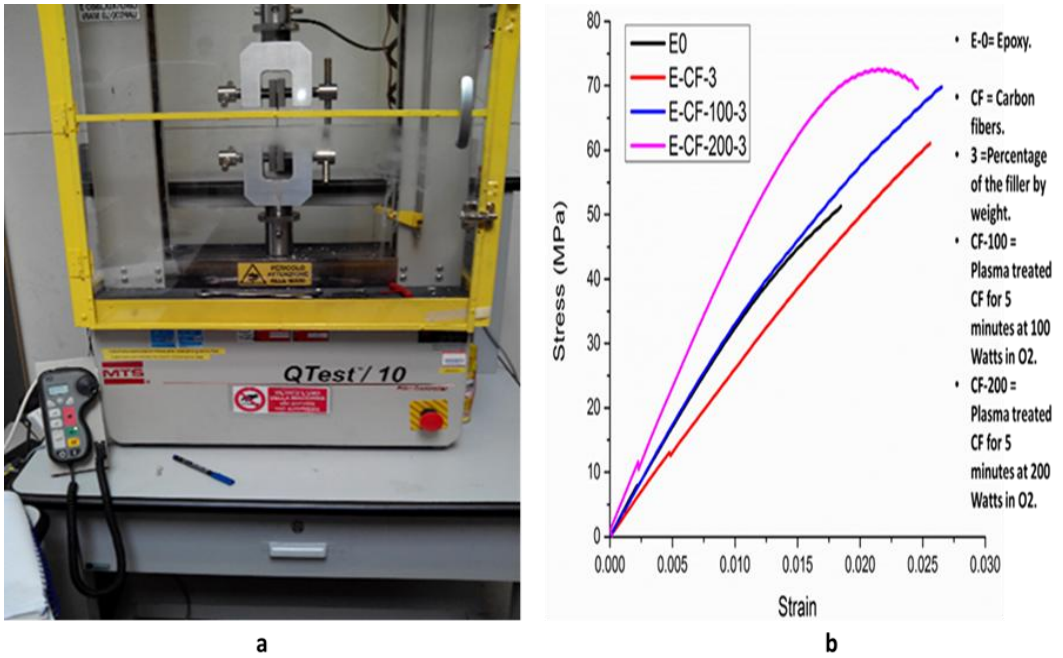

Figure 4.20:(a) Q-TEST 10, (b) Tensile behavior of the plasma treated CF-Epoxy composites.

The improved mechanical properties of the composites with plasma treated CF is due to the oxygen containing functional groups on the surface of CF. The increase of the surface active groups and active sites for chemical bonding generated by plasma treatment enhanced the interfacial adhesion between the fibers and the surrounding matrix [14]. Formation of new surfaces (see fig.4.18) enhanced the contact area with the matrix and ensured higher interfacial adhesion to the matrix. Interfacial adhesion to the matrix allows an adequate stress transfer and reduces the stress concentration at the fiber/polymer interface. Consequently tensile properties increases [38]. The mechanisms leading to better adhesion for the treated CF can be described as a twofold process. On one hand the functionalization increases the wettability of the carbon fibers by the resin. On the other hand the presence of functional groups allow the formation of strong chemical bonding between resin and fibers [8, 39, 40].

4.9.3. Friction analysis.

Tribology studies were carried out using a reciprocating tribometer (Anton-Paar Pin-on-Disk Tribometer TRB). The flat surface of the specimen was abraded against a polished steel sphere (AISI 420) 6 mm in diameter. A normal load of 5 N and a 3.27 mm reciprocating amplitude motion were set. Maximum linear speed of steel sphere was maintained at 0.185 m/s. The coefficient of friction (μ) is calculated as

$$\mu = \frac{F_f}{F_n} \quad \text{.....1}$$

Where, Ff is friction force parallel to the sliding surfaces, and Fn is the load perpendicular (i.e. normal) to the surface. The results are depicted in figure 4.19. Blank epoxy possess a friction coefficient of 1.55. Reinforcement with CF reduces the friction coefficient by 7% to 1.44 Reinforcement with the plasma treated CF further reduces the friction coefficient to 1.33 i.e. 15% less than the blank epoxy and 8% less than the pristine CF composites. Zhang et al. 2007 [40] reported the improved wear and friction properties of functionalized short-cut carbon fiber/polyimide composites. Cui et al.2013 [41] attributed the improved wear and friction properties of MWCNTs/epoxy composites to the addition of oxygen containing functional groups to the MWCNTs through surface modification. After surface modification the interfacial adhesion with the matrix improves and the filler can better protect the matrix by forming chemical bonds with the matrix [41]. Our findings support these views. It is also expected that the improved mechanical properties of polymer lead to better tribological properties [42]. The better dispersion of the plasma treated carbon fibers in the matrix led to a better load transfer at the contact surface with the steel ball [43]. The self-lubricating property of carbon fibers may also helped to reduce the friction co-efficient [44].

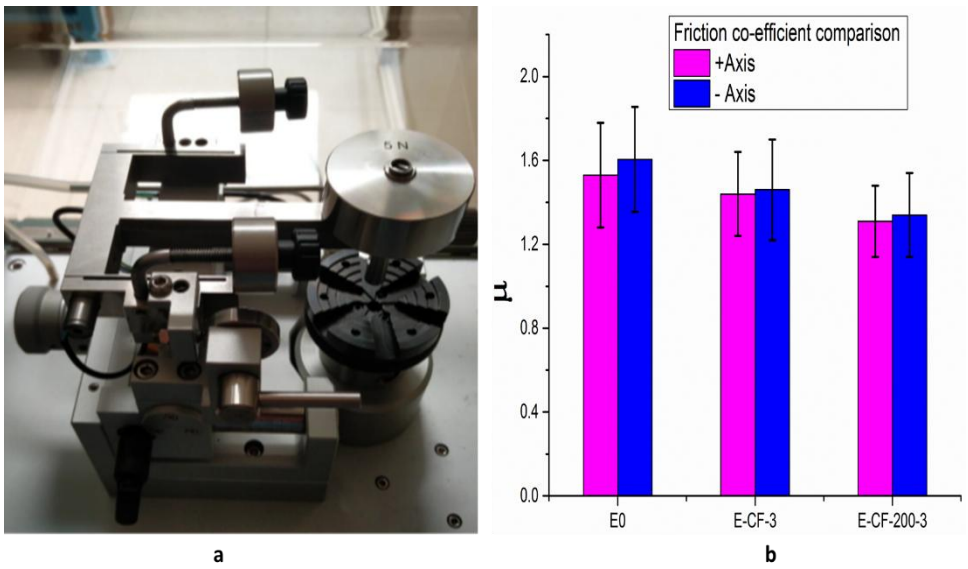

Figure 4.21: (a) Anton-Paar Pin-on-Disk Tribometer, (b) Friciton properties comparison.

4.9.4. Hardness measurement.

Surface hardness was measured with Durometer Shore A according to ASTM D-2240 standard on rectangular specimen as shown in figure 4.22 (a). Samples were placed on an iron flat surface as standard background. Each sample was measured on the 4 corners and at the center. The results are presented in figure 4.22(b). The hardness of the epoxy composites increase after reinforcement with the CF. Plasma treated CF marginally increased the hardness as compared to the pristine CF. The increase in the hardness can be attributed to the addition of carbon fibers which have more stiffness then the epoxy matrix[45]. Further investigation is required to have an in depth knowledge of this phenomena.

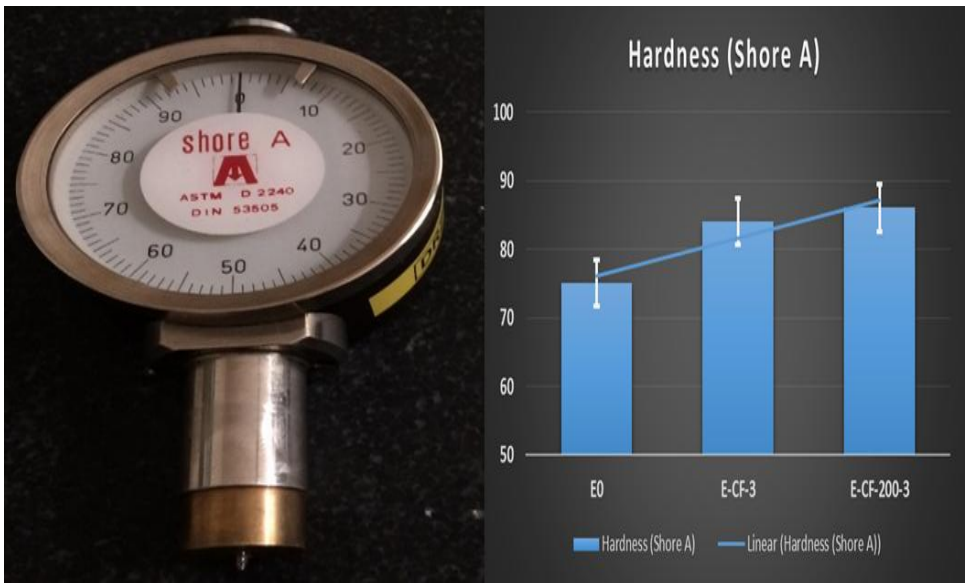

Figure 4.182: (a) Durometer shore A, (b) Hardness comparison.

Gonçalvesa et al. 2014 [46] attributed the increase in hardness of the epoxy/grinitic stone powder to the addition of the filler particles. Ahmed et al. 2017 [47] also reported the increase in hardness of epoxy glass fiber composites. The addition of surface treated carbon fibres increases the cross-linking ratio which inturn reduces molecular movment in the polymer thus making it more resistant to the penetration by indenter.

4.9.5. Wettability test.

Wettability test was carried out as discussed in section 4.7.6. The plasma treated CF retained a higher amount of the epoxy matrix when compared to the pristine CF. 100 W and 200 W treated samples show 22% and 24 % epoxy pick up after 1 hour respectively. After 24 hours the epoxy retention remained higher than for pristine CF case. The retained amounts were 15% and 14% respectively for the 100 W and 200 W treated samples. The high matrix retention can be explained by the FESEM images (figure 4.18) where the formation of crevices and canals favored more surface contact points with the matrix and thus higher pick up of the matrix compared to the pristine CF.

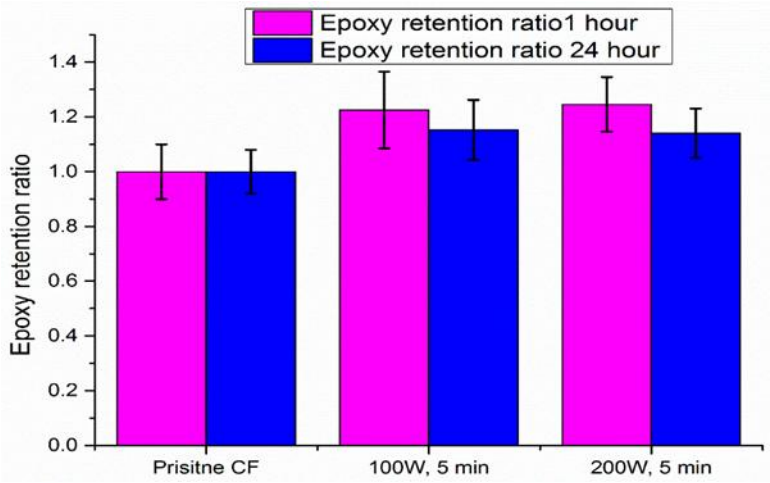

Figure 4.193: Wettability test comparison.

4.10. Conclusions.

- Low pressure plasma treatment in oxygen environment is an effective and suitable technique to modify carbon fibre surface.
- With proper tuning of the parameters we can ensure that the carbon fibres retain 90% of their original tensile strength, which is a key factor for the composite performance.
- XPS, Raman spectroscopy and FTIR results confirm the presence of the oxygen containing functional groups on the surface of the CF.
- Wettability test further strengthens our argument of enhanced interfacial adhesion after the plasma treatment.
- Application to composites show enhanced mechanical and tribology properties which further supports our recommendations to use low pressure oxygen plasma to modify the surface of carbon fibres.
- To further support our recommendations we studied the plasma treatment of carbon fibres generated from waste clothes and application to composites for enhanced properties as discussed in the next chapter.

4.11. References

1. Azarova, M.T.; Kazakov, M.E. World production and consumption of carbon fibres. *Fibre Chemistry* **2011**, *42*, 271.
2. Lee, S.-J.P.a.S.-Y. Carbon fibers, history and structure of carbon fibers. *Springer Series in Materials Science* **2015**, *210*, 1~30.
3. Vaidya, U.K.; Chawla, K.K. Processing of fibre reinforced thermoplastic composites. *International Materials Reviews* **2008**, *53*, 185-218.
4. Liu, Y.; Zhang, X.; Song, C.; Zhang, Y.; Fang, Y.; Yang, B.; Wang, X. An effective surface modification of carbon fiber for improving the interfacial adhesion of polypropylene composites. *Materials & Design* **2015**, *88*, 810-819.
5. Tiwari, S.; Sharma, M.; Panier, S.; Mutel, B.; Mitschang, P.; Bijwe, J. Influence of cold remote nitrogen oxygen plasma treatment on carbon fabric and its composites with specialty polymers. *Journal of Materials Science* **2011**, *46*, 964-974.
6. Zhao, M.; Meng, L.; Ma, L.; Wu, G.; Wang, Y.; Xie, F.; Huang, Y. Interfacially reinforced carbon fiber/epoxy composites by grafting melamine onto carbon fibers in supercritical methanol. *RSC Advances* **2016**, *6*, 29654-29662.
7. Tiwari, S.; Bijwe, J.; Panier, S. Strengthening of a fibre-matrix interface: A novel method using nanoparticles. *Nanomaterials and Nanotechnology* **2013**, *3*, 3.
8. Park, S.-J.; Oh, J.-S.; Rhee, K.-Y. Effect of atmospheric plasma treatment of carbon fibers on crack resistance of carbon fibers-reinforced epoxy composites. *Carbon letters* **2005**, *6*, 106-110.
9. Sharma, M.; Gao, S.; Mäder, E.; Sharma, H.; Wei, L.Y.; Bijwe, J. Carbon fiber surfaces and composite interphases. *Composites Science and Technology* **2014**, *102*, 35-50.
10. Park, S.-J.; Meng, L.-Y. Surface treatment and sizing of carbon fibers. In *Carbon fibers*, Springer Netherlands: Dordrecht, 2015; pp 101-133.
11. Drzal, L.T.; Rich, M.J.; Koenig, M.F.; Lloyd, P.F. Adhesion of graphite fibers to epoxy matrices: Ii. The effect of fiber finish. *The Journal of Adhesion* **1983**, *16*, 133-152.
12. Dai, Z.; Shi, F.; Zhang, B.; Li, M.; Zhang, Z. Effect of sizing on carbon fiber surface properties and fibers/epoxy interfacial adhesion. *Applied Surface Science* **2011**, *257*, 6980-6985.
13. Goan, J.; Prosen, S. Interfacial bonding in graphite fiber-resin composites. In *Interfaces in composites*, ASTM International: 1969.

14. Feih, S.; Schwartz, P. Modification of the carbon fiber/matrix interface using gas plasma treatment with acetylene and oxygen. *Journal of Adhesion Science and Technology* **1998**, *12*, 523-539.
15. Dilsiz, N.; Erinç, N.K.; Bayramli, E.; akovali, G. Surface energy and mechanical properties of plasma-modified carbon fibers. *Carbon* **1995**, *33*, 853-858.
16. Cuesta, A.; Dhamelincourt, P.; Laureyns, J.; Martinez-Alonso, A.; Tascon, J.M.D. Effect of various treatments on carbon fiber surfaces studied by raman microprobe spectrometry. *Appl. Spectrosc.* **1998**, *52*, 356-360.
17. Bellan, P.M. *Fundamentals of plasma physics*. Cambridge University Press: 2008.
18. Bittencourt, J.A. *Fundamentals of plasma physics*. Springer New York: 2004.
19. Lieberman, M.A.; Lichtenberg, A.J. *Principles of plasma discharges and materials processing*. Wiley: 2005.
20. Briggs, D.; Beamson, G. Primary and secondary oxygen-induced c1s binding energy shifts in x-ray photoelectron spectroscopy of polymers. *Analytical Chemistry* **1992**, *64*, 1729-1736.
21. Yuan, L.Y.; Chen, C.S.; Shyu, S.S.; Lai, J.Y. Plasma surface treatment on carbon fibers. Part 1: Morphology and surface analysis of plasma etched fibers. *Composites Science and Technology* **1992**, *45*, 1-7.
22. Han, S.H.; Oh, H.J.; Kim, S.S. Evaluation of fiber surface treatment on the interfacial behavior of carbon fiber-reinforced polypropylene composites. *Composites Part B: Engineering* **2014**, *60*, 98-105.
23. Eren, B.; Hug, D.; Marot, L.; Pawlak, R.; Kisiel, M.; Steiner, R.; Zumbühl, D.M.; Meyer, E. Pure hydrogen low-temperature plasma exposure of hopg and graphene: Graphane formation? *Beilstein Journal of Nanotechnology* **2012**, *3*, 852-859.
24. Garino, N.; Sacco, A.; Castellino, M.; Muñoz-Tabares, J.A.; Chiodoni, A.; Agostino, V.; Margaria, V.; Gerosa, M.; Massaglia, G.; Quaglio, M. Microwave-assisted synthesis of reduced graphene oxide/sno2 nanocomposite for oxygen reduction reaction in microbial fuel cells. *ACS Applied Materials & Interfaces* **2016**, *8*, 4633-4643.
25. Wepasnick, K.A.; Smith, B.A.; Bitter, J.L.; Howard Fairbrother, D. Chemical and structural characterization of carbon nanotube surfaces. *Analytical and Bioanalytical Chemistry* **2010**, *396*, 1003-1014.
26. Kim, S.S.; Yu, H.N.; Lee, D.G.; Murayama, H.; Kageyama, K. Tribological behaviors of plasma-treated carbon composite grooved surfaces. *Composite Structures* **2010**, *92*, 1039-1046.
27. Li, R.; Ye, L.; Mai, Y.-W. Application of plasma technologies in fibre-reinforced polymer composites: A review of recent developments. *Composites Part A: Applied Science and Manufacturing* **1997**, *28*, 73-86.
28. Montes-Morán, M.A.; Martínez-Alonso, A.; Tascón, J.M.D.; Young, R.J. Effects of plasma oxidation on the surface and interfacial properties of

ultra-high modulus carbon fibres. *Composites Part A: Applied Science and Manufacturing* **2001**, *32*, 361-371.

29. Bokobza, L.; Zhang, J. Raman spectroscopic characterization of multiwall carbon nanotubes and of composites.
30. Afanasyeva, N.I.; Jawhari, T.; Klimenko, I.V.; Zhuravleva, T.S. Micro-raman spectroscopic measurements on carbon fibers. *Vibrational Spectroscopy* **1996**, *11*, 79-83.
31. Montes-Morán, M.A.; Young, R.J. Raman spectroscopy study of hm carbon fibres: Effect of plasma treatment on the interfacial properties of single fibre/epoxy composites. *Carbon* **2002**, *40*, 845-855.
32. Wen, H.-C.; Yang, K.; Ou, K.-L.; Wu, W.-F.; Chou, C.-P.; Luo, R.-C.; Chang, Y.-M. Effects of ammonia plasma treatment on the surface characteristics of carbon fibers. *Surface and Coatings Technology* **2006**, *200*, 3166-3169.
33. Long, D.A. Infrared and raman characteristic group frequencies. Tables and charts george socrates john wiley and sons, ltd, chichester, third edition, 2001. Price £135. *Journal of Raman Spectroscopy* **2004**, *35*, 905-905.
34. Park, S.-J.; Chang, Y.-H.; Moon, C.-W.; Suh, D.-H.; Im, S.-S.; Kim, Y.-C. A study of atmospheric plasma treatment on surface energetics of carbon fibers. *Bulletin of the Korean Chemical Society* **2010**, *31*, 335-338.
35. Scheffler, C.; Wölfel, E.; Förster, T.; Poitzsch, C.; Kotte, L.; Mäder, G. Influence of microwave plasma treatment on the surface properties of carbon fibers and their adhesion in a polypropylene matrix. *IOP Conference Series: Materials Science and Engineering* **2016**, *139*, 012046.
36. Castellino, M.; Chiolerio, A.; Shahzad, M.I.; Jagdale, P.V.; Tagliaferro, A. Electrical conductivity phenomena in an epoxy resin–carbon-based materials composite. *Composites Part A: Applied Science and Manufacturing* **2014**, *61*, 108-114.
37. Jagdale, P.; Khan, A.A.; Rovere, M.; Rosso, C.; Tagliaferro, A. 1 multiwalled carbon nanotube–strength to polymer composite. *Nanomaterials in Joining* **2016**.
38. Lau, K.-T.; Hui, D. Effectiveness of using carbon nanotubes as nano-reinforcements for advanced composite structures. *Carbon* **2002**, *40*, 1605-1606.
39. Yuan, H.; Wang, C.; Zhang, S.; Lin, X. Effect of surface modification on carbon fiber and its reinforced phenolic matrix composite. *Applied Surface Science* **2012**, *259*, 288-293.
40. X. R. Zhang, X.Q.P., Q. H. Wang. The effect of fiber oxidation on the friction and wear behaviors of short-cut carbon fiber/polyimide composites. *eXPRESS Polymer Letters* **2007**, *1*, 318–325.
41. Cui, L.-J.; Geng, H.-Z.; Wang, W.-Y.; Chen, L.-T.; Gao, J. Functionalization of multi-wall carbon nanotubes to reduce the coefficient

of the friction and improve the wear resistance of multi-wall carbon nanotube/epoxy composites. *Carbon* **2013**, *54*, 277-282.

42. Zhang, L.C.; Zarudi, I.; Xiao, K.Q. Novel behaviour of friction and wear of epoxy composites reinforced by carbon nanotubes. *Wear* **2006**, *261*, 806-811.
43. Chen, H.; Jacobs, O.; Wu, W.; Rüdiger, G.; Schädel, B. Effect of dispersion method on tribological properties of carbon nanotube reinforced epoxy resin composites. *Polymer Testing* **2007**, *26*, 351-360.
44. Dong, B.; Yang, Z.; Huang, Y.; Li, H.-L. Study on tribological properties of multi-walled carbonnanotubes/epoxy resin nanocomposites. *Tribology Letters* **2005**, *20*, 251-254.
45. Ahmetli, G.; Deveci, H.; Soydal, U.; Gurler, S.P.; Altun, A. Epoxy resin/polymer blends: Improvement of thermal and mechanical properties. *Journal of Applied Polymer Science* **2012**, *125*, 38-45.
46. Gonçalves, J.A.V.; Campos, D.A.T.; Oliveira, G.d.J.; Rosa, M.d.L.d.S.; Macêdo, M.A. Mechanical properties of epoxy resin based on granite stone powder from the sergipe fold-and-thrust belt composites. *Materials Research* **2014**, *17*, 878-887.
47. Ahmed, J.K.; Haleem, A.H.; Omran, A.R. Effect of carbon fiber surface treatment on the flexural strength and interfacial properties of carbon fiber-polyester composite.

Chapter 5

Carbon fibres from waste cotton, functionalization and application to composites

5.1. Introduction

Carbon fibres composites are one of the most employed materials in applications ranging from super capacitors to sport goods, from airplane structural parts to wind turbine blades. This is due to their high strength, low weight, chemical resistant nature and good electrical properties [1-4]. The carbon fibre composites industry is growing at a high pace and is expected to reach a mammoth 140 k tons production in year 2020 [5]. Currently 70 % of carbon fibres are produced using Poly acrylonitrile (PAN) fibres as precursor, but the conversion process is complicated and has environmental impacts. Increasing demands for carbon fibres production and an approach towards sustainable society has made it compulsory to find an environment friendly and renewable sources for carbon fibre production [6, 7]. In recent years, carbon fibres based on renewable cellulose precursors have gained a lot of interest as they are abundant in nature and possess optimal structural properties for carbon fibre production [8, 9]. Cotton fibres mainly consist of cellulose and some traces of waxes, proteins, sugars and organic acids [10]. In recent years cotton fibres and fabrics from waste have been exploited as potential precursor to synthesize carbon fibres for various

applications in published research [11]. Ekrami et al 2014 [12] and Jieying et al 2014 [13] have reported the production of activated carbon fibres from waste cotton fabrics. Wang et al 2014 [14] synthesized hollow carbon fibres from cotton fibres for capacitors application.

Polymer-matrix composites (PMCs) is a class of composites with a great potential for applications in many industries but the poor adhesion at the interface between carbon fibre and the matrix due to their hydrophobic and chemically inert nature has been a long standing issue. This limitation in carbon fibre composites undermine their industrial applications to the full potential [15-17]. To enhance the adhesion at the interface of the carbon fibre and the resin, various surface modifying techniques such as plasma treatments, chemical treatments, surface sizing and surface coating with carbon nano tubes/nano particles have been used in recent years. Plasma treated carbon fibres have found a lot of interest in carbon fibre composite industry owing to several intriguing advantages over the other surface modification treatments such as ease of operation, low treatment time and absence of post treatment hazardous solutions to dispose-off [18-20]. The surface modified carbon fibres confer superior mechanical and tribology properties to the matrix compared to their untreated counterparts due to superior interfacial adhesion to the matrix [21-26]. Feih et al.1998 [27] , Rhee et al. 2012 [28] and Santos et al. 2013 [29] reported the superior mechanical, friction and wear properties of the carbon fibre composites after plasma treatment compared to the untreated carbon fibre composites .

In this chapter we discuss the production of carbon fibres from waste cotton fabrics and their application in composites with better mechanical and tribological properties, after an oxygen plasma treatment.

5.2. Raw material

Fabric strips from waste clothes, 100% cotton in composition, were washed thoroughly with deionized water to remove any foreign matter and dried in the ambient for 24 hours.

Figure 5.1: Cotton strip.

5.2.1. Thermogravimetric analysis (TGA)

Thermogravimetric analysis was carried out on the cotton fibres from waste using a *Mettler Toledo TGA/SDTA85* in argon atmosphere. The flow rate was maintained at 100 ml/min and the ramp rate of 5º C/minute was used for a temperature range of 25 to 800º C. The mass losses of cotton fibres with increase in temperature were analyzed to select appropriate parameters for conversion to carbon fibres [30]. An initial weight loss of 4 wt. % was observed between 25 and 150 °C (Figure 5.1). Cotton fibres at first dehydrate and moisture leaves the cotton. The dehydration process do not affect the strength of the cellulose and leads to the formation of the double-bonded intermediates [31, 32]. The molecular weight of the fibres starts to due to loss in moisture which may reduce the tensile strength of the fibres [33]. Only 5 wt. % losses were observed below the temperature of 300º C. Significant weight loss of around 73 wt% was observed after 300 ºC. At 358° C major weight loss was observed that was followed by a 6 wt. % loss at a temperature of 410° C. The microstructure of carbon forms at a temperature range of 300-450° C [34]. The cellulose chains de-polymerize to monosaccharide derivatives at this temperature range and convert to aromatic structures, releasing the gases containing (O, H) atoms [35]. More ordered carbon structure is obtained by heat treatment at a temperature range of 450 and 800° C. Semi ordered carbon structures are obtained by pyrolysing cotton fibres up to 800° C temperature. These changes are represented in figure 5.6. The mechanism of aromatization is still unknown, owing to the complex reactions occuring during the carbonization process [36].

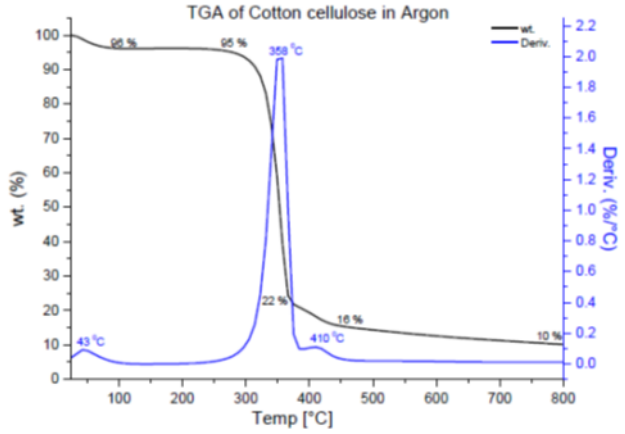

Figure 5.2: TGA analysis on raw cotton in Argon.

5.2.2. Elemental composition analysis

Survey spectra and the high resolution spectra of the cotton fabric are reported in table 5.1. The washed cotton surface has 67.1 at% of carbon and 28.3 at% of oxygen. Traces of other elements, namely Nitrogen, Calcium and Silicon were also present at surface of the cotton fabric. In the high resolution spectra C1s the data has been extracted by curve fitting. C1s curve has been deconvoluted using four curves (Gaussian-Lorentzian sum function). Assignation to each chemical shift has been done according to Briggs chemical shift table [37].

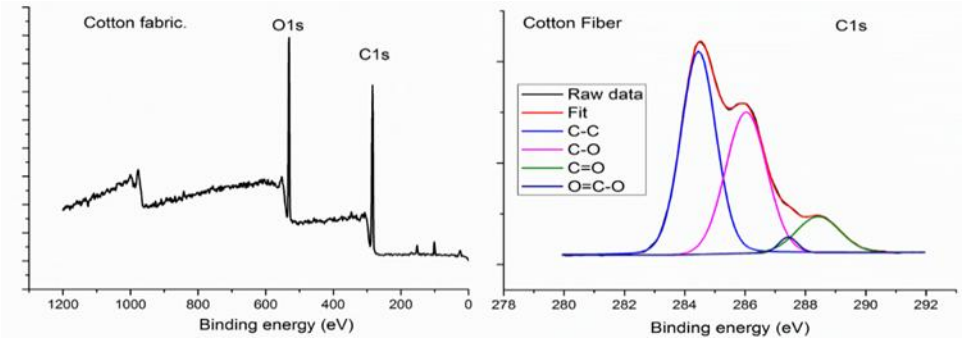

Figure 20: XPS analysis of cotton fibre.

Table 5.1: Elemental composition of cotton from XPS analysis with 5% error bar in the atomic percentage.

XPS analysis of Cotton fabric.						
Survey spectra	**C1s**	**O1s**	**N**	**Ca, Si**	**O/C**	**N/C**
	67.1	28.3	0.8	3.3	0.42	0.01
H.R spectra C1s	**C-C**	**C-O**	**C=O/ O-C-O**	**-O-C=O**		
	49.3	38.4	1.9	10.4		

The C1s spectra of cotton fabric (see table 5.1) comprised of four types of carbon related chemical bondings: (i) un-oxidized carbon at 284.45 eV in form of C–C or C–H bonds, (ii) Carbon bonded to oxygen with a single bond (C-O) at a binding energy of 286.03 eV, (iii) Carbon with two oxygen bonds (O-C-O, C=O), and (iv) carbon with 3 oxygen bonds (O-C=O) at their respective binding energies of 287.43 eV and 288.42 eV. For pure cellulose the C1s spectrum comprises C-O and O-C-O carbon groups only [38]. However the hydrophobic matter e.g. waxes, fats, proteins, and pectin on the surface of the cotton fibres conceal the cellulose backbone by forming laminar layers. The C-C and O-C=O bonds in the C1s spectrum of cotton fibres arise due to these non-cellulosic contaminants that remain on the fibre surface even after process like scouring and bleaching [39].

5.2.3. FTIR-ATR Spectroscopy

Figure 5.4 shows the FT-IR analysis of the raw and washed cotton fabric performed in the absorbance mode. Raw and washed cotton dispaly similiar with no visible difference. Impurities such as wax and oils on the surface of raw cotton were not observed in the spectrum probably due to their low quanitity [40]. The broad peak with center at a wavenumber of 3300 cm^{-1} corresponds to O–H stretching [41]. The sharp peak at 1640 cm^{-1} wavenumber arises probably due to the adsorbed moisture.

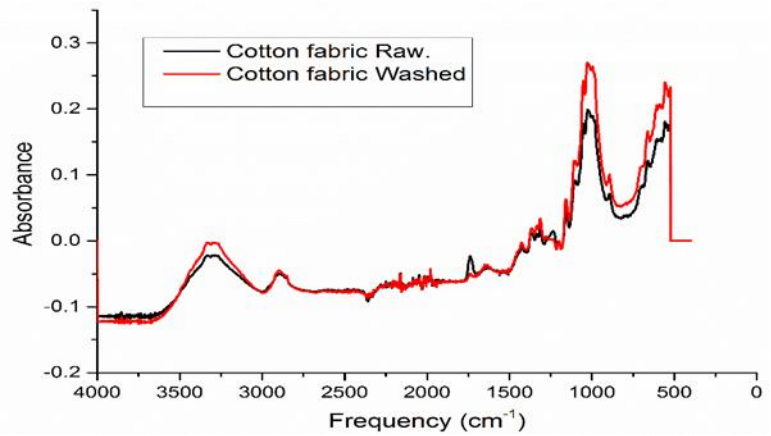

Figure 5.4: ATR-FTIR Spectra of raw and washed cotton fibres.

5.3. Carbonization of the cotton fabric

Carbonization process is defined as a phenomena in which a depolymerized structure converts into a graphitic structure by the re-polymerization process in presence of high temperature and an inert environment [42]. Carbolite (TZF12/65/550) furnace was used to carry out the carbonization at a temperature range of 400° C to 800° C for one hour in nitrogen environment at a ramp rate of 15° C/min. The carbonized fabrics were then left to cool down in the ambient overnight. Figure 5.2 shows the carbon yield obtained after the carbonization process. After 400° C the weight loss is marginal indicating that almost all the carbonization process took place at 400° C. Carbonization and graphitization of the cotton fibres is a two-step process. Low-temperature pyrolysis leads to formation of carbon structures while the high-temperature carbonization leads to graphitization [42]. The final yield of carbonized fibres obtained after carbonization is 18.7 (± 1.9) wt. % at 400° C, 16.5 (± 1.6) wt. % at 600° C and 13.5 (± 1.3) wt. % at 800° C.

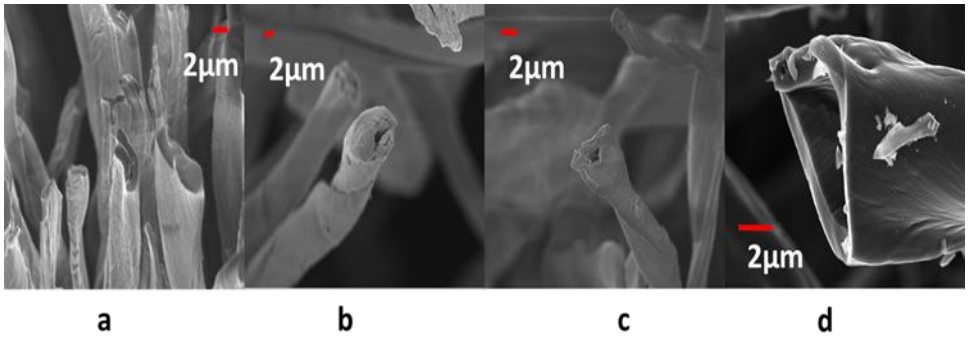

Figure 5.5: a. Cotton fibre, b. 400° C, c.600° C, d. 800°C.

A schematic model of carbonization is depicted in Figure 5.6. The surface layers of the cotton fibre deteriorate with increasing temperature and leads to ordered carbon strucutres formation. The evolution of carbon strucutre with temperature further studied in detail with electron microscopy (figure 5.5). Cotton fibre possess a bean like shape [43] and are composed of concentric layers. The outermost layer on the fibre is separable and comprises of wax and pectin materials. The primary wall of the cotton fibre is composed of cellulose based crystalline fibrils [44, 45]. The secondary wall of the fibre consists of closely packed parallel fibrils. The innermost part of the lumen is composed of the remains of the cell contents.

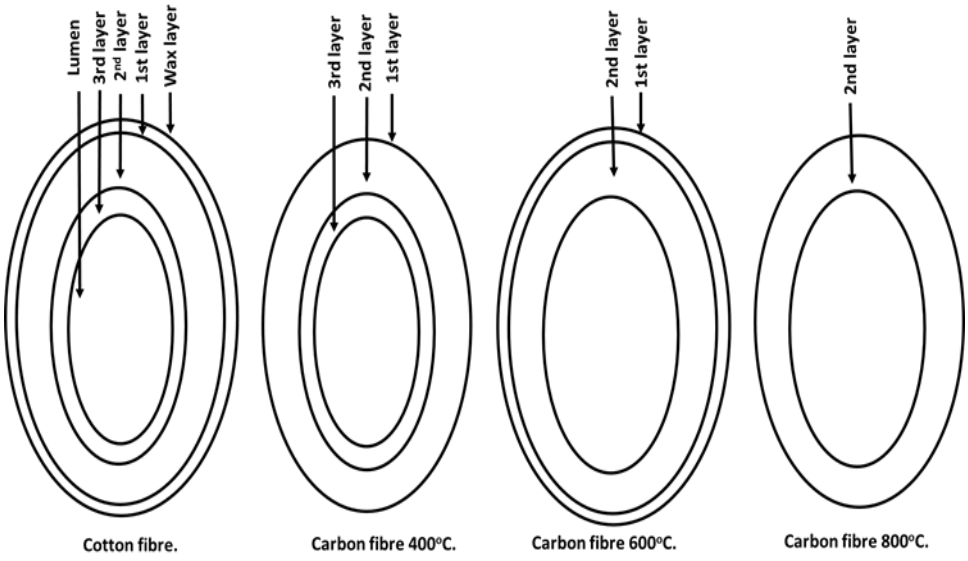

Figure 5.6: Evolution of the CF morphology with change in carbonization temperature.

5.4. Plasma treatment

Low-pressure oxygen plasma treatment was chosen to modify the surface of the CF. The plasma treatment was carried out with a barrel-type reactor (Plasmafab508, see fig. 5.7) equipped with a scroll pump, a radiofrequency (RF) generator working at 13.56 MHz and a mass flow controller for the reactive gas. Plasma process was run for 5 minutes at a RF power of 50 W in order to clean the inside walls of the chamber and the gas lines. Samples were purged with N_2 gas before the treatment in order to remove any contaminant from the surface.

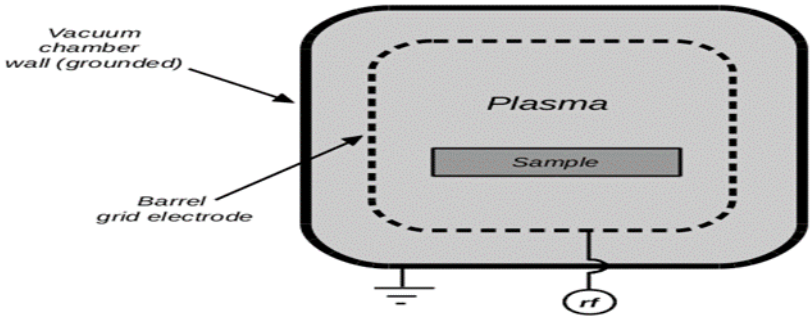

Figure 5.7: Plasma fab 508.

All the samples were treated for 5 minutes in O_2 plasma, using a RF power of 100 W and 200 W. The samples were stored in plastic boxes and in ambient conditions for further characterizations.

5.5. Characterizations on carbon fibres before and after plasma treatment

5.5.1. Morphology analysis

The surface of the carbon fibres (CF) before and after plasma treatment were studied by FESEM-ZEISS Merlin. Figure 5.8 shows that the CF possess a smooth surface after the carbonization process (see fig.5.8-a). The top surface of the CF is eroded due to the action of the plasma radicals, forming pits, holes and canals on the surface of the fibres (see fig. 5.8 b and c). This effect increases the surface area (see surface area measurements) and contribute to enhanced surface adhesion with the matrix in the composite application.

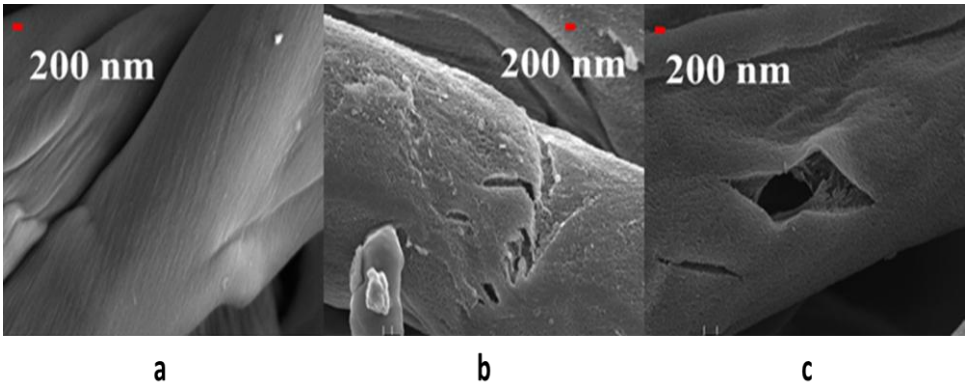

Figure 5.8: Morphology of (a) CF as it is, (b) CF-100W, (c) CF- 200W.

5.5.2. X-ray Photoelectron Spectroscopy (XPS)

Chemical changes on the surface of the treated samples was studied with XPS and compared with the pristine CFs sample. Figure 5.9 shows the survey spectra of the untreated and treated fibres at 100 W and 200 W shows the presence of C and O and small amount of impurities like sodium, calcium and silicon. The relative concentration of O after O_2 plasma treatment increases from 6.9 at% to 21.5 at% and 21.2 at% for the CF100W and CF200W samples compared to untreated CF respectively.

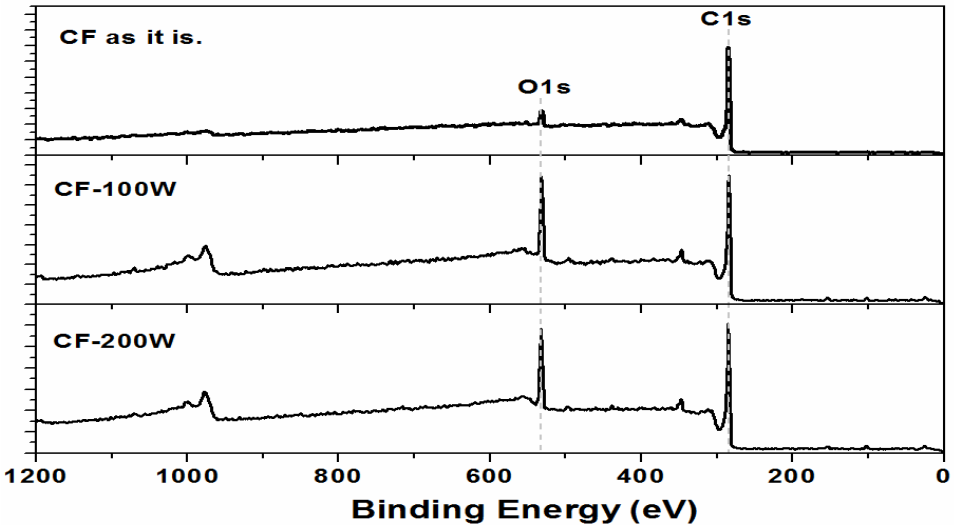

Figure 5.9: Survey spectra comparison of CFs after plasma treatment.

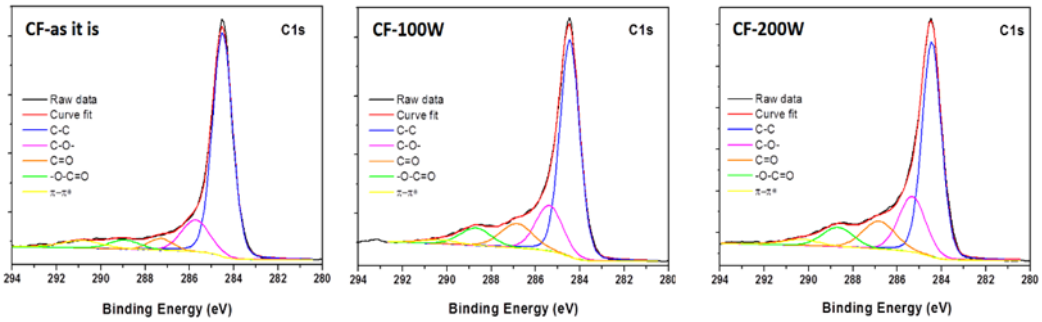

Figure 5.10: XPS C1s HR spectra for untreated (left) and plasma treated (CF-100W. center, CF-200W. right).

The H.R C1s curves were deconvoluted with five curves (Gaussian-Lorentzian sum function) and atomic percentage of the functional groups with a 5% error bar is reported in table 5.2. Assignation to each chemical shift has been done according to Briggs chemical shift table [37]. The C-C peak at the binding energy of 284.5 eV decreases with the increment in the plasma power. While the quantity of C-O- bonds at their respective binding energy increases with an increase in the plasma power. The C=O and -O-C=O fucntional groups increases after the treatment but remains almost unchanged on increasing to treatment power. The π–π* (HOMO–LUMO) component is a characteristic shake-up line for aromatic carbon compounds is generated by the ring excited by the photoelectrons. This feature is the fingerprint of extended delocalized electrons in the material and it is present in graphitic material such as Highly Oriented Pyrolytic Graphite (HOPG) [46], reduced Graphene Oxide (rGO) [47], Carbon NanoTube (CNT) [48]. The π–π* component in the treated carbon fibres decreases after the plasma treatments. A comparison is made in the last row of table 5.2 with percentage of C-O bonds in the various samples confirming an increase with an increase in the plasma treatment power.

Table 5.2: XPS C1s components peak position and relative percentage (%), for all samples, obtained from deconvolution procedure. In the last row the total % of C-O bonds has been reported.

	C1s components (%)		
Type of bonds	**CF as it is**	**CF-100W**	**CF-200W**

C-C (284.5 eV)	70.6	60.8	55.6
C-O- (285.3-285.7eV)	14.5	17.7	20.2
C=O (286.8-287.3 eV)	4.7	11.5	12.4
-O-C=O (288.7-288.9 eV)	4.7	7.9	8.5
π-π* (>290 eV)	5.5	2.1	3.3
C—O bonds (%)	23.9	36.1	41.1

5.5.3. Raman Spectroscopy

The structural quality of the carbon fibres and the effects of the plasma treatment were studied with Raman spectroscopy using a Renishaw ® Ramanscope InVia H43662 model equipped with a green laser source (λ=514 nm). Raman spectra of the untreated and treated CF are reported in figure 5.11. Carbon fibres show the characteristic D and G peaks [49]. The D and G bands were fitted with Gaussian-shaped functions to estimate the I_D/I_G ratio between the areas of the peaks. The positions of D and G peaks of the various carbon fibres along with the I_D/I_G ratios are reported in table 5.3. The I_D/I_G ratio depicts the degree of disorder in a material medium [50]. The untreated fibres possess a larger degree of disorder probably due to the gases expelled during the carbonization process. The degree of disorder decreases slightly as we increase the power of the plasma process. This effect can be explained by the FESEM images (fig. 5.8) where the ablation of the surface most layers expose the inner part of the fibre that probably has a more ordered crystalline structure [51]. Contrary to our findings in this study, an increase in the I_D/I_G ratio has been reported in the literature after surface treatment of commercial carbon fibres [23, 52]. Such an opposite trend in

the I_D/I_G ratio can be due to the fact that commercial carbon fibres are produced from synthetic precursors and possess high degree of order and orientation during manufacturing while our material is based on natural sources with no definite near-surface order. We recommend further investigation in this dimension.

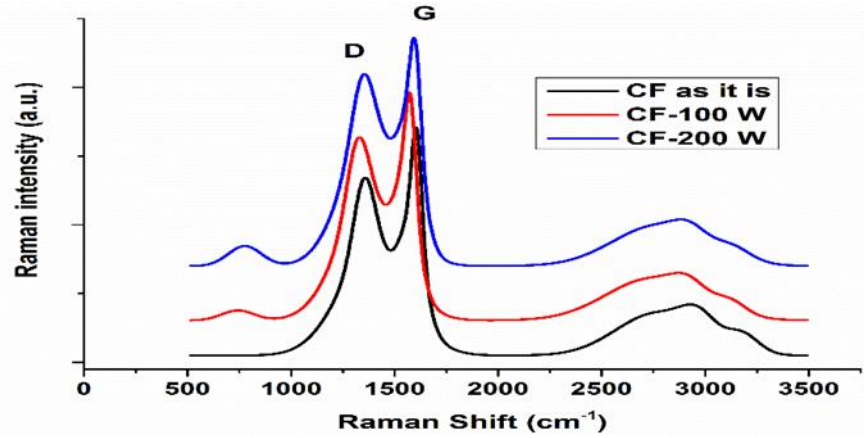

Figure 5.11: Raman spectroscopy of untreated and treated CF.

Table 5.3:Raman spectra comparison of untreated and treated CFs.

S/no.	Sample Id	D peak position (Cm^{-1})	G peak position (Cm^{-1})	Id/Ig
1	CF as it is	1356	1607	0.58
2	CF-100 W	1333	1570	0.53
3	CF-200 W	1352	1587	0.43

5.5.4. Fourier Transform Infrared Spectroscopy (FTIR)

FTIR analysis was performed on the untreated and the treated CF, diluted in KBr pallet, using Equinox, Bruker instrument with a resolution of 2 cm^{-1} in the wavenumber range 400 to 4500 cm^{-1}. The analysis is shown in figure 5.12.

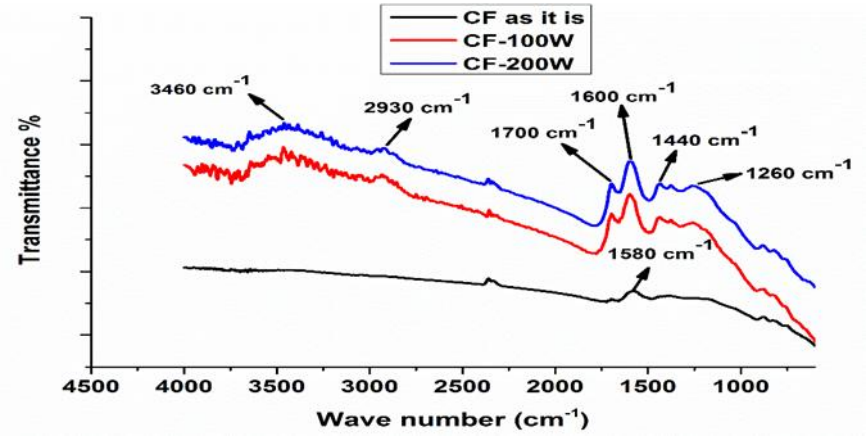

Figure 5.12: FTIR analysis before and after treatment.

The functional groups at their respective frequencies are identified referring to ref. 53. In the spectra of plasma treated carbon fibres the functional group at the frequency of 1260 cm^{-1} is associated to ethers. The functional groups in the frequency range of 1500–1680 cm^{-1} region are assigned to the aromatic C=C bonds and various substitution modes of the aromatic ring. The weak band in the spectra of the plasma treated CF at 1440 cm^{-1} is attributed to the C-O stretching and/or the O-H deformation of the carboxylic acid group. The peaks in the 1700 cm^{-1} and 3460 cm^{-1} regions are associated with the carboxylic acid and alcohol functional groups. The C-O, O=C and O-C=O functional groups are formed due to plasma treatment [54]. XPS analysis (see XPS section) of the plasma treated CF confirms the presence of C-O, C=O and O-C=O bonds. These functional groups contributed to enhance the adhesion between the fibre and the matrix that lead to improved mechanical and tribology properties. Further details are elaborated in the mechanical and tribology analysis section.

5.5.5. Surface area measurement.

The surface area of the carbon fibres before and after plasma treatment was evaluated with nitrogen adsorption at -196^{o} C according to the standard Brunauer, Emmett, and Teller (BET) method using Auto Sorb AS1Win^{TM}, Quantachrome instrument. The various specimen were outgassed at 220 ^{o}C for 3 hours prior to measurements. Analysis shows that the surface area of the CF increased after the plasma treatment. The surface area values are 2 $\pm$ 0.2 m^2/g for untreated CF, 2.9 $\pm$

0.1 m^2/g for CF-100W and 3.4 $\pm$ 0.2 m^2/g for CF-200W respectively. The enhancement of the surface area is due to the micro-pitting and erosion of the surface of CF due to the action of the plasma radicals [55, 56].

5.5.6. Wettability Test

Wettability test was utilized to study the effects of surface modification on the adhesion of the carbon fabric with the epoxy matrix. Carbonized cotton fabrics before and after plasma treatment were cut in dimensions of 2.5 cm x 2.5 cm, weighed and dipped in epoxy resin (HEXION. EPIKOTE TM Resin MGS® RIM 135) for 5 minutes. The specimen were then hanged under the fume hood to drop off the excess epoxy. The amount of the epoxy retained by the untreated and the treated fabrics was studied by weighing the specimen after 1 hour and 24 hours. The plasma treated fabrics showed a better epoxy adhesion to the matrix. The retention of epoxy by the untreated CF was taken as reference. After 1 hour the 100 W treated specimen showed a 28% larger resin retention while the 200W treated specimen showed a 26% larger retention as compared to the reference. After 24 hours, the analysis showed that the resin retention to the matrix was still larger than reference: 23% more for CF-100W and 25% more for CF-200W (fig. 5.13 b). The higher retention of the matrix is due to the surface morphology and chemical groups induced on CF after the plasma treatment. Similar studies have been reported by Tiwari et.al [57].

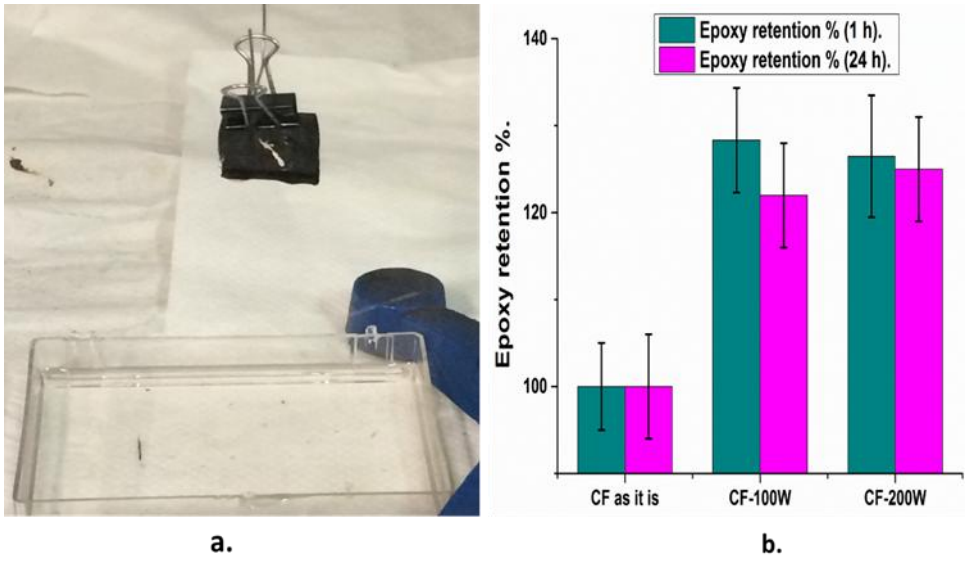

Figure 5.13: Wettability test.

5.6. Composite preparation

Carbonized strips were shredded to fibrous form with the aid of an industrial pulverizer (Savatec BB90E). The carbon fibres were then dispersed in epoxy resin (HEXION. EPIKOTE TM Resin MGS® RIM 135). An overhead mixer (Ultra-Turrax T18) was employed at a speed of 20,000 rpm for 2 minutes. Cross linker (EPIKURE TM Curing Agent MGS ® RIM H 137) was then added. The composite mixture was subsequently sonicated in Elma sonic (S15H) for 15 minutes. For degasing, the composite mixture was left in a vacuum chamber (50 mbar) for 20 minutes. The composite mixture was cured at 60 °C for 4 hours in the oven and molded into dog-bone shape (ASTM D 638-04 standard) for mechanical analysis [58, 59] and 25 mm X 25 mm X 5 mm blocks for the tribology analysis.

5.7. Composites analysis

5.7.1. Morphology of the composites

The dispersion and the interaction of the fibres in the matrix was studied through FESEM. The specimens were fragile fractured by liquid nitrogen and

coated with a 5 nm thick Chromium layer to avoid the charging effects during the measurements. The dispersion and interaction of the CF with the matrix is shown in figure 5.14. Carbon fibres are unbundled and homogenously dispersed in the matrix. The fibres extend between the layers of the matrix (fig.5.14 b-f). The fibres are anchoring the applied stress in this way by retarding the crack onset and accumulation as well as the obstructing the layer slippage of the polymer matrix. The pullout and cavitation phenomena of the carbon fibres from the matrix during the applied stress is visible in FESEM images (fig.5.14 d-e). The effects of these mechanisms on the polymer properties are discussed in the mechanical section.

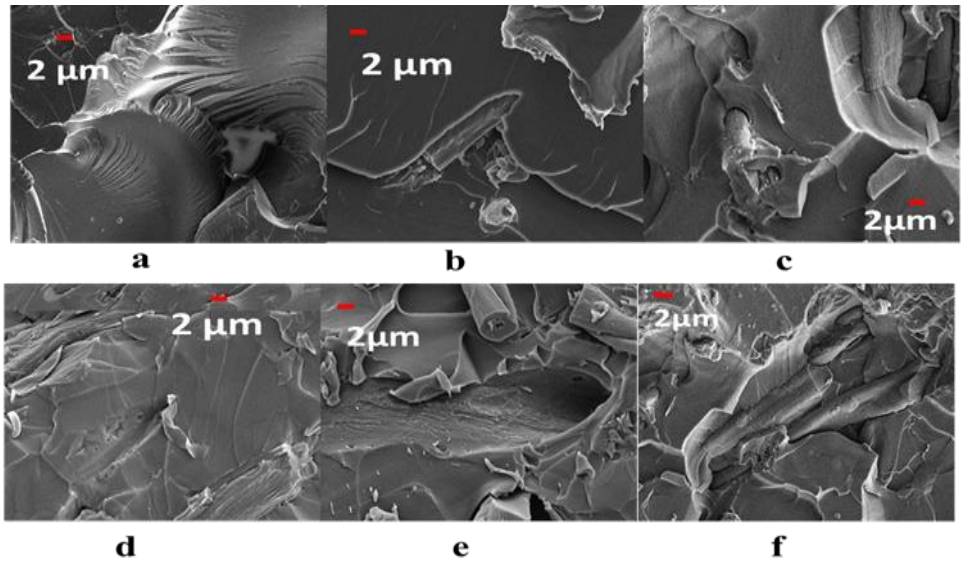

Figure 5.14: Morphology of the composites. (a) E-0, (b) E-CF-1, (c) E-CF-3, (d) E-CF-3, (e) E-CF100-3, and (f) E-CF200-3.

5.7.2. Mechanical analysis

The mechanical behavior of the composites was studied using a mechanical tester (*MTS Q-test 10*). All specimen were measured with a load cell of 10 kN and a strain rate of 1 mm/min. Stress vs strain curves were plotted and compared with neat epoxy and with composites fabricated with untreated and treated CF. Mechanical behavior is elaborated in the figures 5.15 ~ 5.17. Addition of a small amount of the carbon fibres altered the mechanical behavior of the epoxy matrix. Ductility was induced in the brittle matrix. Important design parameters like ultimate tensile strength (UTS), resilience and tensile toughness enhanced due to the addition of the carbon fibre. The plasma treated CF further enhanced the robustness of the matrix. Resilience (the measure of the energy absorbed per unit

volume in the elastic region) increased by 2.5 times by using only 3 wt% of carbon fibre as compared to the neat epoxy. Surface modified CF further enhanced the resilience by almost 4 times with the same weight percent. Carbon fibres functionalized at higher plasma powers (200W) didn't affect the resilience substantially as shown in figure 5.16 a.

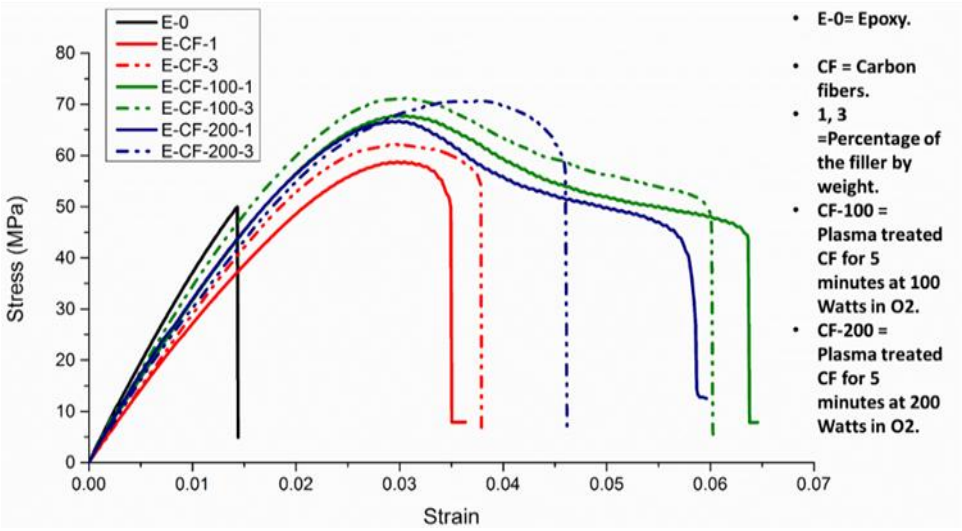

Figure 5.15: Mechanical analysis on the compoistes.

UTS of the epoxy matrix enhanced from 50 MPa to 62 MPa after reinforcement with carbon fibres. Plasma treated CF further enhanced the load bearing capacity of the matrix. A UTS value of 71 MPa, almost 1.5 times the blank epoxy was shown by the specimen E-CF-100-3. CF treated at higher powers didn't contribute much to the UTS.

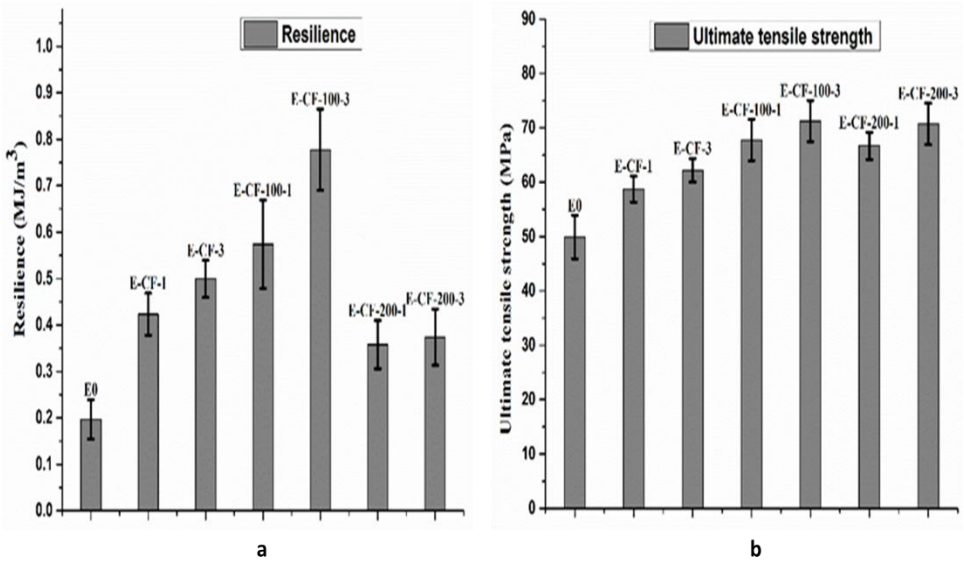

Figure 5.16: (a) Resilience and (b) UTS comparison of the composites.

Addition of small amounts of the carbon fibres enhanced the tensile toughness too. Tensile toughness is the amount of energy absorbed during the total course of load application until the failure of the specimen. The composite specimen of 100 W plasma treated carbon fibres at 3 wt% show the best results by increasing the toughness by 8.5 times compared to blank epoxy value (fig. 5.17 a). The important mechanical properties were improved without significantly affecting the stiffness of the matrix as shown in figure 5.16 b. This shows that ductility can be induced in the fragile epoxy matrix by adding small amounts of the carbon fillers without compromising its stiffness.

The improvement in the tensile properties of the composites of plasma treated carbon fibres is due to the chemical groups formed on the surface after the plasma treatment. A large amount of surface active groups and sites for chemical bonding generated by plasma treatment enhanced the adhesion between the fibres and the matrix at the interface [27]. The higher surface area of the plasma treated CF also ensured better interfacial adhesion with the matrix. Adhesion between the CF and the matrix at the interface provides an adequate stress transfer through the matrix and reduces the stress concentration at the fibre/polymer interface. Consequently the composite increases its ability to withstand the applied tensile load [60]. The mechanisms of enhanced interfacial adhesion is a twofold process. On one hand the functionalization increases the wettability of the carbon fibres by the resin due to change in surface morphology. On the other hand the functional groups allow the formation of strong chemical bonding between the matrix and fibres [61-63].

Saleh et al.2011 [64] and Pittmann et al.1998 [65] reported the enhancement of mechanical properties of the epoxy/carbon fibres composites after plasma treatment. Jimenez et al.2007 [66] reported improved mechanical properties of polymer matrix using oxidized carbon nano fibres.

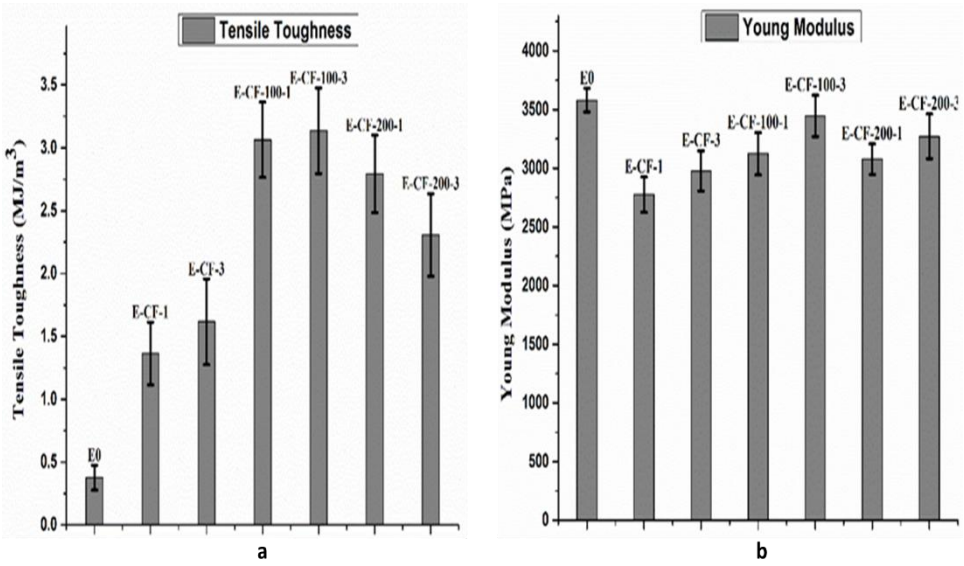

Figure 5.17: Tensile toughness and (b) Young modulus comparison of the composites.

The improvement in the mechanical properties can also be attributed to the uniform and even dispersion of the carbon fibres in the matrix (See fig. 5.14). A good even level of dispersion of the CF minimizes the stress concentration centers and improves the stress distribution uniformity [67]. The enhanced mechanical properties of the composites can further be explained by stress transfer mechanisms such as micro mechanical interlocking (fig. 5.14), chemical bonds (see XPS, FTIR analysis and wettability test) with a marginal contribution from weak Van der Waals forces between the matrix and the filler. These mechanisms are responsible for the better stress transfer through the matrix and interlocking of the matrix layers under the tensile loads which enhances the ability of the composite to resist failure under the tensile force [68, 69]. Addition of the carbon filler may also have increased the cross link ratio of the matrix which blocked the molecular motion and enhanced the matrix robustness [69-72].

5.7.3. Friction and wear properties analysis

Tribology analysis was carried out using a reciprocating tribometer (*Anton-Paar Pin-on-Disk Tribometer TRB*). The surface of the specimen was eroded with a polished steel sphere (*AISI 420*) 6 mm in diameter using a normal load of 5 N and a 3.27 mm reciprocating amplitude motion. Maximum linear speed of steel sphere was maintained at 0.185 m/s. Coefficient of friction (μ) and specific wear rate (W_r) can be estimated as

$$\mu = \frac{F_f}{F_n} \quad \text{..... (1)}$$

$$Wr = \frac{\Delta m}{L \cdot \rho \cdot Fn} \quad \text{..... (2)}$$

Where, 'F_f' is friction force parallel to the sliding surfaces, 'F_n' is the normal load, 'ρ' is the density (g/cm^3) of the specimen, 'L' is sliding distance and 'Δm' (g) is the mass loss after the test.

Neat epoxy shows high values of friction coefficient and high mass loss during the sliding contact with the steel ball. Addition of a small amount of the carbon fibres reduces the friction coefficient and the mass loss significantly. At 3 wt% addition of the untreated fibre the friction coefficient decreased by 50% while the weight loss was reduced to 52% as shown in figure 5.18 a. The composites containing 1 wt% and 3 wt% of functionalized carbon fibres reduced the friction co-efficient by 66% and 77% respectively for 100 W plasma treatment. The values for 200 W plasma treated CF show a 58% and 84% reduction in friction coefficient for 1 wt% and 3 wt% respectively (fig. 5.18a). The specific wear rate was reduced by 71% by using 3 wt% of fibres treated at 100 W and by 76% by using 3 wt% of fibres treated at 200 W. For the untreated and the treated CF the increase in the CF amount reduces the friction coefficient and the specific wear rate. Plasma treated carbon fibres performed better than their untreated counterparts as depicted in figure 5.18. Zhang et al 2007 [63] reported the improved wear and friction properties of functionalized short-cut carbon fibre/polyimide composites. Cui et al 2013 [73] attributed the improved wear and friction properties of MWCNTs/epoxy composites to the addition of oxygen containing functional groups to the MWCNTs through surface modification. After surface modification the interfacial adhesion with the matrix improves and the filler can better protect the matrix by forming chemical bonds with the matrix [73]. Our findings are in conformance to the published research. It is also expected that the improved mechanical properties of polymer lead to better

tribological properties [74]. The better dispersion of the plasma treated carbon fibres in the matrix led to a better load transfer at the contact surface with the steel ball [75]. The carbon fibres protected the matrix from deterioration as evidenced by FESEM images (fig. 5.19). The width of the canal made by steel ball was highest in the blank epoxy and lowest in the E-CF 200-3 samples with values of 720 μm and 205 μm respectively.

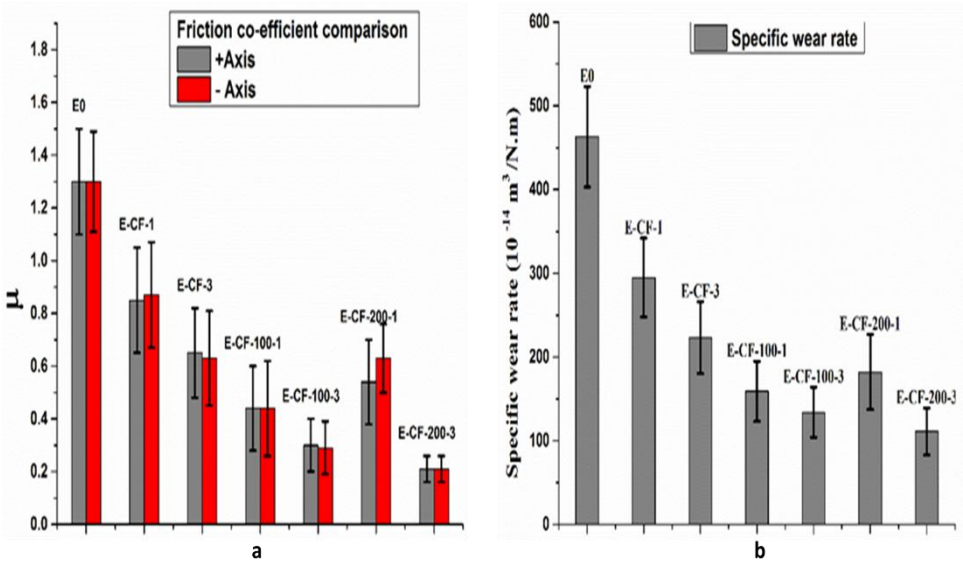

Figure 5.18: (a) Friction and (b) wear properties comparison of the composites.

Phenomena like micro melting and mechanical deterioration caused by the friction heat can be seen on the surface of all the composites samples, though the magnitude of the surface damage varies among different samples. Surface of the untreated CF composites show large and deep surface cracks and crevices and debris in the worn area which indicates a high wear loss. On the other hand, the plasma treated fibres protected the matrix from deterioration (fig.5.19 e&f) due to better interfacial adhesion to the matrix [26, 73]. The carbon fibres acted as spacers between the steel abrader and matrix and thus reduced the matrix deterioration as evident in the FESEM (fig.5.19 d~f) images. Schon 2004 [76], and Lei Yan et al 2013 [77] reported a similar behavior for carbon fibres/epoxy and MWCNTs/epoxy composites for better friction and wear properties. The self-lubricating property of carbon fibres may also help to reduce the friction co-efficient [78]. We recommend further research in this area for better understanding the mechanisms leading to tribological properties.

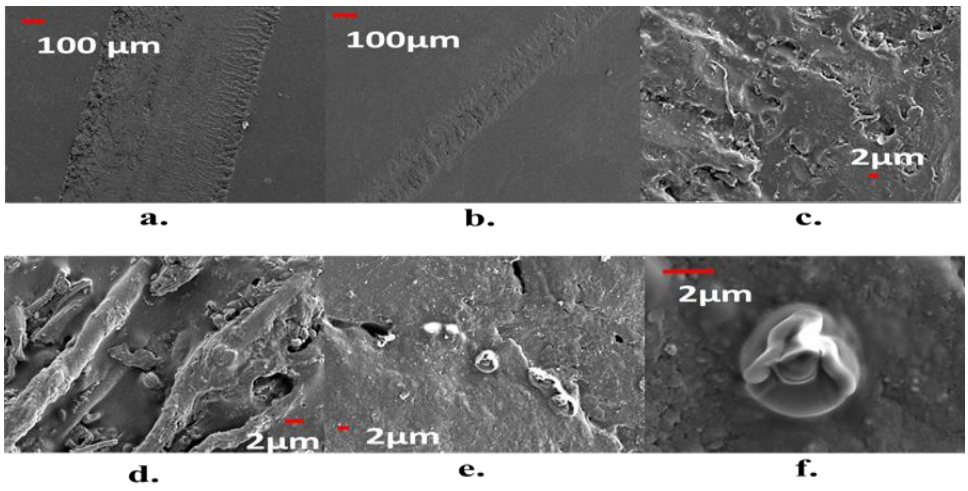

Figure 5.19: FESEM images of the worn surfaces, (a) blank, (b) E-CF200-3, (c) E-CF-1, (d) E-CF-3, (e) E-CF200-3, and (f) E-CF200-3.

5.8. Conclusions

In this chapter we reported the following achievements.

- Waste cotton clothes can be used as an alternate cheap precursor to synthesize carbon fibres.The obtained carbon fibres can reinforce polymers for improved tensile and tribology properties. The surface of CF can be modified by the plasma treatment. The surface modified CF can further enhance the polymer properties.
- Vacuum Plasma treatment on CF in an oxygen environment efficiently modifies the surface morphology of the fibres as shown in the FESEM images. Specific surface area increases after the plasma treatment. The chemical modification of the CF surface due to plasma treatment was confirmed by FTIR and XPS analysis. A high surface area and the functional groups provided better adhesion between the carbon fibres and the epoxy matrix, manifested by the wettability test. Consequently the tensile and tribology properties of the epoxy resin improved significantly.

5.9. References

1. Azarova, M.T.; Kazakov, M.E. World production and consumption of carbon fibres. *Fibre Chemistry* **2011**, *42*, 271.
2. Kim, K.-W.; Kim, D.-K.; Kim, B.-S.; An, K.-H.; Park, S.-J.; Rhee, K.Y.; Kim, B.-J. Cure behaviors and mechanical properties of carbon fiber-reinforced nylon6/epoxy blended matrix composites. *Composites Part B: Engineering* **2017**, *112*, 15-21.
3. Liu, Y.; Zhang, X.; Song, C.; Zhang, Y.; Fang, Y.; Yang, B.; Wang, X. An effective surface modification of carbon fiber for improving the interfacial adhesion of polypropylene composites. *Materials & Design* **2015**, *88*, 810-819.
4. Vaidya, U.K.; Chawla, K.K. Processing of fibre reinforced thermoplastic composites. *International Materials Reviews* **2008**, *53*, 185-218.
5. Lee, S.-J.P.a.S.-Y. Carbon fibers, history and structure of carbon fibers. *Springer Series in Materials Science* **2015**, *210*, 1~30.
6. Jazaeri, E.; Tsuzuki, T. Effect of pyrolysis conditions on the properties of carbonaceous nanofibers obtained from freeze-dried cellulose nanofibers. *Cellulose* **2013**, *20*, 707-716.
7. O. Naboka, K.R., A. F. Toomadj, A. Sanz-Velasco, G. Toriz, P. Lundgren, P. Enoksson, P. Gatenholm Carbon nanofibers synthesized from electrospun cellulose for advanced material applications. *Materials Science Forum* **2013**, *730-732*, 903-908.
8. Nogi, M.; Kurosaki, F.; Yano, H.; Takano, M. Preparation of nanofibrillar carbon from chitin nanofibers. *Carbohydrate Polymers* **2010**, *81*, 919-924.
9. Salmon, S.; Hudson, S.M. Crystal morphology, biosynthesis, and physical assembly of cellulose, chitin, and chitosan. *Journal of Macromolecular Science, Part C* **1997**, *37*, 199-276.
10. Inbakumar, S.; Morent, R.; De Geyter, N.; Desmet, T.; Anukaliani, A.; Dubruel, P.; Leys, C. Chemical and physical analysis of cotton fabrics plasma-treated with a low pressure dc glow discharge. *Cellulose* **2010**, *17*, 417-426.
11. Kawasaki, N.; Tominaga, H.; Ogata, F.; Inoue, K.; Kankawa, M. Development of novel carbon fiber produced from waste fiber by carbonization. *Journal of oleo science* **2012**, *61*, 593-600.

12. Ekrami, E.; Dadashian, F.; Soleimani, M. Waste cotton fibers based activated carbon: Optimization of process and product characterization. *Fibers and Polymers* **2014**, *15*, 1855-1864.

13. Jieying, Z.; Zhao, Q.; Ye, Z. Preparation and characterization of activated carbon fiber (acf) from cotton woven waste. *Applied Surface Science* **2014**, *299*, 86-91.

14. Wang, S.; Ren, Z.; Li, J.; Ren, Y.; Zhao, L.; Yu, J. Cotton-based hollow carbon fibers with high specific surface area prepared by ammonia etching for supercapacitor application. *RSC Advances* **2014**, *4*, 31300-31307.

15. Tiwari, S.; Sharma, M.; Panier, S.; Mutel, B.; Mitschang, P.; Bijwe, J. Influence of cold remote nitrogen oxygen plasma treatment on carbon fabric and its composites with specialty polymers. *Journal of Materials Science* **2011**, *46*, 964-974.

16. Shen, X.-J.; Pei, X.-Q.; Liu, Y.; Fu, S.-Y. Tribological performance of carbon nanotube–graphene oxide hybrid/epoxy composites. *Composites Part B: Engineering* **2014**, *57*, 120-125.

17. Montes-Morán, M.A.; Martínez-Alonso, A.; Tascón, J.M.D.; Young, R.J. Effects of plasma oxidation on the surface and interfacial properties of ultra-high modulus carbon fibres. *Composites Part A: Applied Science and Manufacturing* **2001**, *32*, 361-371.

18. Dilsiz, N.; Erinç, N.K.; Bayramli, E.; akovali, G. Surface energy and mechanical properties of plasma-modified carbon fibers. *Carbon* **1995**, *33*, 853-858.

19. Li, R.; Ye, L.; Mai, Y.-W. Application of plasma technologies in fibre-reinforced polymer composites: A review of recent developments. *Composites Part A: Applied Science and Manufacturing* **1997**, *28*, 73-86.

20. Sharma, M.; Gao, S.; Mäder, E.; Sharma, H.; Wei, L.Y.; Bijwe, J. Carbon fiber surfaces and composite interphases. *Composites Science and Technology* **2014**, *102*, 35-50.

21. Nie, Y.; Hübert, T. Surface modification of carbon nanofibers by glycidoxysilane for altering the conductive and mechanical properties of epoxy composites. *Composites Part A: Applied Science and Manufacturing* **2012**, *43*, 1357-1364.

22. Nohara, L.B.; Petraconi Filho, G.; Nohara, E.L.; Kleinke, M.U.; Rezende, M.C. Evaluation of carbon fiber surface treated by chemical and cold plasma processes. *Materials Research* **2005**, *8*, 281-286.

23. Wen, H.-C.; Yang, K.; Ou, K.-L.; Wu, W.-F.; Chou, C.-P.; Luo, R.-C.; Chang, Y.-M. Effects of ammonia plasma treatment on the surface

characteristics of carbon fibers. *Surface and Coatings Technology* **2006**, *200*, 3166-3169.

24. Zhu, Y.; Bakis, C.E.; Adair, J.H. Effects of carbon nanofiller functionalization and distribution on interlaminar fracture toughness of multi-scale reinforced polymer composites. *Carbon* **2012**, *50*, 1316-1331.

25. Zhao, M.; Meng, L.; Ma, L.; Wu, G.; Wang, Y.; Xie, F.; Huang, Y. Interfacially reinforced carbon fiber/epoxy composites by grafting melamine onto carbon fibers in supercritical methanol. *RSC Advances* **2016**, *6*, 29654-29662.

26. Kim, S.S.; Yu, H.N.; Lee, D.G.; Murayama, H.; Kageyama, K. Tribological behaviors of plasma-treated carbon composite grooved surfaces. *Composite Structures* **2010**, *92*, 1039-1046.

27. Feih, S.; Schwartz, P. Modification of the carbon fiber/matrix interface using gas plasma treatment with acetylene and oxygen. *Journal of Adhesion Science and Technology* **1998**, *12*, 523-539.

28. Rhee, K.Y.; Park, S.J.; Hui, D.; Qiu, Y. Effect of oxygen plasma-treated carbon fibers on the tribological behavior of oil-absorbed carbon/epoxy woven composites. *Composites Part B: Engineering* **2012**, *43*, 2395-2399.

29. Santos, A.L.; Botelho, E.C.; Kostov, K.G.; Nascente, P.A.P.; Silva, L.L.G.d. Atmospheric plasma treatment of carbon fibers for enhancement of their adhesion properties. *IEEE Transactions on Plasma Science* **2013**, *41*, 319-324.

30. Baker, R.R. Thermal decomposition of cellulose. *Journal of thermal analysis* **1975**, *8*, 163-173.

31. Várhegyi, G.; Antal, M.J.; Jakab, E.; Szabó, P. Kinetic modeling of biomass pyrolysis. *Journal of Analytical and Applied Pyrolysis* **1997**, *42*, 73-87.

32. Scheirs, J.; Camino, G.; Tumiatti, W. Overview of water evolution during the thermal degradation of cellulose. *European Polymer Journal* **2001**, *37*, 933-942.

33. Naithani, S.C.; Rao, N.R.; Singh, Y.D. Physiological and biochemical changes associated with cotton fibre development. *Physiologia Plantarum* **1982**, *54*, 225-229.

34. Tang, M.M.; Bacon, R. Carbonization of cellulose fibers—i. Low temperature pyrolysis. *Carbon* **1964**, *2*, 211-220.

35. Lie, J.A.; Hägg, M.-B. Carbon membranes from cellulose: Synthesis, performance and regeneration. *Journal of Membrane Science* **2006**, *284*, 79-86.

36. Huang, X. Fabrication and properties of carbon fibers. *Materials* **2009**, *2*, 2369.

37. Briggs, D.; Beamson, G. Primary and secondary oxygen-induced c1s binding energy shifts in x-ray photoelectron spectroscopy of polymers. *Analytical Chemistry* **1992**, *64*, 1729-1736.

38. Wang, M.; Long, X.; Du, J.; Sun, C.; Fu, S.; Xu, C. X-ray photoelectron spectroscopy analysis of cotton treated with the tbcc/h2o2/nahco3 system. *Textile Research Journal* **2014**, *84*, 2149-2156.

39. Mitchell, R.; Carr, C.M.; Parfitt, M.; Vickerman, J.C.; Jones, C. Surface chemical analysis of raw cotton fibres and associated materials. *Cellulose* **2005**, *12*, 629-639.

40. Fortier, C. Fourier transform spectroscopy of cotton and cotton trash. In *Fourier transform-materials analysis*, InTech: **2012**.

41. Chung, C.; Lee, M.; Choe, E.K. Characterization of cotton fabric scouring by ft-ir atr spectroscopy. *Carbohydrate Polymers* **2004**, *58*, 417-420.

42. Heo, S.-J.P.a.G.-Y. Precursor and manufacturing of carbon fibres. *Springers Series in Materials Science* **2015**, *210*, 31-63.

43. Wakelyn, P.J.; Bertoniere, N.R.; French, A.D.; Thibodeaux, D.P.; Triplett, B.A.; Rousselle, M.-A.; Goynes Jr, W.R.; Edwards, J.V.; Hunter, L.; McAlister, D.D. *Cotton fiber chemistry and technology*. CRC Press: **2006**.

44. Bunsell, A.R. *Handbook of tensile properties of textile and technical fibres*. Elsevier: **2009**.

45. Schick, M.J. *Surface characteristics of fibers and textiles*. CRC Press: **1977**, Vol. 7.

46. Eren, B.; Hug, D.; Marot, L.; Pawlak, R.; Kisiel, M.; Steiner, R.; Zumbühl, D.M.; Meyer, E. Pure hydrogen low-temperature plasma exposure of hopg and graphene: Graphane formation? *Beilstein Journal of Nanotechnology* **2012**, *3*, 852-859.

47. Garino, N.; Sacco, A.; Castellino, M.; Muñoz-Tabares, J.A.; Chiodoni, A.; Agostino, V.; Margaria, V.; Gerosa, M.; Massaglia, G.; Quaglio, M. Microwave-assisted synthesis of reduced graphene oxide/sno2 nanocomposite for oxygen reduction reaction in microbial fuel cells. *ACS Applied Materials & Interfaces* **2016**, *8*, 4633-4643.

48. Wepasnick, K.A.; Smith, B.A.; Bitter, J.L.; Howard Fairbrother, D. Chemical and structural characterization of carbon nanotube surfaces. *Analytical and Bioanalytical Chemistry* **2010**, *396*, 1003-1014.

49. Bokobza, L.; Zhang, J. Raman spectroscopic characterization of multiwall carbon nanotubes and of composites.

50. Cuesta, A.; Dhamelincourt, P.; Laureyns, J.; Martinez-Alonso, A.; Tascon, J.M.D. Effect of various treatments on carbon fiber surfaces studied by raman microprobe spectrometry. *Appl. Spectrosc.* **1998**, *52*, 356-360.

51. Afanasyeva, N.I.; Jawhari, T.; Klimenko, I.V.; Zhuravleva, T.S. Micro-raman spectroscopic measurements on carbon fibers. *Vibrational Spectroscopy* **1996**, *11*, 79-83.

52. Montes-Morán, M.A.; Young, R.J. Raman spectroscopy study of hm carbon fibres: Effect of plasma treatment on the interfacial properties of single fibre/epoxy composites. *Carbon* **2002**, *40*, 845-855.

53. Long, D.A. Infrared and raman characteristic group frequencies. Tables and charts george socrates john wiley and sons, ltd, chichester, third edition, 2001. Price £135. *Journal of Raman Spectroscopy* **2004**, *35*, 905-905.

54. Park, S.-J.; Chang, Y.-H.; Moon, C.-W.; Suh, D.-H.; Im, S.-S.; Kim, Y.-C. A study of atmospheric plasma treatment on surface energetics of carbon fibers. *Bulletin of the Korean Chemical Society* **2010**, *31*, 335-338.

55. Smiley, R.J.; Delgass, W.N. Afm, sem and xps characterization of pan-based carbon fibres etched in oxygen plasmas. *Journal of Materials Science* **1993**, *28*, 3601-3611.

56. Jang, J.; Yang, H. The effect of surface treatment on the performance improvement of carbon fiber/polybenzoxazine composites. *Journal of materials science* **2000**, *35*, 2297-2303.

57. Tiwari, S.; Bijwe, J.; Panier, S. Strengthening of a fibre-matrix interface: A novel method using nanoparticles. *Nanomaterials and Nanotechnology* **2013**, *3*, 3.

58. Castellino, M.; Chiolerio, A.; Shahzad, M.I.; Jagdale, P.V.; Tagliaferro, A. Electrical conductivity phenomena in an epoxy resin–carbon-based materials composite. *Composites Part A: Applied Science and Manufacturing* **2014**, *61*, 108-114.

59. Jagdale, P.; Khan, A.A.; Rovere, M.; Rosso, C.; Tagliaferro, A. 1 multiwalled carbon nanotube–strength to polymer composite. *Nanomaterials in Joining* **2016**.

60. Lau, K.-T.; Hui, D. Effectiveness of using carbon nanotubes as nano-reinforcements for advanced composite structures. *Carbon* **2002**, *40*, 1605-1606.

61. Park, S.-J.; Oh, J.-S.; Rhee, K.-Y. Effect of atmospheric plasma treatment of carbon fibers on crack resistance of carbon fibers-reinforced epoxy composites. *Carbon letters* **2005**, *6*, 106-110.

62. Yuan, H.; Wang, C.; Zhang, S.; Lin, X. Effect of surface modification on carbon fiber and its reinforced phenolic matrix composite. *Applied Surface Science* **2012**, *259*, 288-293.

63. X. R. Zhang, X.Q.P., Q. H. Wang. The effect of fiber oxidation on the friction and wear behaviors of short-cut carbon fiber/polyimide composites. *eXPRESS Polymer Letters* **2007**, *1*, 318–325.

64. Al-Saleh, M.H.; Sundararaj, U. Review of the mechanical properties of carbon nanofiber/polymer composites. *Composites Part A: Applied Science and Manufacturing* **2011**, *42*, 2126-2142.

65. Pittman, C.U.; Jiang, W.; He, G.R.; Gardner, S.D. Oxygen plasma and isobutylene plasma treatments of carbon fibers: Determination of surface functionality and effects on composite properties. *Carbon* **1998**, *36*, 25-37.

66. Jimenez, G.A.; Jana, S.C. Oxidized carbon nanofiber/polymer composites prepared by chaotic mixing. *Carbon* **2007**, *45*, 2079-2091.

67. Coleman, J.N.; Khan, U.; Gun'ko, Y.K. Mechanical reinforcement of polymers using carbon nanotubes. *Advanced Materials* **2006**, *18*, 689-706.

68. Allaoui, A.; Bai, S.; Cheng, H.M.; Bai, J.B. Mechanical and electrical properties of a mwnt/epoxy composite. *Composites Science and Technology* **2002**, *62*, 1993-1998.

69. Bai, J.B.; Allaoui, A. Effect of the length and the aggregate size of mwnts on the improvement efficiency of the mechanical and electrical properties of nanocomposites—experimental investigation. *Composites Part A: Applied Science and Manufacturing* **2003**, *34*, 689-694.

70. Godara, A.; Mezzo, L.; Luizi, F.; Warrier, A.; Lomov, S.V.; van Vuure, A.W.; Gorbatikh, L.; Moldenaers, P.; Verpoest, I. Influence of carbon nanotube reinforcement on the processing and the mechanical behaviour of carbon fiber/epoxy composites. *Carbon* **2009**, *47*, 2914-2923.

71. Frankland, S.J.V.; Caglar, A.; Brenner, D.W.; Griebel, M. Molecular simulation of the influence of chemical cross-links on the shear strength of carbon nanotube−polymer interfaces. *The Journal of Physical Chemistry B* **2002**, *106*, 3046-3048.

72. Wang, W.; Murthy, N.S. Characterization of nanotube- reinforced polymer composites. In *Carbon nanotubes - polymer nanocomposites*, Yellampalli, S., Ed. InTech: Rijeka, 2011; p Ch. 08.

73. Cui, L.-J.; Geng, H.-Z.; Wang, W.-Y.; Chen, L.-T.; Gao, J. Functionalization of multi-wall carbon nanotubes to reduce the coefficient of the friction and improve the wear resistance of multi-wall carbon nanotube/epoxy composites. *Carbon* **2013**, *54*, 277-282.

74. Zhang, L.C.; Zarudi, I.; Xiao, K.Q. Novel behaviour of friction and wear of epoxy composites reinforced by carbon nanotubes. *Wear* **2006**, *261*, 806-811.

75. Chen, H.; Jacobs, O.; Wu, W.; Rüdiger, G.; Schädel, B. Effect of dispersion method on tribological properties of carbon nanotube reinforced epoxy resin composites. *Polymer Testing* **2007**, *26*, 351-360.

76. Schön, J. Coefficient of friction and wear of a carbon fiber epoxy matrix composite. *Wear* **2004**, *257*, 395-407.

77. Yan, L.; Wang, H.; Wang, C.; Sun, L.; Liu, D.; Zhu, Y. Friction and wear properties of aligned carbon nanotubes reinforced epoxy composites under water lubricated condition. *Wear* **2013**, *308*, 105-112.

78. Dong, B.; Yang, Z.; Huang, Y.; Li, H.-L. Study on tribological properties of multi-walled carbonnanotubes/epoxy resin nanocomposites. *Tribology Letters* **2005**, *20*, 251-254.

Chapter 6

Synthesis of carbon nano materials from waste plastic and application to composites

6.1. Introduction

Carbon Nano Tubes (CNTs) are allotropes of carbon element. They have been branded as the revolutionary material in the new age owing to their outstanding thermal, mechanical and electrical properties. CNTs possess high length to diameter ratio, large specific surface area, low-density and their resistance towards chemicals make them ideal for composite application in various industries [1-4]. CNTs reinforced polymer matrices composites have been explored for various applications in industry owing to their high strength-to-weight ratio, good resistance towards chemical and inertness to weathering affects [5-8]. The increased demand for lightweight high strength materials in the current era make CNTs reinforced polymer matrix composites an ideal material for structural applications [9,10]. But the industry of polymer–CNTs composites is still far from reaching their full potential owing to various downsides in the synthesis of CNTs at commercial scale. CNTs production processes are energy and resource intensive. Moreover high precursor cost is among the key factors [11-17]. Waste plastics like polythene and PET bottles are carbon rich materials

and have been exploited as a cheap precursor for the synthesis of CNTs in the last decade [18-20]. Waste polyethylene bags pollute the environment, both land and water, and have devastating impacts on the marine, human and wildlife health. The commonly used recycling techniques for polythene bags are incineration and landfills [21]. Unfortunately, these techniques fail to provide a permanent solution for this problem [22,23]. The use of carbon rich polythene precursor to synthesize CNTs have been explored by many researchers [24,25]. Jagdale et al. 2012, Ahmetli et al. 2013 and Borsodi et al. 2016 have exploited waste polyethylene as a cheap precursor to synthesize carbon nano materials and CNTs [26-28]. This technique reduces the production costs and may provide a permanent and profitable solution for the recycling of waste polythene bags.

A number of polymer matrices are available today. Epoxy is the most commonly utilized matrix in composite industry due to its intriguing properties. Epoxy resins show low shrinkage during curing and good mechanical properties, high degree of adhesion, good chemical and corrosion resistance [29]. Epoxy resin based components are vastly used in structural applications in aerospace industry, for joining of materials, as surface coatings and lamination of circuit boards in electronics industry [30]. Despite these intriguing properties and vast range of applications, epoxy resins are not without limitations. They become brittle after curing, consequently fracture resistance reduces, which undermines greatly their utility in applications requiring safety and durability [31]. Many researchers have reported the enhancement of mechanical and friction properties of epoxy matrix by reinforcement with CNTs. CNTs are expensive and adds cost to the final product.

In this chapter, we report the strengthening of the epoxy matrix with carbon nano materials (CNMs) based on waste plastic precursor. This approach provides a cheap filler as an alternative to expensive commercial CNTs. We compared the mechanical and the tribology properties of the composites of CNMs with the commercial CNTs composites and observed that in-house generated CNMs composites performed overall better than the commercial CNTs composites.

6.2. Materials and Methods

Two types of CNMs were synthesized from waste plastic bags. The CNMs were used as fillers to reinforce epoxy matrix. Commercial Multiwall carbon nanotubes, MWCNTs, (MW2, *Cheap Tubes, USA, purity 95%*) based composite

were fabricated to compare with the composites of the CNMs. The CNMs were synthesized by chemical vapour deposition (CVD) technique with waste polyethylene bags were used as precursors. Nitrogen gas atmosphere (50 ml/min) was maintained during the CVD process. The CNMs growth was carried out for 1 hour at 800º C at a heating ramp rate of 15º C/ minute. The CVD system was let to cool down in ambient after the synthesis process in presence of nitrogen gas. The morphology of the CNMs depends upon the gas pressure inside the CVD reactor [32]. Carbon nano beads (CNBs) named as P1 were obtained at a gas pressure of 2 bar. The other sample P2, combination of CNTs and CNBs was obtained at a reactor pressure of 1bar. 20-30 wt. % yield of carbon nano material was obtained in both cases [26, 32].

6.3. Material characterizations

6.3.1. Morphology analysis

Morphology of all carbon fillers was studied by Field Emission Scanning Electron Microscope (*FESEM-ZEISS Merlin*).Morphology of the in-house CNMs is depicted in figure 6.1 below. The morphology of the CNMs differ. P1 is an aggregate of fused carbon nano beads/balls (CNBs) while P2 type of the CNMs is a mix of carbon nano beads and carbon nanotubes (CNBs + CNTs). The beads in P1 possess diameter in the range 100 to 1000 nm while in P2 the CNTs show an estimated diameter range from 50~200 nm and CNBs depict a diameter range of 200 ~ 1000 nm. This confirms that changing the carrier gas pressure in the CVD reactor alters the morphology of the carbon particles.

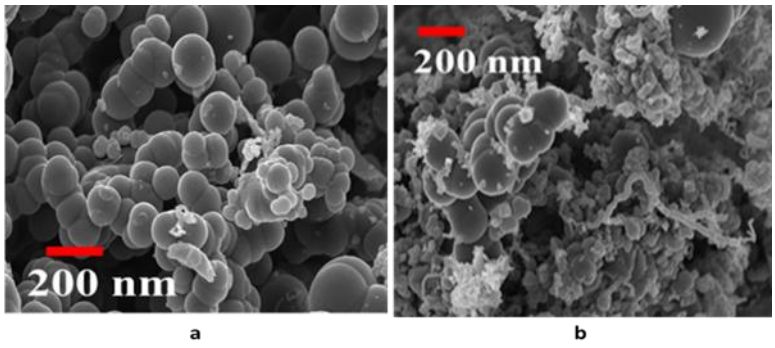

Figure 6.1: Morphology analysis (a) P1 (CNBs), (b) P2 (CNBs +CNTs).

6.3.2. Thermogravimetric analysis

The thermal stability and purity of in-house made carbon material were studied through Thermogravimetric Analysis (*TGA-Mettler Toledo*). TGA was carried out in the air at flow rate of *100 ml/min* with heating ramp rate of 5 ºC/minute at the temperature range of 25-1000º C. The CNMs start major weight losses by oxidation in air at around 400-450º C. The CNBs show a higher thermal stability compared to CNTs +CNBs. P1 degradation peaks at 581º C in DTG-TGA analysis. While P2 degradation peak is downshifted at 553º C. This slight variation in thermal stability is probably due to the mixture of two different morphological structures (CNTs and CNBs). Both P1 and P2 CNMs show the same purity level with a residue just exceeding 9 wt. % as shown in figure 6.2

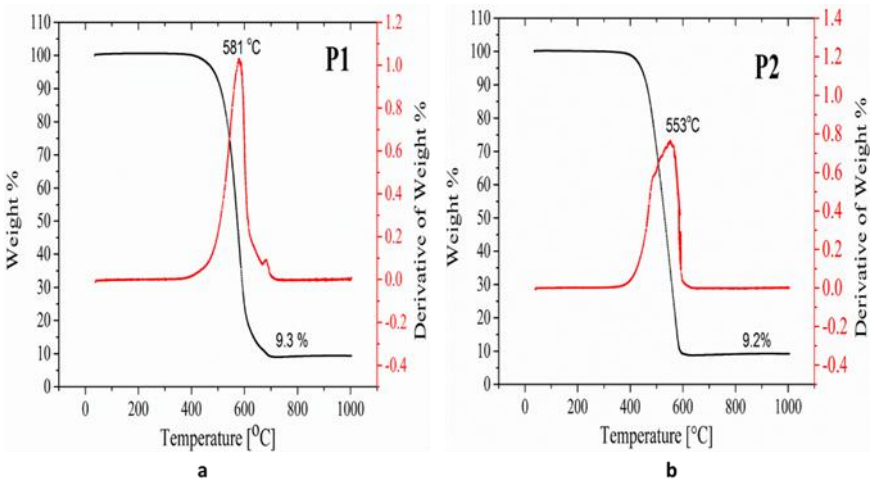

Figure 6.2: TGA analysis on the in-house generated CNMs.

The morphology and TGA analysis of all the carbon fillers are summarised in table 6.1.

Table 6.1:Morphology and purity of the various carbon materials.

Code	Type	Make	Diameter (nm)	Length (µm)	Purity %
MW2	MWCNTs	Cheap-tubes	< 8	10~30	95
P1	Beads	In house	100-1000	NA	> 90
P2	MWCNTs Beads mix	In house	Tubes 50-200 Beads 200-1000	Several	> 90

6.3.3. Raman analysis

The purity of all the carbon materials was studied with Raman (Renishaw ® Ramanscope InVia H43662 model) spectroscopy using a green laser as a source with $\lambda=514nm$.The Raman spectra of the different carbon fillers MW2, P1, and P2 are reported in figure 6.3. All the fillers show the characteristic Raman D and G peaks associated with carbon materials at the respective frequencies [33]. The D and G peaks were fitted with a Gaussian function to estimate the area under the curve to calculate I_D/I_G ratio. The I_D/I_G ratio is a parameter related to the degree of order and structural defects in the carbon materials [34,35]. The commercial MWCNTs (MW2) showed the lowest value of I_D/I_G ratio 0.43 while P1 and P2 showed I_D/I_G ratios of 0.95 and 0.86 respectively (see table 6.2).

Table 6.2: D & G raman peaks position and ID/IG ratio of the carbon materials.

Sample	D-peak position	G-peak position	I_D/I_G
	cm^{-1}	cm^{-1}	
MW2	1340	1572	0.43
P1	1355	1576	0.95
P2	1343	1573	0.86

The D peak is related to the size of ordered regions [36], which means a lower I_D/I_G value indicates a more ordered structure, i.e. a more graphitized structure. Other features of the Raman spectra like peak width and 2D region further assists to comment on the degree of order of the carbon materials. In the spectrum of MWCNTs, the D and G peaks are sharper compared to the width of D and G peaks in P1 and P2 spectra. Linewidths of D and G peaks are related to the spread in local disorder around Raman active bonding [37]. Thus the sharp peaks of MW2 indicate a more ordered structure. Also the 2D region in the frequency region 2400 cm^{-1} to 3500 cm^{-1} clearly show overtones in the spectrum of MW2 and only small bulges for P1 and P2 Raman spectra. MWCNTs are expected to have a more ordered structure as the more evident are the overtones the more ordered is the material [38]. That again supports the I_D/I_G value indication that MWCNTs have a more ordered structure.

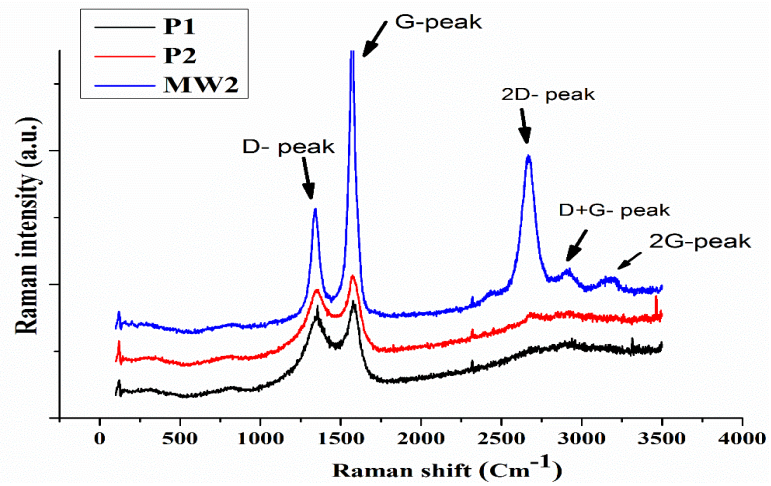

Figure 6.3: Raman analysis on the carbon materials.

6.4. Composite preparation

Epoxy resin (T19-36/700, LEUNA-Harze) was used to fabricate the composites. Carbon fillers were mixed in the matrix using an overhead mixer (ULTRA-TURRAX *T18*) was used at 20,000 rpm for two minutes according to the recipe in table one. Sonication (*Elma sonic S15H*) was subsequently utilized for 15 minutes. Degassing was carried out in a low pressure vacuum chamber (50 mbar) for 20 minutes. Curing was carried out in an oven at 70° C for 4 hours [6] and molded in dog-bone shapes according to the *ASTM D 638-4*. The dimension accuracy was set at ± 0.1 mm for all samples [11]. Four specimen for every filler type and concentration were prepared to verify reproducibility.

Table 6.3: Recipe for compoiste preparation.

Specimen	Monomer (g)	Cross-linker (g)	Nano-filler (g)
Blank epoxy	63.00	37.00	-
1% Filler	62.37	36.63	1.00
3% Filler	61.11	35.89	3.00

6.5. Composites analysis

6.5.1. Morphology of the composites

The dispersion of the carbon fillers in the matrix was studied with electron microscopy.The composites specimens were fragile fractured in liquid nitrogen and coated with a 5 nm thick chromium layer to avoid the charging effect in FESEM. Neat epoxy resin shows plain surface as depicted in figure 6.4 a. MW2 show a good dispersion in the matrix although agglomerations of MW2 can be seen in the matrix. MWCNTs bridge between the layers of polymer that leads to interlocking of the matrix layers see figure 6.4 b. Increasing weight of the MW2 (3%) shows large agglomerates in the matrix. P1 can be seen evenly dispersed in the matrix and fixed firmly between the polymer layers. The CNBs leave a detaching / pull out mark while the composite failed during the mechanical analysis (see fig. 6.4d). This behaviour indicates a better surface contact and physical bonds with the matrix. Higher weight (3%) of the filler forms large agglomerates in the matrix. P2 filler shows a uniform dispersion throughout the matrix. The beads can be seen resting firmly in the matrix while the tubes extend through the polymer layers. This way of interaction confirms a superior interlocking of the matrix leading to better mechanical properties (figure 6.4 f &g).

<table>
<tr><td></td><td colspan="2">FESEM</td></tr>
<tr><td>Neat Epoxy</td><td colspan="2"> 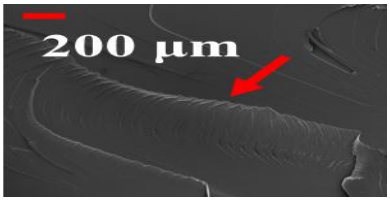

(a).</td></tr>
<tr><td></td><td>1wt. %</td><td>3 wt.%</td></tr>
<tr><td>MW2</td><td> 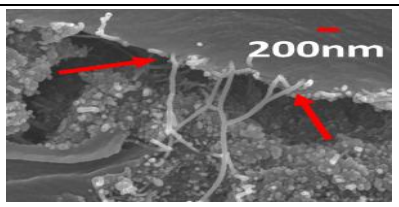

(b).</td><td> 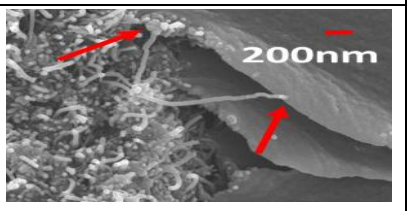

(c).</td></tr>
</table>

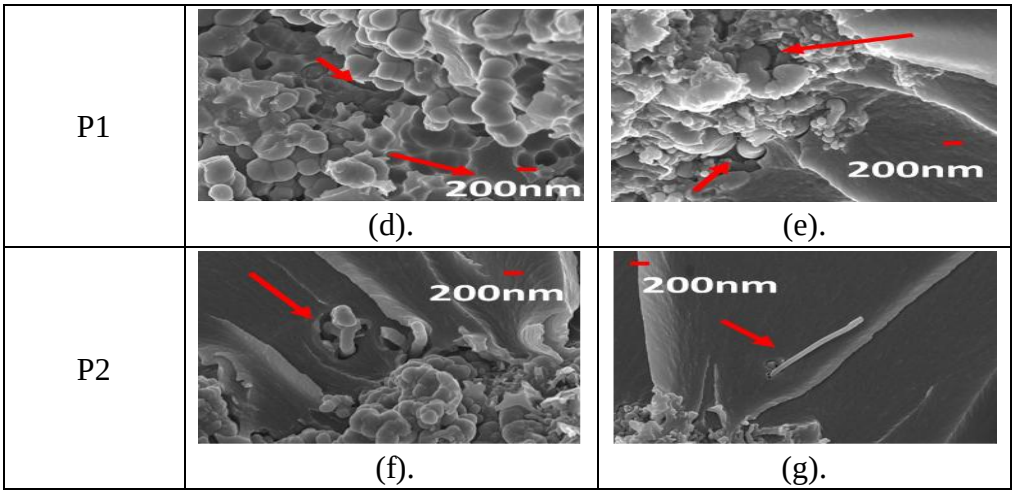

Figure 6.4: Morphology of compoistes based on the various carbon fillers.Arrows elaborate the interaction of the filler with the matrix.

6.5.2. Mechanical analysis

The mechanical properties of the composites was studied using a tensile tester (*MTS Q-test 10*) with a load cell of 10kN and a strain rate of 0.5 mm/min. Stress vs. strain data was plotted in Origin 9.0 software and compared with the neat epoxy resin and among each other. The evolution of mechanical properties of the polymer matrix with the addition of the different weight of the carbon fillers used is presented in the figure 6.5 below. Pure epoxy displays a brittle behaviour with an ultimate tensile strength (UTS) at 17.7 MPa and a strain limit of 0.01. Addition of the various carbon fillers in epoxy changes the brittle behaviour to ductile. Addition of 1 wt. % of MW2 enhanced the UTS to 32.18 MPa. Increasing the filler weight didn't add to the mechanical properties substantially. Similar behaviour was displayed by the composites formed with P1 and P2. Important mechanical properties like Ultimate tensile strength, Resilience and tensile toughness increased with a slight compromise of the Young modulus. The nominal stress vs strain graphs are discussed in detail in the following paragraphs.

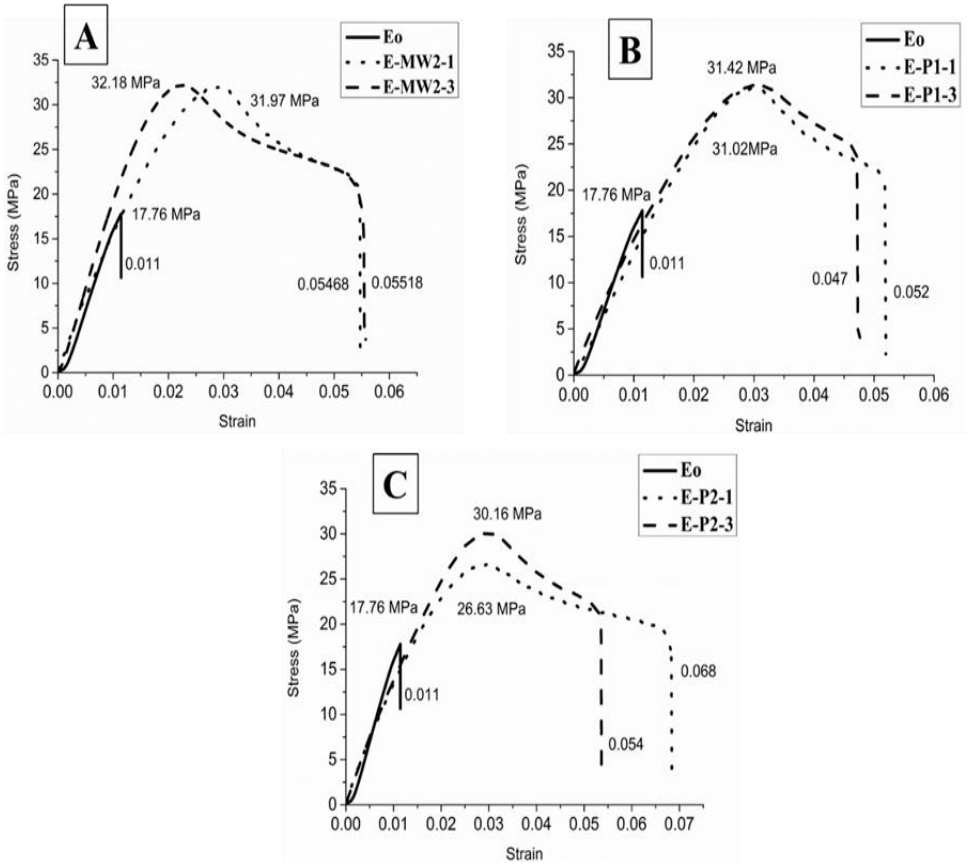

Figure 6.5: Tensile behavior of the various composites based on the carbon fillers.

a. Ultimate tensile strengths (UTS)

Addition of 1 wt. % and 3 wt. % of all the carbon fillers increased the UTS of the epoxy matrix (17.7 MPa). MWCNTs at 1 wt. % show the best improvement in UTS with 82%, compared to the blank epoxy. The in-house generated CNMs (P1) show a slightly lower UTS of 31.42 MPa at 1 wt. % while the P2 filler show a maximum strength of 30.16 MPa. This indicates that the cheap precursor based CNMs can be used as an alternative to the expensive commercial MWCNTs. The comparison of the UTS of the various fillers and their respective percentages with respect to neat epoxy is presented in the figure 6.6 a.

b. Young Modulus

Neat epoxy displays a Young modulus of roughly 1700 MPa. Mechanical analysis depicts that the addition of the carbon fillers slightly undermines this value apart from the MWCNTs 3 wt. % sample. While the other important mechanical properties increase a slight compromise in the Young modulus is acceptable w.r.t to the design safety. Figure 6.6 b shows a comparison of Young modulus of the different composites.

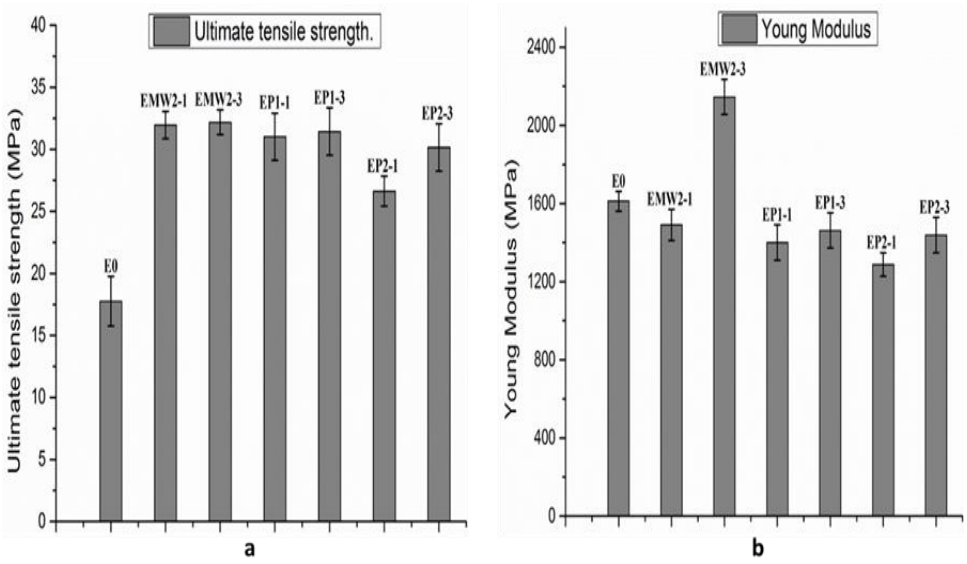

Figure 6.6: (a) Ultimate tensile strenght and (b) Young Modulus comparison.

c. Yield point

The plastic region starts at the yield point and is very important in the design of an element. The yield point is the failure threshold for any material where the material starts inheriting plasticity before the complete failure under a tensile load. Addition of a small amounts of the carbon fillers increased the yielding limit of the neat epoxy. Composites fabricated from CNMs and MWCNTs show comparable values of the yield stress and yield strain as shown in the figure 6.7.

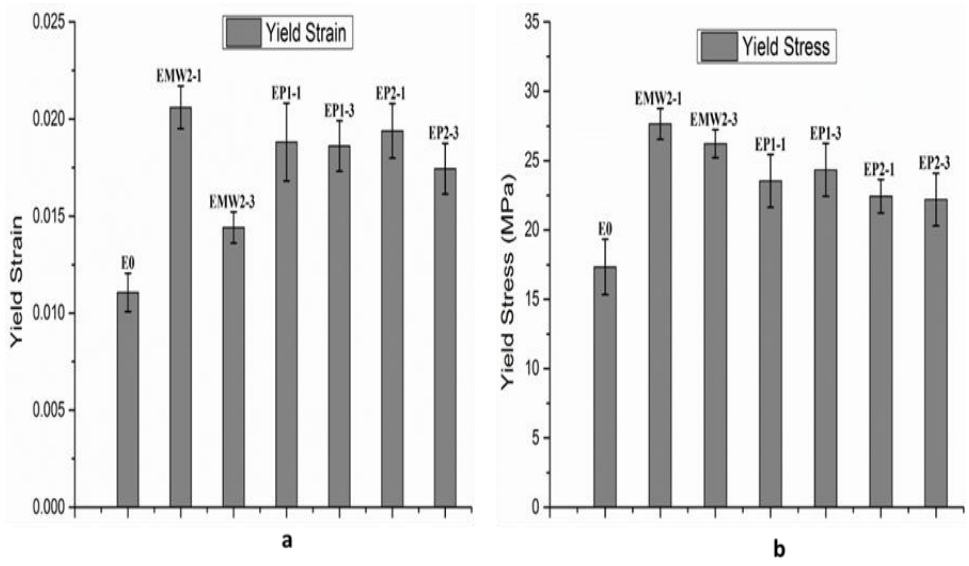

Figure 6.7: (a) Yield strain, (b) Yield stress comparison.

d. Resilience

Resilience corresponds to the maximum value of the elastic energy density that the material can withstand before the onset of plastic deformation. Addition of the carbon fillers enhanced the resilience of the neat epoxy with MWCNTs showing best results. An increase of 300% has been observed by 1 wt. % addition of MW2. As soon as the filler weight is increased the resilience goes down by roughly half the value at 1 wt. % MW2. CNMs show a better trend in this regard. An increase of 125% is observed for both fillers P1 and P2 that remains quite stable at higher wt. % of the filler used. A comparison is shown in the figure 6.8 a.

e. Tensile Toughness

Tensile toughness is the total energy density absorbed by the material during the course of a tensile test before complete failure. High toughness values guarantee a less sensitivity of the material to the stress intensity factor. Additionally, the higher is the tensile toughness (ductility), the higher is the fracture toughness [39-41] and this is the reason why for increasing the safety of structural applications, a ductile material is preferred to a brittle one. An increase of 11x to 13x has been observed in tensile toughness by the addition of the various carbon fillers with P2 filler the outstanding candidate at 1 wt. % concentration as depicted in the fig. 6.8 b.

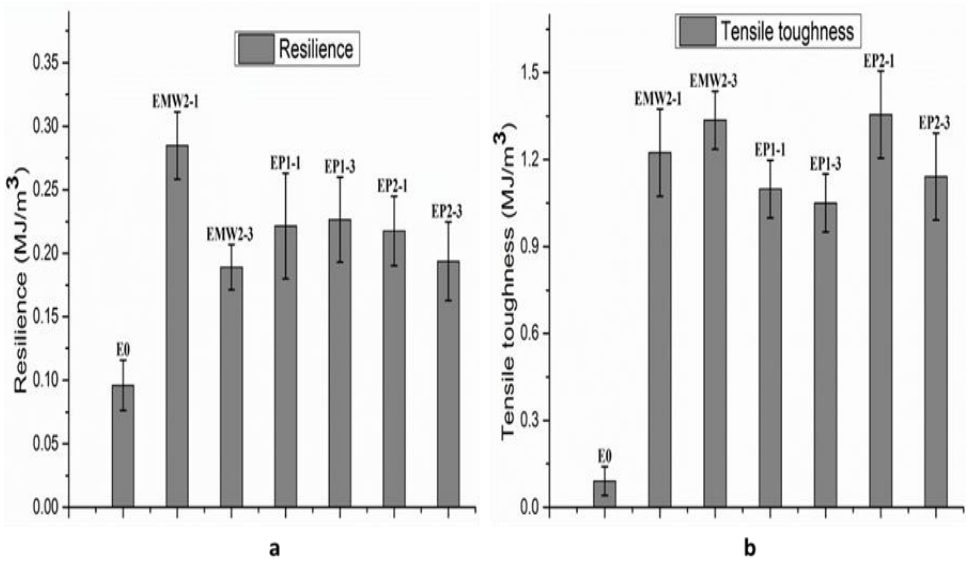

Figure 6.8: (a) Resilience, (b) Tensile toughness comparison.

6.5.3. Discusssion on the mechanical properties

Reinforcement with carbon nano fillers increases the mechanical strength of neat epoxy up to ~ 80 % and extensibility up to ~ 600 %. Addition of 1 wt. % filler seems to be more favorable for enhancing most of the tensile properties as compared to higher weight percent of the filler (3 wt. %). This behavior can be associated to the high volume of the filler (3 wt. %) for which the filler particles can be seen dispersed in large agglomerates in the matrix [42,43]. The in-house synthesized CNMs composites show comparable / better tensile properties with respect to the commercial MWCNTs. Fillers particles anchored the applied stress through the matrix and retarded the crack onset and accumulation as seen in the FESEM images [44, 45]. The CNTs protrude between the polymer layers and promote mechanical interlocking while the CNBs obstruct / divert the crack propagation during the application of the load. For this reason the combination of CNTs and CNBs over performed the other carbon fillers in the mechanical and tribology analysis. The pull out phenomenon of the filler particles from the matrix during the application of the tensile load also ensured the necessity of extra load for composite failure [46,47]. Ma et al. 2009 [48] used a hybrid filler of CNTs and carbon black particles to enhance the mechanical and electrical properties of epoxy composites with the emphasis on the hybrid filler being responsible for

better performance. Tang et al. 2012 [49] also confirmed the same phenomenon. The way the different carbon fillers interact with the matrix and anchor the applied stress is illustrated in figure 6.9. Reinforcement with carbon fillers may increase cross-link density of the polymer matrix which blocks the molecular motion and thus enhances the robustness of the matrix [50,51]. The mechanical and friction behavior changes with the higher concentration of the filler. This phenomena can be assigned to uneven dispersion of the filler particles in the polymer [52-54].

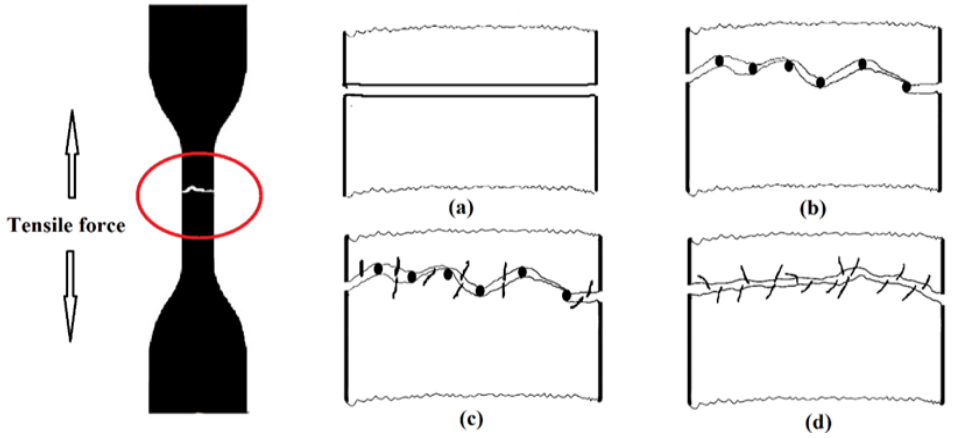

Figure 6.9: Fracture behaviour for the different composites, (a) Neat epoxy, (b) EP1, (c) EP2, (d) EMW2.

6.5.4. Tribology analysis

Anton-Paar Pin-on-Disk Tribometer TRB was used (fig.6.10 a) in reciprocating mode to study the friction coefficient and wear rate. The surface of the specimen with dimensions *20 mm x 22 mm x 5 mm* was eroded with a polished steel (*AISI 420*) sphere 6 mm in diameter with a normal load of 5N and a reciprocating amplitude of 3.27mm.

Maximum linear speed of steel sphere was maintained at 0.185 m/s. The coefficient of friction (μ) and specific wear rate are calculated as.

$$\mu = \frac{F_f}{F_n} \quad \ldots\ldots\ldots\ldots\ldots\ldots (1)$$

$$Wr = \frac{\Delta m}{L.\ \rho.\ Fn} \quad \ldots\ldots\ldots\ldots (2)$$

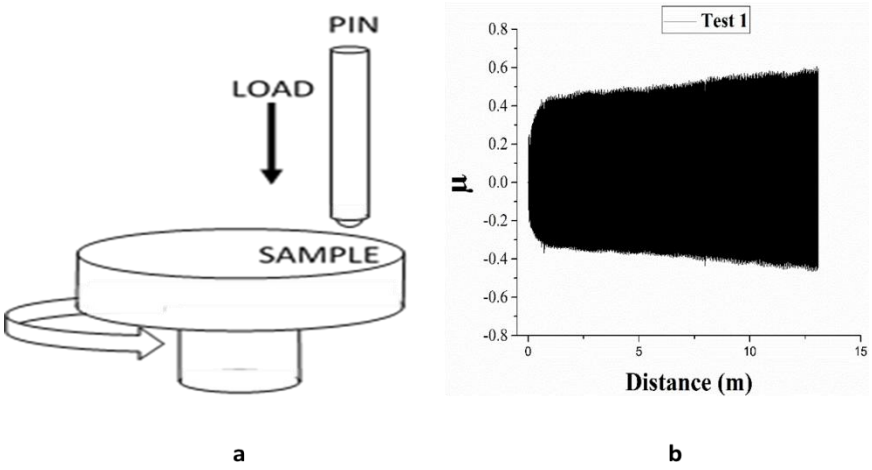

Figure 6.10: (a) Pin on disc tribometer, (b) An example of tribometer test.

Here 'F_f' is friction force parallel to the sliding surfaces, 'F_n' the normal load, 'ρ' is the density (g/cm$^{3)}$ of the specimen, 'L' is sliding distance and 'Δm' (g) is the mass loss after the after the test.

The friction co-efficient values obtained from the tribology analysis are shown in the figure 6.11 a. MWCNTs show no impact on the friction co-efficient of the epoxy resin. A steady state was reached in both 1 wt. % and 3 wt. % samples with no considerable difference. On the other hand CNMs greatly reduce the friction co-efficient and weight loss during the tribology analysis. Composites of P1 and P2 filler performed better than the commercial MWCNTs. P2 filler at 1 wt. % shows the best results with a 70 % reduction of the friction coefficient when compared to the neat epoxy. While the P1 filler reported a 35% decrease in the friction co-efficient. P1 and P2 fillers also have the lowest mass loss compared to neat epoxy and MWCNTs in the wear analysis. A comparison of friction co-efficient values for various fillers used is shown in the figure 6.11 a. Addition of 1 wt. % of the fillers decreases the wear rate of the matrix with P2 filler showing best results of 57% decrease in the wear rate. Using higher weight percentage of the filler alters the wear rate and deterioration can be seen in the wear protection capability of the composites as shown in the figure 6.11 b. Electron microscopy was performed to study the effects of abrasion on the surface of the composites as shown in figure 6.12. Neat epoxy shows a high wear rate and the width of the canal made by the abrasion of the steel ball is the broadest in neat epoxy and narrowest in the P2 filler composites. Neat epoxy, MW2, P1, P2 composites show the canal widths of 643 μm, 446 μm, 287 μm and 229 μm respectively.

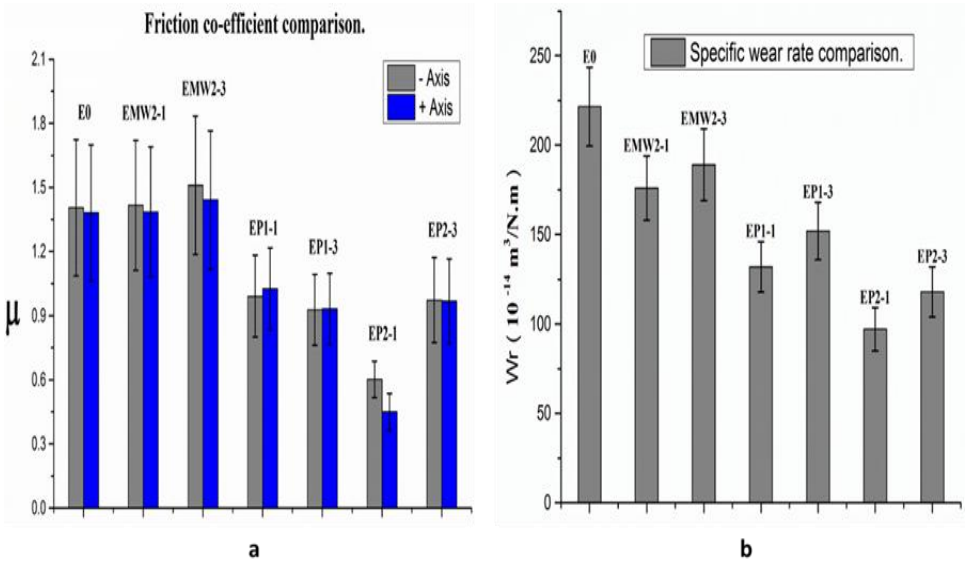

Figure 6.11: (a) Friction co-efficient, (b) Specific wear rate comparison.

Mechanical deterioration of the surface due to the abrasion of the steel ball is visible in all the samples though the magnitude of damage varies among the different samples. Neat epoxy shows deeper surface cracks and debris in the worn area indicating a high wear loss. Reinforcement with the carbon fillers protected the matrix from damage with P2 filler seems to better protect the matrix comparatively. The composites of P2 filler show least surface damage. The combination of CNBs and CNTs held the matrix well and protected it when subjected to steel ball induced wear as shown in the FESEM images. The wear rate seems to be directly proportional to the friction coefficient. This behaviour can be associated to the reduction of the tangential forces. A low co-efficient of friction means a low amount of tangential force transmitted to the surface while the normal force remains the same. In this way the global stress field reduces and consequently the wear of the matrix reduces.

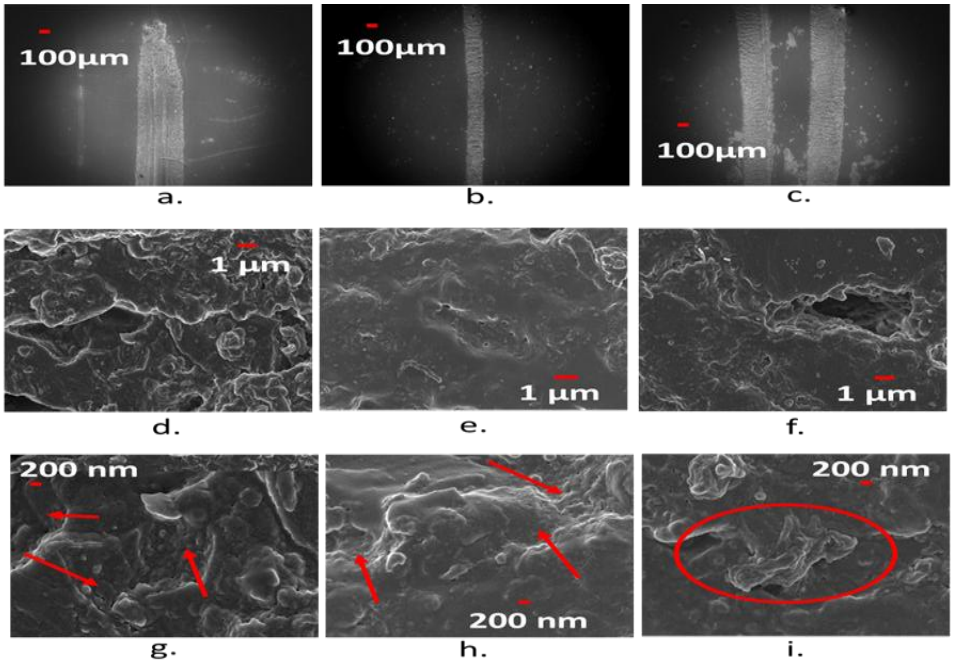

Figure 6.12: Morphology of the worn surfaces. (a) E0, (b)E-P2, (c) E-MW2, (d) E-P1, (e) E-P2, (f)E-MW2, (g) E-P1, (h) E-P2, (i) E-MW2. Arrows indicate the filler particles.

6.5.5. Discussions on the tribology behavior

Commercial MWCNTs didn't reduce the friction co-efficient and marginally reduced the matrix wear and tear of the epoxy matrix. The reason behind this behaviour can be the dispersion of the MWCNTs in form of large agglomerates in the matrix. Chen et al. 2007 [55] reported the improved tribology behaviour of epoxy composites with a uniform dispersion of the carbon nano tubes in the matrix. They reported disintegration of CNT agglomerates using a speed mixer simultaneously with an ultrasound bath. This technique ensured uniform distribution of CNTs in the epoxy matrix which conferred better friction and wear resistance properties to the composites. However we resorted to the simpler dispersion technique to further project the advantages of the waste based CNMs. The CNMs reduced the friction co-efficient and wear rate substantially at 1 wt% loading. Higher loading didn't reduce the friction co-efficient while the wear rate increased slightly. This behaviour is due to the high specific surface area of the filler (3% by weight) that results in large agglomerations of the particles in the matrix [56,57]. The improved tribological properties of the CNMs epoxy

composites can further be supported by the enhanced mechanical properties of the neat epoxy after reinforcement. The release of the carbon fillers during the course of abrasion at the interface may have served as spacers between the matrix and the ball. Consequently the filler particles prevented the close touch between the steel ball face and the matrix and slowing down the wear rate [58,59]. P2, the hybrid filler of CNTs and CNBs outperformed the other two fillers in this case. Similar behaviour was reported by Shen et al. 2014 for improved tribology properties of the epoxy resin/ CNTs-Graphene Oxide composites [60]. Tang et al. 2011[61] also confirmed the improved tribology properties of Polyamide 6 composites with a hybrid filler of para aramid fibres and nano-MOS_2 particles.

Further research in the filler dimensions, shape and orientation in the matrix can help to understand the mechanisms associated with improved tribology properties of the composites.

6.6. Conclusions

We conclude that

- Waste polyethylene bags can be used as a cheap alternative precursor for the synthesis of CNMs via CVD process. Morphology of the CNMs can be altered by varying the gas pressure inside the CVD chamber.
- The hybrid filler P2 (CNBs + CNT) outperformed the commercial MWCNTs in the mechanical and tribology properties of the composites. P2 fillers shows tensile toughness, and strength comparable to the MW2 composites and superior tribology properties.
- The mechanical and tribology properties of the composites depict that CNMs synthesized from waste polyethylene can replace commercial MWCNTs as a cheap and environment friendly filler in composite applications.

6.7. References

1. Iijima, S.; Ichihashi, T. Single-shell carbon nanotubes of 1-nm diameter. *Nature* **1993**, *363*, 603-605.
2. Kratschmer, W.; Lamb, L.D.; Fostiropoulos, K.; Huffman, D.R. Solid c60: A new form of carbon. *Nature* **1990**, *347*, 354-358.
3. Kenny, J.M.; Valentini, L.; Puglia, D.; Terenzi, A. 8 - epoxy–carbon nanotube composites. In *Polymer–carbon nanotube composites*, Woodhead Publishing: 2011; pp 230-261.
4. Zhang, J.; Ju, S.; Jiang, D.; Peng, H.-X. Reducing dispersity of mechanical properties of carbon fiber/epoxy composites by introducing multi-walled carbon nanotubes. *Composites Part B: Engineering* **2013**, *54*, 371-376.
5. Kausar, A.; Rafique, I.; Muhammad, B. Review of applications of polymer/carbon nanotubes and epoxy/cnt composites. *Polymer-Plastics Technology and Engineering* **2016**, *55*, 1167-1191.
6. Castellino, M.; Chiolerio, A.; Shahzad, M.I.; Jagdale, P.V.; Tagliaferro, A. Electrical conductivity phenomena in an epoxy resin–carbon-based materials composite. *Composites Part A: Applied Science and Manufacturing* **2014**, *61*, 108-114.
7. Chiolerio, A.; Castellino, M.; Jagdale, P.; Giorcelli, M.; Bianco, S.; Tagliaferro, A. Electrical properties of cnt-based polymeric matrix nanocomposites. In *Carbon nanotubes - polymer nanocomposites*, Yellampalli, S., Ed. InTech: Rijeka, 2011; p Ch. 11.
8. Wang, W.; Murthy, N.S. Characterization of nanotube- reinforced polymer composites. In *Carbon nanotubes - polymer nanocomposites*, Yellampalli, S., Ed. InTech: Rijeka, 2011; p Ch. 08.
9. Zakaria, M.R.; Abdul Kudus, M.H.; Md. Akil, H.; Mohd Thirmizir, M.Z. Comparative study of graphene nanoparticle and multiwall carbon nanotube filled epoxy nanocomposites based on mechanical, thermal and dielectric properties. *Composites Part B: Engineering* **2017**, *119*, 57-66.
10. Viet, N.V.; Wang, Q.; Kuo, W.S. Effective young's modulus of carbon nanotube/epoxy composites. *Composites Part B: Engineering* **2016**, *94*, 160-166.
11. Koumoulos, E.P.; Jagdale, P.; Kartsonakis, I.A.; Giorcelli, M.; Tagliaferro, A.; Charitidis, C.A. Carbon nanotube/polymer nanocomposites: A study on mechanical integrity through nanoindentation. *Polymer Composites* **2015**, *36*, 1432-1446.

12. Bazargan, A.; McKay, G. A review – synthesis of carbon nanotubes from plastic wastes. *Chemical Engineering Journal* **2012**, *195–196*, 377-391.

13. Hsiao, K.-T.; Advani, S.; Antonucci, V. Review of polymer composites with carbon nanotubes. In *Advanced polymeric materials*, CRC Press: 2003.

14. Harris †, P.J.F. Fullerene-related structure of commercial glassy carbons. *Philosophical Magazine* **2004**, *84*, 3159-3167.

15. Shaffer, M.S.P.; Sandler, J.K.W. Carbon nanotube/nanofibre polymer composites. In *Processing and properties of nanocomposites*, WORLD SCIENTIFIC: 2012; pp 1-59.

16. O'Connell, M.J. *Carbon nanotubes: Properties and applications*. CRC Press: 2006.

17. Moniruzzaman, M.; Winey, K.I. Polymer nanocomposites containing carbon nanotubes. *Macromolecules* **2006**, *39*, 5194-5205.

18. Bazargan, A.; Hui, C.W.; McKay, G. Porous carbons from plastic waste. In *Porous carbons – hyperbranched polymers – polymer solvation*, Long, T.E.; Voit, B.; Okay, O., Eds. Springer International Publishing: Cham, 2015; pp 1-25.

19. Bajad, G.; Guguloth, V.; Vijayakumar, R.P.; Bose, S. Conversion of plastic waste into cnts using ni/mo/mgo catalyst—an optimization approach by mixture experiment. *Fullerenes, Nanotubes and Carbon Nanostructures* **2016**, *24*, 162-169.

20. Jagdale, P. Waste plastic to carbon nano material a new source for carbon nanotechnology. *Lap-Lambert publication, Germany* **2012**, 180.

21. Singh, N.; Hui, D.; Singh, R.; Ahuja, I.P.S.; Feo, L.; Fraternali, F. Recycling of plastic solid waste: A state of art review and future applications. *Composites Part B: Engineering* **2017**, *115*, 409-422.

22. Wu, C.; Nahil, M.A.; gt; Miskolczi; gt; Norbert; Huang, J.; Williams, P.T. Production and application of carbon nanotubes, as a co-product of hydrogen from the pyrolysis-catalytic reforming of waste plastic. *Process Safety and Environmental Protection* **2016**, *103*, 107-114.

23. Mishra, N.; Das, G.; Ansaldo, A.; Genovese, A.; Malerba, M.; Povia, M.; Ricci, D.; Di Fabrizio, E.; Di Zitti, E.; Sharon, M., *et al.* Pyrolysis of waste polypropylene for the synthesis of carbon nanotubes. *Journal of Analytical and Applied Pyrolysis* **2012**, *94*, 91-98.

24. Wu, C.; Nahil, M.A.; Miskolczi, N.; Huang, J.; Williams, P.T. Processing real-world waste plastics by pyrolysis-reforming for hydrogen and high-value carbon nanotubes. *Environmental Science & Technology* **2014**, *48*, 819-826.

25. Arnaiz, N.; Gomez-Rico, M.F.; Martin Gullon, I.; Font, R. Production of carbon nanotubes from polyethylene pyrolysis gas and effect of temperature. *Industrial & Engineering Chemistry Research* **2013**, *52*, 14847-14854.

26. Jagdale, P.; Sharon, M.; Kalita, G.; Maldar, N.M.N.; Sharon, M. Carbon nano material synthesis from polyethylene by chemical vapour deposition. *Advances in Materials Physics and Chemistry* **2012**, *Vol.02No.01*, 10.

27. Borsodi, N.; Szentes, A.; Miskolczi, N.; Wu, C.; Liu, X. Carbon nanotubes synthetized from gaseous products of waste polymer pyrolysis and their application. *Journal of Analytical and Applied Pyrolysis* **2016**, *120*, 304-313.

28. Ahmetli, G.; Kocaman, S.; Ozaytekin, I.; Bozkurt, P. Epoxy composites based on inexpensive char filler obtained from plastic waste and natural resources. *Polymer Composites* **2013**, *34*, 500-509.

29. Gardea, F.; Lagoudas, D.C. Characterization of electrical and thermal properties of carbon nanotube/epoxy composites. *Composites Part B: Engineering* **2014**, *56*, 611-620.

30. Nam, T.H.; Goto, K.; Yamaguchi, Y.; Premalal, E.V.A.; Shimamura, Y.; Inoue, Y.; Arikawa, S.; Yoneyama, S.; Ogihara, S. Improving mechanical properties of high volume fraction aligned multi-walled carbon nanotube/epoxy composites by stretching and pressing. *Composites Part B: Engineering* **2016**, *85*, 15-23.

31. Ghosh, P.K.; Kumar, K.; Chaudhary, N. Influence of ultrasonic dual mixing on thermal and tensile properties of mwcnts-epoxy composite. *Composites Part B: Engineering* **2015**, *77*, 139-144.

32. Jagdale, P.; Tulliani, J.M.; Tagliaferro, A.; Lopez, A.; Prestini, I.; Ferro, G. In *Carbon nano beads (cnbs): A new ingredient in reinforcing materials*, Workshop IGF, Forni di Sopra (UD), 2012; pp 113-119.

33. Bokobza, L.; Zhang, J. Raman spectroscopic characterization of multiwall carbon nanotubes and of composites. *Express Polym. Lett* **2012**, *6*, 601-608.

34. Afanasyeva, N.I.; Jawhari, T.; Klimenko, I.V.; Zhuravleva, T.S. Micro-raman spectroscopic measurements on carbon fibers. *Vibrational Spectroscopy* **1996**, *11*, 79-83.

35. Ferrari, A.C.; Robertson, J. Interpretation of raman spectra of disordered and amorphous carbon. *Physical Review B* **2000**, *61*, 14095-14107.

36. Koenig, F.T.a.J.L. Raman spectrum of graphite. *The Journal of Chemical Physics* **1970**, *53*, 1126-1130.

37. Jorio, A.; Ferreira, E.H.M.; Cançado, L.G.; Achete, C.A.; Capaz, R.B. Measuring disorder in graphene with raman spectroscopy. In *Physics and applications of graphene-experiments*, InTech: 2011.

38. Pimenta, M.A.; Dresselhaus, G.; Dresselhaus, M.S.; Cancado, L.G.; Jorio, A.; Saito, R. Studying disorder in graphite-based systems by raman spectroscopy. *Physical chemistry chemical physics : PCCP* **2007**, *9*, 1276-1291.

39. Weiss, V.; Sengupta, M. In *Correlation between the fracture toughness and material ductility*, ICF3, Munich (Germany) 1973, 2013.

40. Konur, O.; Matthews, F.L. Effect of the properties of the constituents on the fatigue performance of composites: A review. *Composites* **1989**, *20*, 317-328.

41. Manson, S.S.; Hirschberg, M.H. The role of ductility, tensile strength and fracture toughness in fatigue. *Journal of the Franklin Institute* **1970**, *290*, 539-548.

42. Tarfaoui, M.; Lafdi, K.; El Moumen, A. Mechanical properties of carbon nanotubes based polymer composites. *Composites Part B: Engineering* **2016**, *103*, 113-121.

43. Hosseini Farrash, S.M.; Shariati, M.; Rezaeepazhand, J. The effect of carbon nanotube dispersion on the dynamic characteristics of unidirectional hybrid composites: An experimental approach. *Composites Part B: Engineering* **2017**, *122*, 1-8.

44. Godara, A.; Mezzo, L.; Luizi, F.; Warrier, A.; Lomov, S.V.; van Vuure, A.W.; Gorbatikh, L.; Moldenaers, P.; Verpoest, I. Influence of carbon nanotube reinforcement on the processing and the mechanical behaviour of carbon fiber/epoxy composites. *Carbon* **2009**, *47*, 2914-2923.

45. Guan, Q.; Yuan, L.; Zhang, Y.; Gu, A.; Liang, G. Improving the mechanical, thermal, dielectric and flame retardancy properties of cyanate ester with the encapsulated epoxy resin-penetrated aligned carbon nanotube bundle. *Composites Part B: Engineering* **2017**, *123*, 81-91.

46. Üstün, T.; Ulus, H.; Karabulut, S.E.; Eskizeybek, V.; Şahin, Ö.S.; Avcı, A.; Demir, O. Evaluating the effectiveness of nanofillers in filament wound carbon/epoxy multiscale composite pipes. *Composites Part B: Engineering* **2016**, *96*, 1-6.

47. Chandra, Y.; Scarpa, F.; Adhikari, S.; Zhang, J.; Saavedra Flores, E.I.; Peng, H.-X. Pullout strength of graphene and carbon nanotube/epoxy composites. *Composites Part B: Engineering* **2016**, *102*, 1-8.

48. Ma, P.-C.; Liu, M.-Y.; Zhang, H.; Wang, S.-Q.; Wang, R.; Wang, K.; Wong, Y.-K.; Tang, B.-Z.; Hong, S.-H.; Paik, K.-W., *et al.* Enhanced

electrical conductivity of nanocomposites containing hybrid fillers of carbon nanotubes and carbon black. *ACS Applied Materials & Interfaces* **2009**, *1*, 1090-1096.

49. Tang, L.-C.; Wan, Y.-J.; Peng, K.; Pei, Y.-B.; Wu, L.-B.; Chen, L.-M.; Shu, L.-J.; Jiang, J.-X.; Lai, G.-Q. Fracture toughness and electrical conductivity of epoxy composites filled with carbon nanotubes and spherical particles. *Composites Part A: Applied Science and Manufacturing* **2013**, *45*, 95-101.

50. Bai, J.B.; Allaoui, A. Effect of the length and the aggregate size of mwnts on the improvement efficiency of the mechanical and electrical properties of nanocomposites—experimental investigation. *Composites Part A: Applied Science and Manufacturing* **2003**, *34*, 689-694.

51. Allaoui, A.; Bai, S.; Cheng, H.M.; Bai, J.B. Mechanical and electrical properties of a mwnt/epoxy composite. *Composites Science and Technology* **2002**, *62*, 1993-1998.

52. Vaisman, L.; Wagner, H.D.; Marom, G. The role of surfactants in dispersion of carbon nanotubes. *Advances in Colloid and Interface Science* **2006**, *128–130*, 37-46.

53. Kumar, A.; Ghosh, P.K.; Yadav, K.L.; Kumar, K. Thermo-mechanical and anti-corrosive properties of mwcnt/epoxy nanocomposite fabricated by innovative dispersion technique. *Composites Part B: Engineering* **2017**, *113*, 291-299.

54. Jiménez-Suárez, A.; Campo, M.; Gaztelumendi, I.; Markaide, N.; Sánchez, M.; Ureña, A. The influence of mechanical dispersion of mwcnt in epoxy matrix by calendering method: Batch method versus time controlled. *Composites Part B: Engineering* **2013**, *48*, 88-94.

55. Chen, H.; Jacobs, O.; Wu, W.; Rüdiger, G.; Schädel, B. Effect of dispersion method on tribological properties of carbon nanotube reinforced epoxy resin composites. *Polymer Testing* **2007**, *26*, 351-360.

56. Cui, L.-J.; Geng, H.-Z.; Wang, W.-Y.; Chen, L.-T.; Gao, J. Functionalization of multi-wall carbon nanotubes to reduce the coefficient of the friction and improve the wear resistance of multi-wall carbon nanotube/epoxy composites. *Carbon* **2013**, *54*, 277-282.

57. Zhang, L.C.; Zarudi, I.; Xiao, K.Q. Novel behaviour of friction and wear of epoxy composites reinforced by carbon nanotubes. *Wear* **2006**, *261*, 806-811.

58. Dong, B.; Yang, Z.; Huang, Y.; Li, H.-L. Study on tribological properties of multi-walled carbonnanotubes/epoxy resin nanocomposites. *Tribology Letters* **2005**, *20*, 251-254.

59. Yan, L.; Wang, H.; Wang, C.; Sun, L.; Liu, D.; Zhu, Y. Friction and wear properties of aligned carbon nanotubes reinforced epoxy composites under water lubricated condition. *Wear* **2013**, *308*, 105-112.

60. Shen, X.-J.; Pei, X.-Q.; Liu, Y.; Fu, S.-Y. Tribological performance of carbon nanotube–graphene oxide hybrid/epoxy composites. *Composites Part B: Engineering* **2014**, *57*, 120-125.

61. Tang, G.; Huang, W.; Chang, D.; Nie, W.; Mi, W.; Yan, W. The friction and wear of aramid fiber-reinforced polyamide 6 composites filled with nano-mos2. *Polymer-Plastics Technology and Engineering* **2011**, *50*, 1537-1540.

Chapter 7

Bio char: A versatile material to exalt polymer properties

7.1. Introduction

Different kinds of composites based on polymer matrix matrices are nowadays available on the market. In particular, composites based on epoxy resins are used as high-tech materials because of their excellent mechanical properties, chemical resistance, thermal stability and low production cost [1-5]. Some examples of such applications are glues, adhesives, surface coatings and electrical insulator. In recent years, there has been an increased interest in materials such as carbon nanotubes and graphene as reinforcements for polymers in order to increase the material performances [6-12]. However, an important aspect related to the commercialization of carbon-polymer composites is the cost reduction that can be achieved not only by cutting down the production costs but also by reducing the cost of the filler. Additionally, carbon nano tubes (CNTs) in large amounts are difficult to disperse in the matrix through conventional mechanical mixing methods. Expensive treatments such as surface functionalization with acids, plasma or coupling of CNTs with polymers are essential to achieve an optimum level of dispersion [13,14].This procedure further increases the cost of the end product and undermines the industrial application potential of CNTs.

Recently, polymer scientists and technologists have been devoting their attention to the study of ecofriendly materials derived from recycling for composites production. The development of new structural and functional materials relying on ecofriendly (i.e. biochar) sources is particularly desirable in geographical areas where biomass and other biogenic wastes are abundant [15-18]. Waste materials, obtained after removing organic components (e.g. carboxylic acids, phenols, aromatic hydrocarbon, ketons, alcohools, etc.) by pyrolysis, can be used as a new type of carbon filler to increase carbon percentage in the final products [19,20].

In this work we investigate the mechanical, friction and electrical (i.e. microwave) behavior of two different kinds of epoxy resin composites prepared using Multi-walled Carbon Nanotubes (MWCNTs) and Maple biochar as fillers. The impact of each filler on the composites' mechanical, friction and microwave properties is evaluated related to their concentration, chemical and physical properties.

7.2. Materials and methods.

- Two biochar materials were used - pristine biochar (BC) and heat-treated biochar (BCHT). BC was made from maple wood by pyrolysis at 800^{o} C under an inert atmosphere, while BCHT was produced by heating BC at 950° C under nitrogen for 4 hours. Heat treatment is known to further carbonize biochar and make it more conductive. For comparison, MWCNTs were purchased from Nanothinx Greece.
- Morphology of the bio char material, MWCNTs and composites was studied through Field Emission Scanning Electron Microscope (FESEM-ZEISS SUPRA-40TM).
- Reactivity of the two biochars was evaluated by thermal analysis and N2 physio sorption measurements. TGA and DSC analyses were accomplished by using a Q Series SDT Q600 Model (TA Instruments) thermos analyzer and by burning the samples in air, with a flow rate of 50 ml/min. Samples of approximately 30 mg were gradually heated from 30 to 1000^{o} C at a rate of 5^{o} C/min.
- The specific surface area (SSA) of the biochar powders was determined by N2 adsorption with a Quantachrome Nova 1200e

surface analyzer. Samples were degassed under vacuum for 3h at 250^{o} C prior to measurement.

- The structural quality of the biochar carbon materials and MWCNTs was investigated with Raman spectroscopy (Renishaw ® Ramanscope InVia H43662 model) with a green laser (λ = 514 nm).
- Organic functional groups charactericterizations of biochar and biochar HT were performed thorugh IR spectroscopy by using Nicolet 5700 FTIR spectrometer equipped with a Diamond crystal.
- LPL (Cores Ocean) was used as matrix to produce polymer composites with bio chars to study the mechanical and friction properties. Results are compared to ones produced from commercial multiwall carbon nanotubes.

7.3. Results

7.3.1. Morphology of the biochar and biochar HT

Fig. 7.1shows the surface morphology of the biochar and heat-treated biochar samples, determined with FESEM. It is anticipated that they have a similar surface morphology as they were manufactured from the same biomass precursor (maple wood).Heat treatment further carbonizes the biochar sample by reducing oxygen, hydrogen and nitrogen contents in biochar. Consequently, heat-treated biochar should be more electrically conductive and have a surface that is more hydrophobic. The large pores in micrometers size as shown in Fig. 1(a&b) were part of the wood structure (vessel lumen) that was retained after pyrolysis. Incidentally, the heat-treated biochar sample (BCHT) had larger vessel lumens in its precursor than the untreated biochar (BC). It should be pointed out that heat-treatment can alter micro-pores, which could lead to changes in SSA.

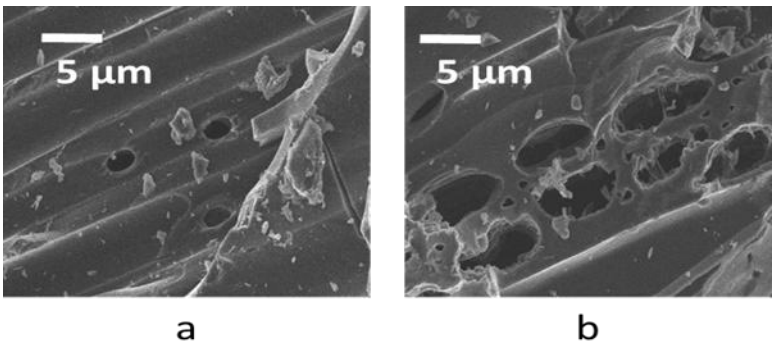

Figure 7.1: FESEM images of (a) biochar (BC) and (b) heat-treated biochar (BCHT).

7.3.2. Thermogravimetric analysis

Thermograms for Maple Biochar and HT Maple Biochar are reported in Figure 7.2 (a), and (b), respectively. Maximum combustion rate occurs at about 450^{o} C in both samples. Although none of the sample was subjected to acid treatment the residual amount of ashes (stemming from the oxidation of biochar's inorganic components. K, Ca, Na, Mg, etc.) is quite low (2.45 wt. % for the Maple Biochar and 3.0% for the HT maple biochar). The additional peak detectable in the DSC graph for the heat-treated biochar is related to the morphology and surface properties of the material. In fact, as illustrated by FESEM micrographs, the macro pores diameter for the HT Maple biochar have approximately twice the size of those of its non-treated counterpart (≈ 5 µm vs 2 µm, respectively). Needless to say, the larger macro pores size is brought about by the thermal treatment instrumental in removing the organic residues from the pores. Thus, the HT Maple biochar`s pores are more oxygen-accessible and the combustion begins at lower temperatures. Furthermore, the FESEM analysis reveals a relevant inhomogeneity in the macro pores size of the heat treat sample causing the combustion process to be multi-stepped.

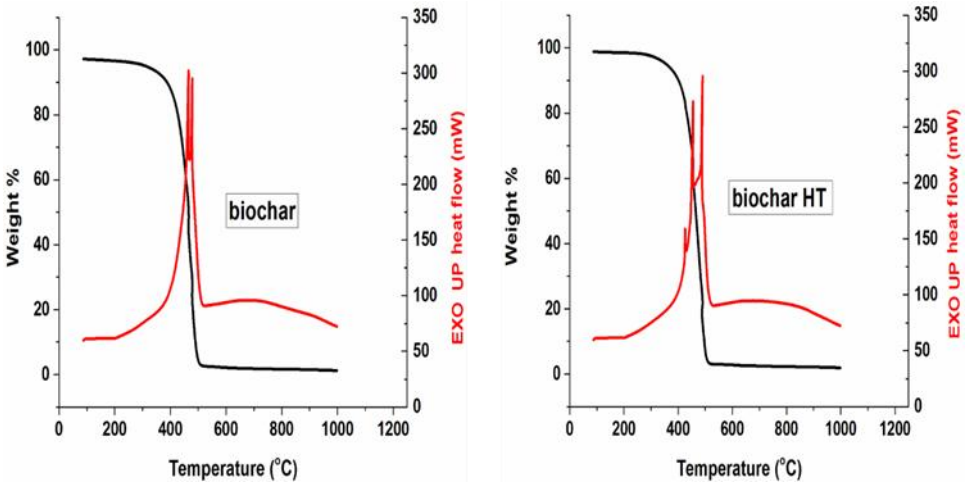

(a) (b)

Figure 7.2: TGA-DSC curves of (a) biochar and (b) biochar HT.

7.3.3. Surface area measurement

Fig. 7.3 reports the complete N2 adsorption-desorption isotherm for the HT sample and the BET fit performed in the linear range of the desorption branch. HT biochar (as well as its non-heat treated counterpart) shows a gas adsorption behavior belonging to the type II isotherms family (according to the IUPAC classification), which is typical of non-porous or microporous materials. Indeed, the adsorption branch shows the unrestricted formation of an adsorption monolayer (with a monolayer volume Vm of 9.1 cc/g) and then of multilayers. The H3 like type open hysteresis is consistent with the behavior of macro porous layered materials (e.g. clays) and it has been already reported in literature [21,22] and in the 1985 IUPAC technical report about porous materials. The biochar layered structured is confirmed by the FESEM micrographs (Fig. 1). In addition, the low pressure hysteresis without closure point is not uncommon to layered materials, especially those containing micro pores besides macro porosity [21,22] .As expected, the SSA for the HT Maple biochar is two orders of magnitude higher than the one of the non-treated biochar (170 ± 3 m2/g vs 3.4 ± 0.3 m2/g. In fact, organic residues brought about by the incomplete de-methanation, de-carboxylation and de-carbonylation of oligosaccharides, remain in the biochar's pores after the pyrolysis plugging them. The thermal treatment carried out on the HT Maple biochar unclogs the macro pores consequently increasing the SSA [23].

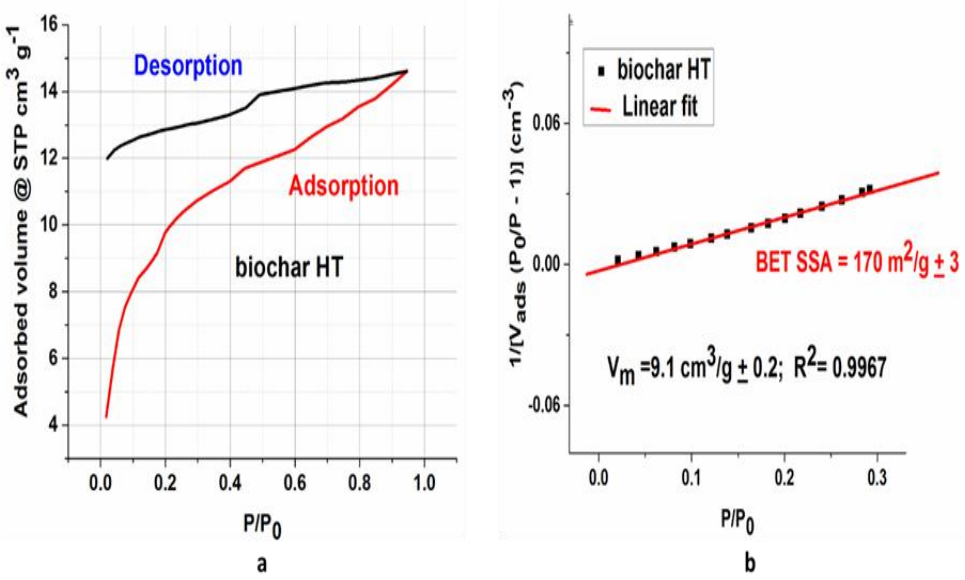

Figure 7.3: (a) biochar HT surface characterization. (b) Complete nitrogen adsorption-desorption. BET linear fit performed on the desorption branch.

7.3.4. Raman Spectroscopy

Raman spectra of commercial MWCNTs (MW8) and biochar materials, collected from 500 to 3500 cm^{-1} are illustrated in Fig. 4. Raman was used to study the graphitic behaviour of the three carbon species under analysis. The Raman spectrum of carbon materials is usually comprised of two relevant ranges with different features; the first set of features, located in the 1000-1700 cm^{-1} range is related to the D and G bands of carbon bonds [24]. These features are used to estimate defects (D) and graphitization grade (G), respectively. The second spectral range (2200-3500 cm^{-1}) contains the second-order Raman spectrum. In this frequency range it is possible to identify the overtones of the D vibration mode, namely, the G' or 2D second-harmonic, and the second order product of the D and G peaks.

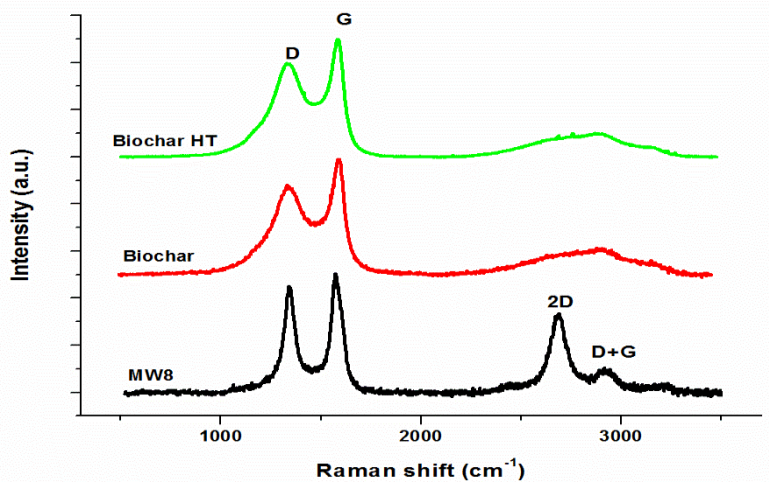

Figure 7.4: Raman spectra of MWCNTs, biochar and biochar HT.

7.4. Composite preparation

Biochar were grinded using an industrial pulverizer (Savatec BB90E) and dispersed in the epoxy resin LPL (Cores Ocean) according to the recipe in table7.1 usin the same technique as already mentioned in previous chapters.

Table 7.1: Recipe for composite preparation.

S/No.	Sample	Resin (g)	Hardener (g).	Filler (g).
1	Blank Epoxy	66.67	33.33	0.0
2	1 wt. %	66.00	33.00	1.0
3	2 wt. %	65.33	32.67	2.0
4	4 wt. %	64.00	32.00	4.0
5	20 wt. %	53.33	26.67	20

7.5. Composite analysis.

- The dispersion of the biochar materials and MWCNTs in the epoxy matrix was studied through Field Emission Scanning Electron Microscope (FESEM-ZEISS SUPRA-40TM). The composites specimens were fragile fractured in liquid nitrogen and coated with chromium (5 nm) layer to avoid the charging effects in FESEM.

- The tensile behavior of the composites was studied using tensile testing machine (MTS Q-test10). All specimen were measured with a load cell of 10kN and a strain rate of 5 mm/min according to the standard ASTM D-638-4. Specimen broken at the center were considered for further analysis. Stress Vs. strain data was plotted and compared with blank epoxy resin and with each other.
- Composites and pristine epoxy resin were characterized for their electrical properties in the microwave frequency range. Characterization was performed on samples of dimensions (34 mm x 34 mm x 20 mm) using a commercial open-ended coaxial sensor (Agilent 85070D) and a network analyzer (Agilent E8361A). The main advantage of this method is its smaller sample size (< 20 mm in diameter) compared to the free-space method. This method is also less sensitive to sample dimension than waveguide methods. Thus, small quantities of filler materials are needed for the measurement. Drawback of this method is that the roughness of the surface should be smaller than a given value in order to ensure a good contact with the sensor. The measurements were done considering different positions on the surface of the sample.
- Friction properties were studied by a reciprocating tribometer (Anton-Paar Pin-on-Disk Tribometer TRB). Same measurement parameters were used to analyze the samples as discussed in previous chapters.

7.5.1. Morphology of the composites

FESEM images (Fig. 7.5 a) show that the pristine epoxy possesses a layered structure with a smooth surface and that carbon fillers are well dispersed within the polymer matrix. Biochar particles are dispersed evenly and uniformly throughout the matrix. Large agglomerates can be seen in the specimen containing higher percentages of the filler due to their high volume and surface area (Fig. 7.5 e & f). The biochar particles fix firmly in the matrix as seen in the FESEM images. A homogeneous dispersion of the filler particles is instrumental in improving composite properties compared to the neat polymer. In fact, biochar sub micrometric structures evenly distributed across the epoxy resin matrix hinder the crack propagation caused by the accumulation of micro-cracks. During the application of the tensile load these particles are de-bonded / pulled out of the

matrix, as shown in the FESEM images, and thus help the matrix to withstand higher loads. Conversely, the MWCNTs are dispersed in large chunks and bridge between the layers of the matrix. Such a geometry promote matrix interlocking leading to enhanced tensile properties.

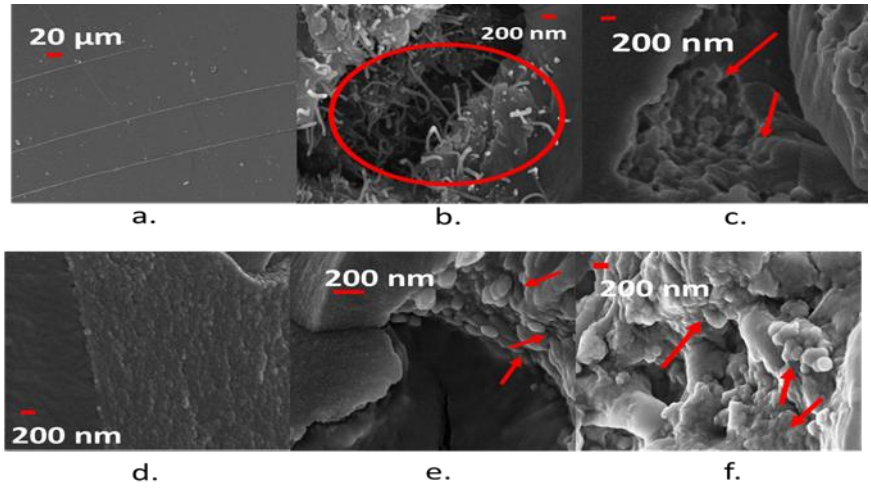

Figure 7.5: Morphology of neat epoxy (a) MWCNTs 1 wt. %, (b) biochar 2 wt. %, (c) biochar HT 2 wt. %, (d) biochar 20 wt. %, (e) biochar HT 20 wt. %, (f) Composites. Arrows indicate phenomena of crack bridging and obstruction by the various fillers used.

7.5.2. Mechanical analysis

The results of the tensile behaviour are depicted in figure 7.6 below. Interestingly addition of 1 wt. % biochar filler didn't change the brittle nature of the epoxy matrix. A slight increase in the strain at break along with a 63% increase in ultimate tensile strength was recorded for biochar 1 wt. % specimen. Addition of higher amounts (2 to 4 wt. %) changes the behaviour of epoxy from brittle to ductile. An increase the tensile strength up to ~ 48 % and ~ 500 % in elongation was observed (both for Biochar 2 wt. % and Biochar HT 2 wt. %). Higher loadings of the biochars changed the mechanical behavior and the composites showed reduced strength and extension, i.e. a trend towards semi-brittle behavior. This behavior could be attributed to high specific volume of the filler (20 wt. %). Das et al. 2016 [25] also reported the improved mechanical properties of the bio-char polypropylene composites and the same semi brittle trend at high weight percentage of the bio char.

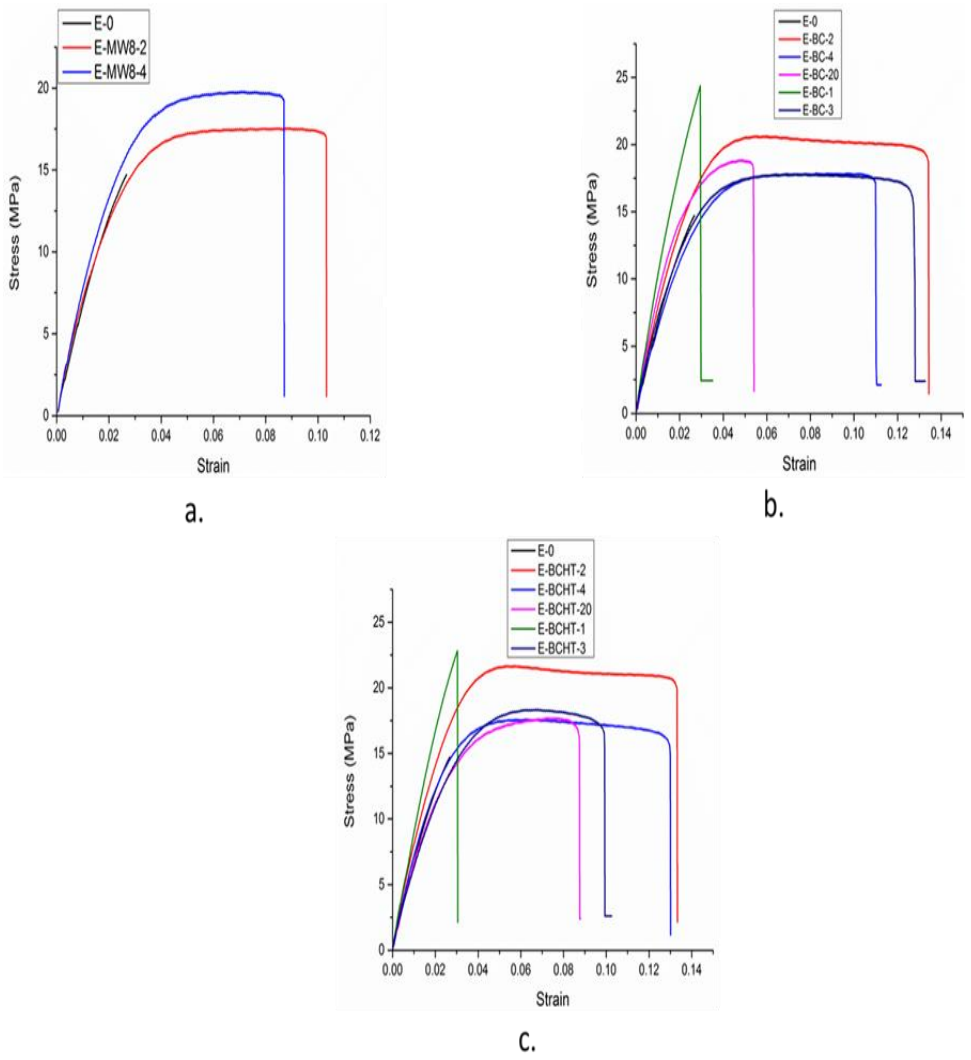

Figure 7.6: Stress vs. Strain behavior of blank epoxy compared to (a) MWCNTs 2 wt.% and 4 wt. % (b) biochar 1 wt. %, 2wt.%, 3 wt. %, 4wt.% and 20wt.% (c) biochar HT 1 wt. %, 2wt.%, 3 wt. %, 4wt.% and 20wt.% .

a. Ultimate tensile strength (UTS)

Addition of the carbon fillers increased the load bearing capacity of the epoxy matrix and best results were shown by the bio char with 1 wt. % concentration. An increase of 63% in the maximum load bearing capacity has been observed by the addition of small amount of filler. The comparison is shown in the figure 7.7. Increase in the mechanical strength of the composite can be attributed to the fact that biochar particles anchored the applied stress through the matrix and

obstructed the crack onset and accumulation as shown in the FESEM images. Cavitation / debonding of the filler from the matrix due to applied stress is also evident in the FESEM analysis. This pull out and cavitation phenomenon of the bio char filler from the matrix during the applied stress is the main cause of enhanced mechanical properties [26, 27]. The cross-link ratio of the epoxy resin may also have enhanced due the addition of bio char fillers which effectively blocked the molecular motion in the polymer matrix reducing its deformability and thus strengthening the polymer matrix [28, 29].

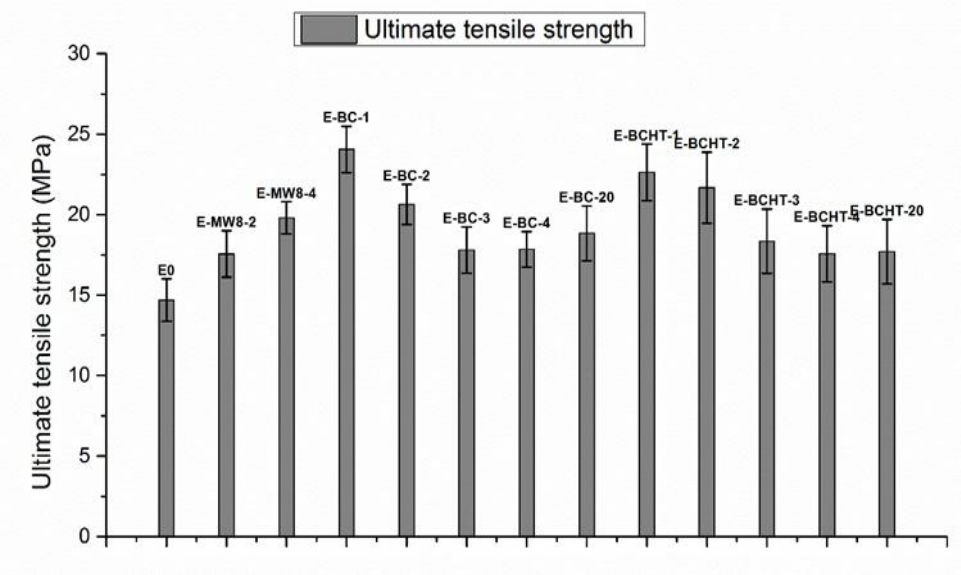

Figure 7.7: Ultimate tensile strength comparison for blank epoxy and different fillers.

b. Young Modulus

Addition of small amounts of the biochar enhanced the stiffness of the matrix. Addition of 1 wt% biochar and biochar HT enhanced the young modulus by 63% and 50% respectively. Higher loading didn't enhanced the stiffness considerably. 2 wt. % of bio char increased the stiffness by 33 % while 20 wt. % biochar composite enhance the stiffness by 41% compared to the blank epoxy. All three fillers used in different loading percentages enhanced the stiffness of the material as shown in figure 7.8. The enhanced stiffness of the matrix can be attributed to better stress transfer from the matrix to the biochar filler due to its high surface area. Fu et.al 2008 [30] reported the same phenomena for the enhanced stiffness

of the matrix by the addition of micron size particles. Nan et.al 2016 [31] also confirmed the same behavior in bio char/ PVA composites.

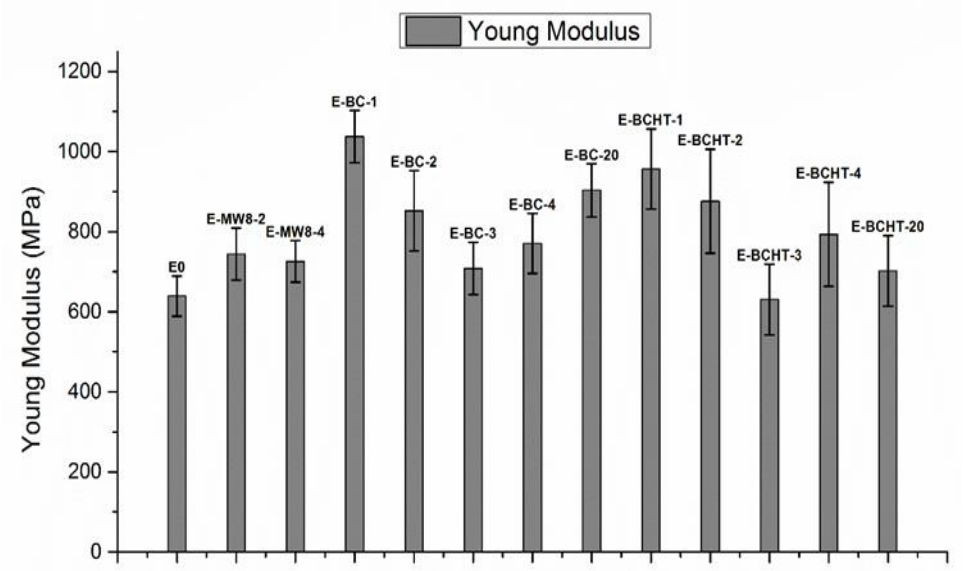

Figure 7.8: Young modulus comparison.

c. Resilience

Resilience is the measure of the energy absorbed by a material per unit volume in its elastic zone while being pulled under tensile load. Addition of small amount of the bio char enhanced the ability of the epoxy matrix to absorb more energy in its elastic limit under the tensile loads. Biochar HT at 1 wt% showed best results with an increase of 100% in the resilience. Bio char 1 wt% and MWCTNs 4 wt% samples enhanced the resilience by 23% and 7% respectively. Other concentrations of the carbon fillers didn't affect the resilience considerably as shown in figure 7.9.

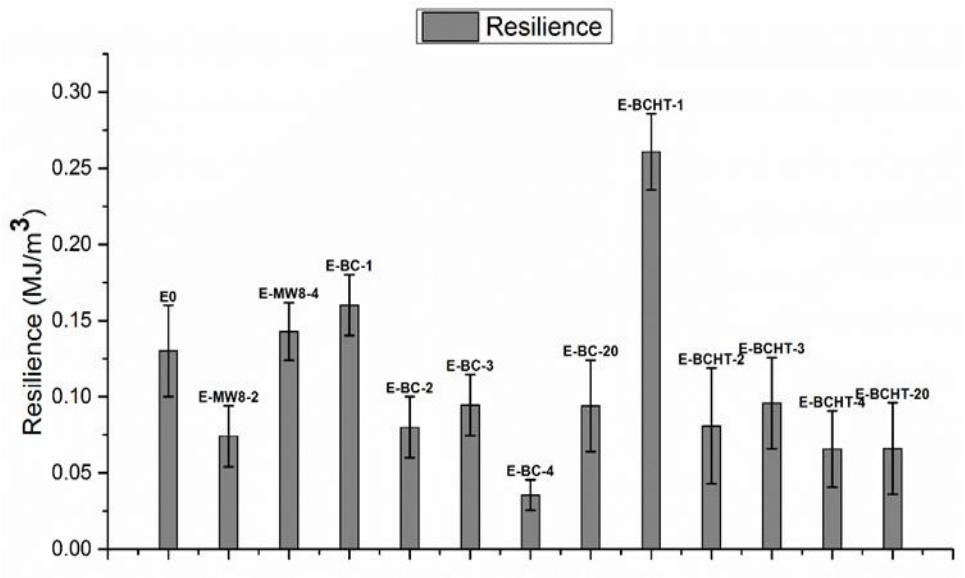

Figure 7.9: Resilience comparison.

d. Tensile Toughness

Tensile toughness is the measure of the maximum capacity of the material to withstand load before breakage. Addition of a small amount of the filler enhanced the overall load bearing capacity. The load bearing capacity deteriorated with the increase in the filler loading. An increase of roughly 11 times in the tensile toughness was recorded for 2 wt% sample for biochar and biochar HT as shown in the figure 7.10. Biochar based fillers have performed better in comparison to MWCNTs. The lower tensile toughness at higher loading of biochar fillers is due the change of the plastic behavior into semi- brittle behavior [31].

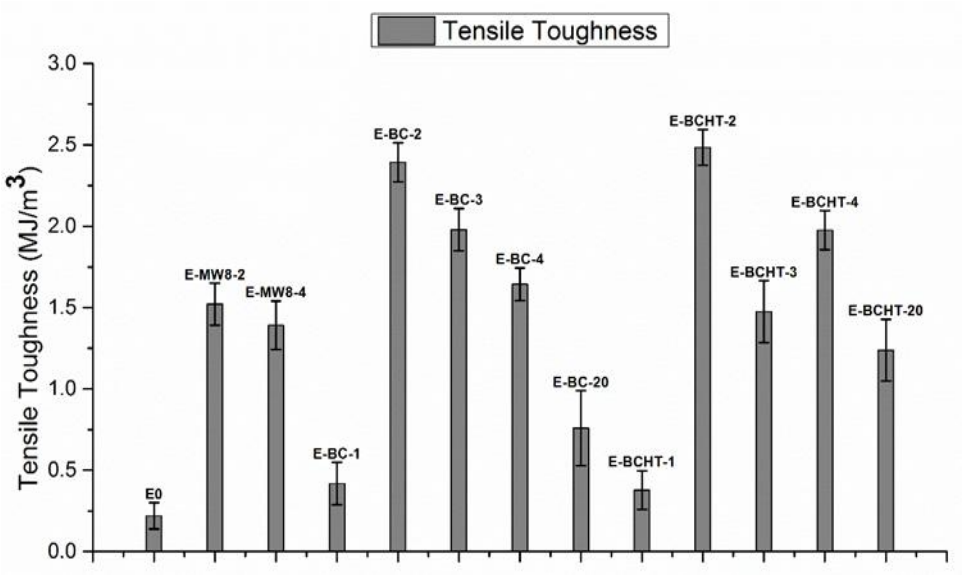

Figure 7.10: Tensile toughness comparison.

7.5.3. Complex permittivity measurements

The real part of permittivity and the conductivity in the microwave range (1-4 GHz) of the pure resin and the resin filled with MWCNT 2 and 4 wt. % vs frequency as shown in Fig. 7.11.

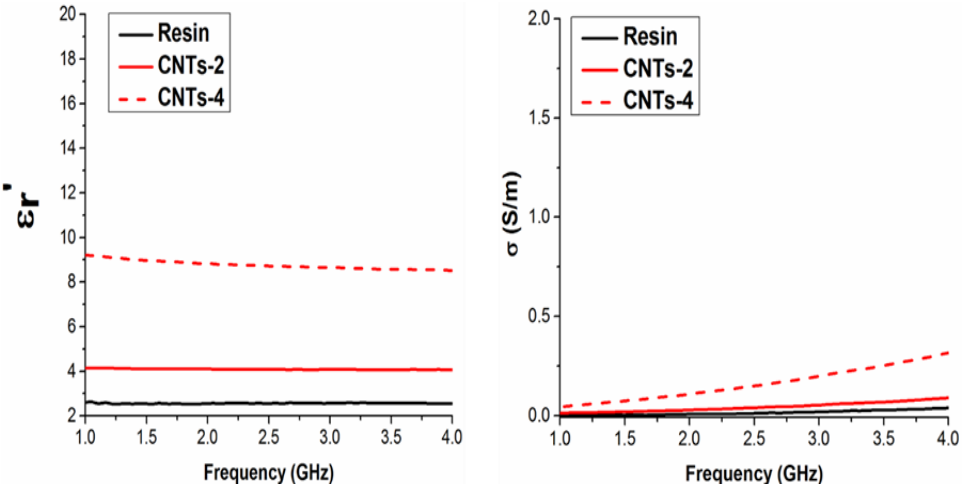

Figure 7.11: Real part of permittivity (left panel) and conductivity (right panel) in the MW range for pure epoxy and epoxy composites filled with 2 and 4 wt. % of MWCNT.

As expected, the real part of the dielectric constant and the conductivity values both increase as filler percentage is increased. In Fig. 7.12 the results obtained for biochar with 2wt. % and 20wt. % are shown.

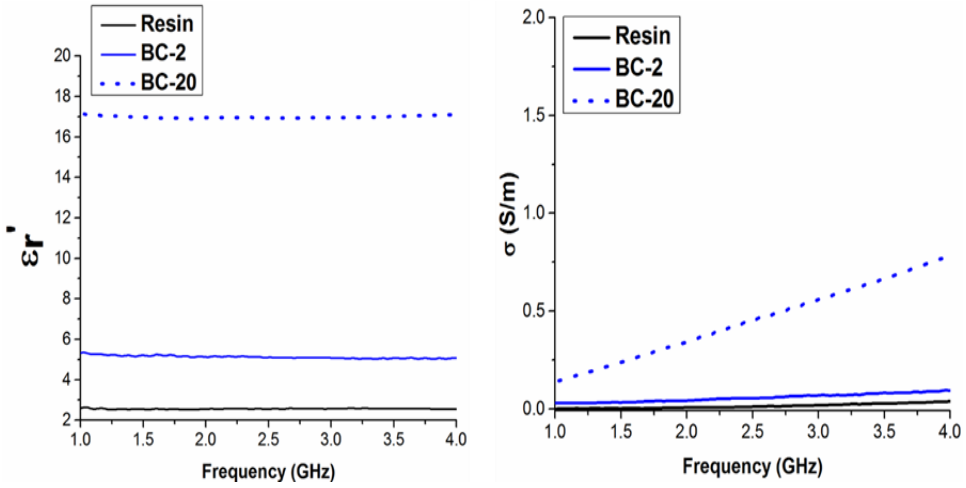

Figure 7.12: Real part of permittivity (left panel) and conductivity (right panel) in the MW range for pure epoxy and epoxy composites filled with 2 and 20 wt. % of biochar.

In order to have a significant increase of the values of the complex permittivity, it is necessary to load the composite with at least 10wt. % of biochar. Conversely, MWCNTs bring about a dielectric constant increase (i.e. real part of complex permittivity) even at lower concentrations because of their low percolation threshold required to modify composite's electrical properties [32-36]. Moreover, MWCNTs-containing composites also benefit from the carbon nanotubes' high aspect ratio (800~1000) resulting in an improved electrical conductivity in the microwave range (compared to the bare resin). On the other hand, biochar's three-dimensional structure results in worse particle interconnectivity consequently raising the percolation threshold to create a conductive path throughout the composite. In fact, DC conductivity measurements carried out on biochar samples showed an insulating behavior. On the other hand, conductivity values for pure biochar and biochar HT are of the order of 0.1-0.2 S/m.

It is worth noticing the biochar real permittivity trend against the frequency of the applied field. A decreasing trend, due to the relaxation of polar organic groups (e.g. OH, C=O, COOH, etc.), is observed in the non-heat treated sample. Conversely, the lower electronic delocalization due the removal of alkene, amides, nitrile, moieties is responsible for the lower electrical conductivity at the

microwave frequencies shown by the HT samples. Furthermore, also the removal of thiols by heat treatment contributes to the electrical conductivity's reduction (see Fig. 7.13). Indeed, Sulphur electron lone pairs play a role in the conductivity at the microwave frequencies. Such assumptions are supported by IR spectra of biochar and biochar HT (see Fig. 7.14) where it is possible to observe the decreasing of functional groups after thermal treatment.

In Fig. 7.13 the samples of biochar 20wt. %, non-heat treated and activated are compared with MWCNT 4wt. %. The results show that similar microwave properties (permittivity and electrical conductivity in the microwaves) of composites can be obtained by biochar and MWCNT but at a higher wt. % in the biochar case. At last but not least, the different graphitic structures of MWCNTs respect to the biochar, as reported by Raman analysis, could play a role in the electrical behavior.

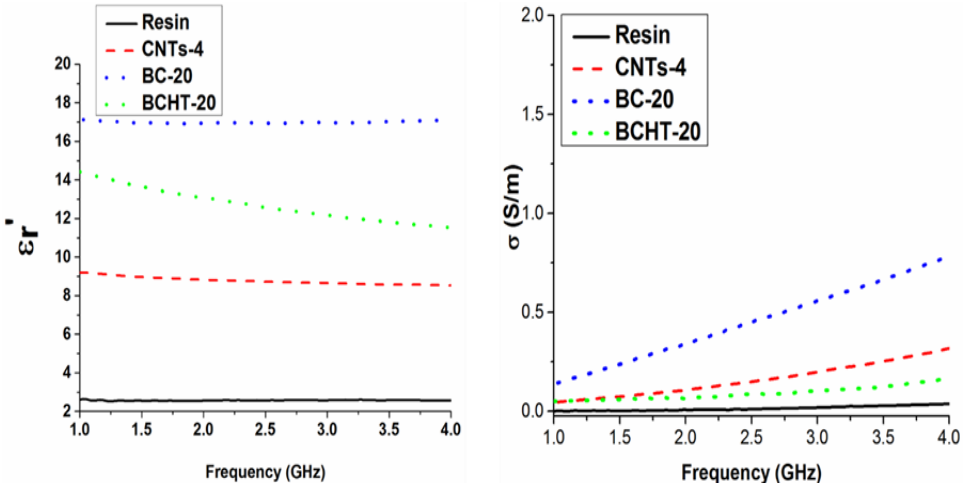

Figure 7.13 : Comparison among the real part of permittivity (left panel) and conductivity (right panel) in the MW range for pure epoxy and epoxy composites filled with 4 wt. % of MWCNT and 20 wt. % of each biochar types.

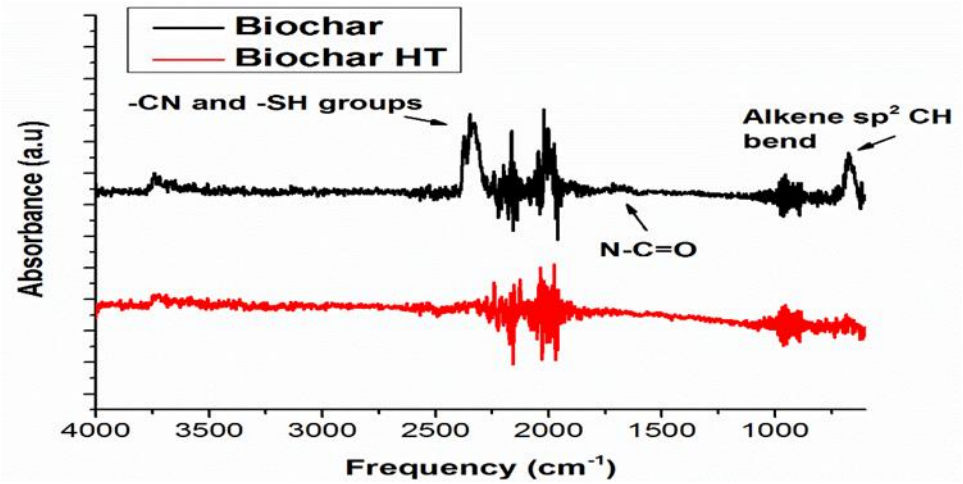

Figure 7.14: IR spectra of biochar and biochar HT.

7.5.4. Friction properties.

Comparison of friction co-efficient of blank epoxy with the different fillers is shown in the figure 7.15 below. Addition of small amounts of the carbon fillers reduced the sliding friction in both directions designated by +axis and – axis. Addition of just 2 wt% MWCNTs reduces the friction co-efficient by roughly 73%. Further addition of the filler didn't reduce the friction co-efficient significantly. Bio char as it is and activated also reduced the friction co-efficient. Biochar 4 wt% composite shows a 75% decrease in the co-efficient of friction. This effect may be related to the better mechanical properties of the composites. Also the exposure of the fillers at the contact point between the steel ball and the composite may have reduced the friction between the two interfaces [37, 38]. At higher weight of the filler used (20 wt%) the friction properties deteriorated significantly. This effect can be attributed to the high specific surface area of the biochar particles which resulted in large agglomerations of the particles in the matrix [39, 40]. The change in the mechanical and friction properties of the composites at higher concentration of biochar fillers is probably due to uneven dispersion of the particles in the low density polymer matrix and the powder-like nature of the biochar filler [41].

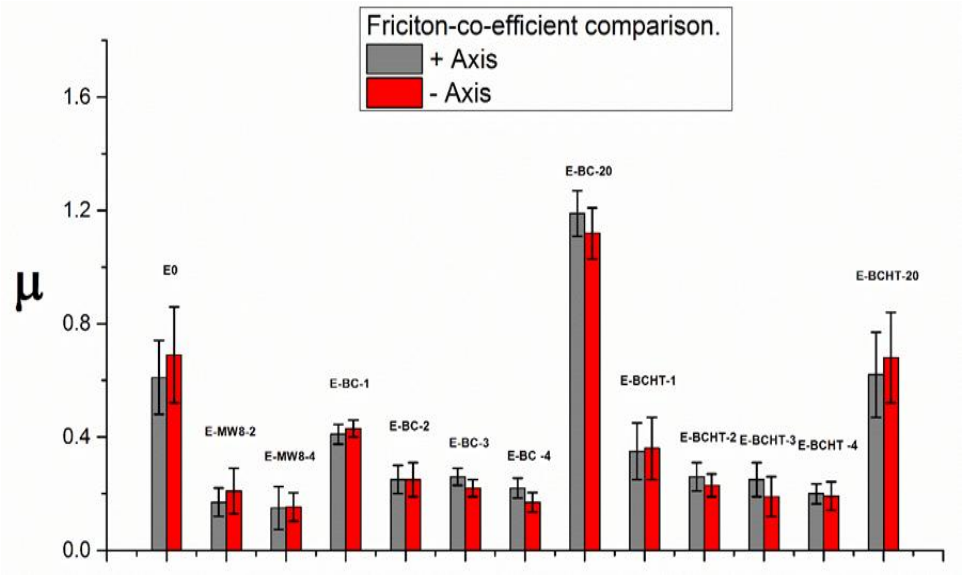

Figure 7.15: Friction properties comparison.

7.6. Conclusions

- The mechanical, friction and electrical performances of two types of carbon filler (MWCNTs and biochar) dispersed in Epoxy resin were investigated. These two types of filler where compared because MWCNTs need somewhat harsh chemical process for production, whereas biochar stems from a renewable low-cost source.
- From the point of view of mechanical properties the most remarkable improvement (in particular in ultimate tensile stress, toughness and young modulus) is obtained for a 2 wt% load of biochar. Still at 20 wt% biochar filler over perform MWCNTs composites in strength and stiffness but show somewhat inferior properties in the plastic zone.
- From the point of view of microwave properties on the other hand the properties obtained by using 4 wt % of MWCNT are improved by using 20 wt% of maple wood biochar.
- From the point of view of frictional properties MWCNTs and biochar both at 4 wt% show almost similar results.

- It has to be noted that 4 wt% is about the maximum dispersion limit of MWCNT and uniform dispersion can be obtained only with dedicated additional steps compared to the standard filler dispersion ones. On the other hand no difficulties are incurred in by dispersing as much as 20 wt% of biochar in resin. In addition biochar is a low cost ecofriendly renewable material.
- The results reported in this chapter suggest that further investigation of the impact of the parameters like filler particle size, shape and orientation in the matrix are worth in order to enhance the overall mechanical and friction performances of the biochar based polymer composites.

7.7. References

1. Thostenson, E.T.; Ren, Z.; Chou, T.-W. Advances in the science and technology of carbon nanotubes and their composites: A review. *Composites Science and Technology* **2001**, *61*, 1899-1912.

2. Ritts, A.C.; Yu, Q.; Li, H.; Lombardo, S.J.; Han, X.; Xia, Z.; Lian, J. Plasma treated multi-walled carbon nanotubes (mwcnts) for epoxy nanocomposites. *Polymers* **2011**, *3*, 2142.

3. Atif, R.; Shyha, I.; Inam, F. Mechanical, thermal, and electrical properties of graphene-epoxy nanocomposites—a review. *Polymers* **2016**, *8*, 281.

4. Moser, A.; Feuchter, M. Mechanical properties of composites used in high-voltage applications. *Polymers* **2016**, *8*, 260.

5. Borowski, E.; Soliman, E.; Kandil, U.; Taha, M. Interlaminar fracture toughness of cfrp laminates incorporating multi-walled carbon nanotubes. *Polymers* **2015**, *7*, 1020.

6. Bauhofer, W.; Kovacs, J.Z. A review and analysis of electrical percolation in carbon nanotube polymer composites. *Composites Science and Technology* **2009**, *69*, 1486-1498.

7. Li, B.; Zhong, W.-H. Review on polymer/graphite nanoplatelet nanocomposites. *Journal of Materials Science* **2011**, *46*, 5595-5614.

8. Byrne, M.T.; Gun'ko, Y.K. Recent advances in research on carbon nanotube–polymer composites. *Advanced Materials* **2010**, *22*, 1672-1688.

9. Koledintseva, M.Y.; Drewniak, J.L.; DuBroff, R.E.; Rozanov, K.N.; Archambeault, B. Modeling of shielding composite materials and structures for microwave frequencies. *Progress In Electromagnetics Research B* **2009**, *15*, 197-215.

10. Liu, L.; Kong, L.B.; Yin, W.-Y.; Matitsine, S. Characterization of single- and multiwalled carbon nanotube composites for electromagnetic shielding and tunable applications. *IEEE Transactions on Electromagnetic Compatibility* **2011**, *53*, 943-949.

11. Micheli, D.; Pastore, R.; Apollo, C.; Marchetti, M.; Gradoni, G.; Primiani, V.M.; Moglie, F. Broadband electromagnetic absorbers using carbon nanostructure-based composites. *IEEE Transactions on Microwave Theory and Techniques* **2011**, *59*, 2633-2646.

12. Olmo, C.; Amestoy, H.; Casas, M.; Martínez, J.; Franco, L.; Sarasua, J.-R.; Puiggalí, J. Preparation of nanocomposites of poly(ε-caprolactone) and multi-walled carbon nanotubes by ultrasound micro-molding. Influence of nanotubes on melting and crystallization. *Polymers* **2017**, *9*, 322.

13. Bisri, S.Z.; Gao, J.; Derenskyi, V.; Gomulya, W.; Iezhokin, I.; Gordiichuk, P.; Herrmann, A.; Loi, M.A. High performance ambipolar field-effect transistor of random network carbon nanotubes. *Advanced Materials* **2012**, *24*, 6147-6152.

14. Gomulya, W.; Costanzo, G.D.; de Carvalho, E.J.F.; Bisri, S.Z.; Derenskyi, V.; Fritsch, M.; Fröhlich, N.; Allard, S.; Gordiichuk, P.; Herrmann, A., *et al.* Semiconducting single-walled carbon nanotubes on demand by polymer wrapping. *Advanced Materials* **2013**, *25*, 2948-2956.

15. Nanda, S.; Dalai, A.K.; Berruti, F.; Kozinski, J.A. Biochar as an exceptional bioresource for energy, agronomy, carbon sequestration, activated carbon and specialty materials. *Waste and Biomass Valorization* **2016**, *7*, 201-235.

16. Tan, X.; Liu, Y.; Zeng, G.; Wang, X.; Hu, X.; Gu, Y.; Yang, Z. Application of biochar for the removal of pollutants from aqueous solutions. *Chemosphere* **2015**, *125*, 70-85.

17. Raclavsky, K.; Raclavska, H.; Kovalova, L.; Skrobankova, H.; Frydrych, J. In *Utilization of carbon produced by torrefaction of grass for energy purposes and related risks*, 2015 IEEE 15th International Conference on

Environment and Electrical Engineering (EEEIC), 10-13 June 2015, 2015; pp 1972-1976.

18. Guizani, C.; Jeguirim, M.; Valin, S.; Limousy, L.; Salvador, S. Biomass chars: The effects of pyrolysis conditions on their morphology, structure, chemical properties and reactivity. *Energies* **2017**, *10*, 796.

19. El-Hendawy, A.-N.A. Surface and adsorptive properties of carbons prepared from biomass. *Applied Surface Science* **2005**, *252*, 287-295.

20. Fryda, L.; Visser, R. Biochar for soil improvement: Evaluation of biochar from gasification and slow pyrolysis. *Agriculture* **2015**, *5*, 1076.

21. Thommes, M.; Kaneko, K.; Neimark Alexander, V.; Olivier James, P.; Rodriguez-Reinoso, F.; Rouquerol, J.; Sing Kenneth, S.W. Physisorption of gases, with special reference to the evaluation of surface area and pore size distribution (iupac technical report). In *Pure and Applied Chemistry*, 2015; Vol. 87, p 1051.

22. Xu, L.; Lu, C.; Zhang, Z.; Yang, X.; Hou, W. Various self-assembled three-dimensional hierarchical architectures of la2(moo4)3: Controlled synthesis, growth mechanisms, luminescence properties and adsorption activities. *Nanoscale* **2010**, *2*, 995-1005.

23. Mandzyuk, V.I.; Lisovskyy, R.P.; Nagirna, N.I. The effect of thermal treatment on porous structure of carbon materials. *Nanoscience and Nanotechnology Research* **2013**, *1*, 23-26.

24. Jiang, J.; Saito, R.; Grüneis, A.; Chou, S.G.; Samsonidze, G.G.; Jorio, A.; Dresselhaus, G.; Dresselhaus, M.S. Intensity of the resonance raman excitation spectra of single-wall carbon nanotubes. *Physical Review B* **2005**, *71*, 205420.

25. Das, O.; Bhattacharyya, D.; Hui, D.; Lau, K.-T. Mechanical and flammability characterisations of biochar/polypropylene biocomposites. *Composites Part B: Engineering* **2016**, *106*, 120-128.

26. Godara, A.; Mezzo, L.; Luizi, F.; Warrier, A.; Lomov, S.V.; van Vuure, A.W.; Gorbatikh, L.; Moldenaers, P.; Verpoest, I. Influence of carbon nanotube reinforcement on the processing and the mechanical behaviour of carbon fiber/epoxy composites. *Carbon* **2009**, *47*, 2914-2923.

27. Nagarajan, V.; Mohanty, A.K.; Misra, M. Biocomposites with size-fractionated biocarbon: Influence of the microstructure on macroscopic properties. *ACS Omega* **2016**, *1*, 636-647.

28. Allaoui, A.; Bai, S.; Cheng, H.M.; Bai, J.B. Mechanical and electrical properties of a mwnt/epoxy composite. *Composites Science and Technology* **2002**, *62*, 1993-1998.

29. Bai, J.B.; Allaoui, A. Effect of the length and the aggregate size of mwnts on the improvement efficiency of the mechanical and electrical properties of nanocomposites—experimental investigation. *Composites Part A: Applied Science and Manufacturing* **2003**, *34*, 689-694.

30. Fu, S.-Y.; Feng, X.-Q.; Lauke, B.; Mai, Y.-W. Effects of particle size, particle/matrix interface adhesion and particle loading on mechanical properties of particulate–polymer composites. *Composites Part B: Engineering* **2008**, *39*, 933-961.

31. Nan, N.; DeVallance, D.B.; Xie, X.; Wang, J. The effect of bio-carbon addition on the electrical, mechanical, and thermal properties of polyvinyl alcohol/biochar composites. *Journal of Composite Materials* **2016**, *50*, 1161-1168.

32. Giorcelli, M.; Savi, P.; Miscuglio, M.; Yahya, M.H.; Tagliaferro, A. Analysis of mwcnt/epoxy composites at microwave frequency: Reproducibility investigation. *Nanoscale Research Letters* **2014**, *9*, 168.

33. Giorcelli, M.; Savi, P.; Yasir, M.; Miscuglio, M.; Yahya, M.H.; Tagliaferro, A. Investigation of epoxy resin/multiwalled carbon nanotube nanocomposite behavior at low frequency. *Journal of Materials Research* **2014**, *30*, 101-107.

34. Savi, P.; Miscuglio, M.; Giorcelli, M.; Tagliaferro, A. Analysis of microwave absorbing properties of epoxy mwcnt composites. *PIER Lett* **2014**, *44*.

35. Giorcelli, M.; Savi, P.; Delogu, A.; Miscuglio, M.; Hajj Yahya, M.; Tagliaferro, A. Microwave absorption properties in epoxy resin multiwalled carbon nanotubes composites. In *Iceaa13 international conference in electromagnetics in advanced applications, torino, september 9-13 2013*, 2013.

36. Miscuglio, M.; Yahya, M.H.; Savi, P.; Giorcelli, M.; Tagliaferro, A. In *Rf characterization of polymer multi-walled carbon nanotube composites*, 2014 IEEE Conference on Antenna Measurements & Applications (CAMA), 16-19 Nov. 2014, 2014; pp 1-4.

37. Chen, H.; Jacobs, O.; Wu, W.; Rüdiger, G.; Schädel, B. Effect of dispersion method on tribological properties of carbon nanotube reinforced epoxy resin composites. *Polymer Testing* **2007**, *26*, 351-360.

38. Yan, L.; Wang, H.; Wang, C.; Sun, L.; Liu, D.; Zhu, Y. Friction and wear properties of aligned carbon nanotubes reinforced epoxy composites under water lubricated condition. *Wear* **2013**, *308*, 105-112.

39. Zhang, L.C.; Zarudi, I.; Xiao, K.Q. Novel behaviour of friction and wear of epoxy composites reinforced by carbon nanotubes. *Wear* **2006**, *261*, 806-811.

40. Cui, L.-J.; Geng, H.-Z.; Wang, W.-Y.; Chen, L.-T.; Gao, J. Functionalization of multi-wall carbon nanotubes to reduce the coefficient of the friction and improve the wear resistance of multi-wall carbon nanotube/epoxy composites. *Carbon* **2013**, *54*, 277-282.

41. Vaisman, L.; Wagner, H.D.; Marom, G. The role of surfactants in dispersion of carbon nanotubes. *Advances in Colloid and Interface Science* **2006**, *128-130*, 37-46.

Chapter 8

Summary, conclusions and future work

a. Our studies on the commercial carbon fibres and later on the lignin based carbon fibres revealed that

- Low pressure plasma treatment in oxygen environment is an effective and suitable technique to modify carbon fibre surface.
- With proper tuning of the parameters such as treatment time, plasma power, gas glow rate and pressure inside the plasma chamber we can ensure that the carbon fibres retain 90% of their original tensile strength, which is a key factor in the composite performance.
- XPS, Raman spectroscopy and FTIR results confirm the presence of the oxygen containing functional groups on the surface of the CF.
- Wettability test further strengthened our argument of enhanced interfacial adhesion after the plasma treatment.
- Application to composites showed enhanced mechanical and tribology properties which further supports our recommendations to use low pressure oxygen plasma to modify the surface of carbon fibres.

- To further support our recommendations we studied the plasma treatment of carbon fibres generated from waste clothes and application to composites for enhanced properties.
- We recommend the use of plasma treatment for the surface functionalization of carbon fibres produced under the European Union FP7 Project "Functionalized Innovative Carbon Fibres Developed from Novel Precursors with Cost Efficiency and Tailored Properties" (FIBRALSPEC) under Grant Agreement No. 604248.

b. Carbon fibres from waste cotton, functionalization and application to composites.

- Waste cotton clothes can be used as an alternate cheap precursor to synthesize carbon fibres which can be used to reinforce polymer matrices for improved mechanical and tribology properties. The surface of CF can be modified by the plasma treatment. The surface modified CF can further enhance the polymer properties.
- Vacuum Plasma treatment on CF in an oxygen environment efficiently modifies the surface morphology of the fibres as shown in the FESEM images. Specific surface area increases after the plasma treatment. The chemical modification of the CF surface due to plasma treatment was confirmed by FTIR and XPS analysis. The high surface area and the functional groups provided better interfacial adhesion between the CF and the epoxy matrix as evident from the wettability test. Consequently the mechanical and tribology properties of the epoxy matrix improved significantly.
- We recommend the application of the carbon fibres from waste in other application like microwave adsorption properties of polymers, gas sensors, Lithium ion batteries due to their cheap nature and good quality of carbon materials.

c. Synthesis of carbon nano materials from waste plastic and application to composites.

- Polythene bags can be used as a cheap alternative precursor for the synthesis of CNMs via CVD process. Morphology of the CNMs can be altered by varying the gas pressure inside the CVD chamber.
- The hybrid filler P2 (CNBs + CNT) outperformed the commercial MWCNTs in the mechanical and tribology properties of the composites. P2 fillers shows tensile toughness, and strength comparable to the MW2 composites and superior tribology properties.
- The mechanical and tribology properties of the composites depict that CNMs synthesized from waste polyethylene can replace commercial MWCNTs as a cheap and environment friendly filler in composite applications.
- Process tuning and further improvement in the composites properties can surely put CNMs from waste plastic in a competitive position against commercial carbon nano tubes.

d. Bio char: A versatile material to exalt polymer properties.

- The mechanical, friction and electrical performances of two types of carbon filler (MWCNTs and biochar) dispersed in Epoxy resin were investigated. These two types of filler where compared because MWCNTs need somewhat harsh chemical process for production, whereas biochar stems from a renewable low-cost source.
- From the point of view of mechanical properties the most remarkable improvement (in particular in ultimate tensile stress, toughness and young modulus) is obtained for a 2 wt. % load of biochar. Still at 20 wt. % biochar filler over perform MWCNTs

composites in strength and stiffness but show somewhat inferior properties in the plastic zone.

- From the point of view of frictional properties MWCNTs at 4 and biochar at 4 % show almost similar results.
- From the point of view of microwave properties on the other hand the properties obtained by using 4 wt. % of MWCNT are improved by using 20 wt. % of maple wood biochar.
- It has to be noted that 4 wt. % is about the maximum dispersion limit of MWCNT and uniform dispersion can be obtained only with dedicated additional steps compared to the standard filler dispersion ones. On the other hand no difficulties are incurred in by dispersing as much as 20 wt. % of biochar in resin. In addition biochar is a low cost ecofriendly renewable material.
- The results reported suggest that further investigation of the impact of the parameters like filler particle size, shape and orientation in the matrix are worth in order to enhance the overall mechanical and friction performances of the biochar based polymer composites.
- Future plans include the evaluation of European woods like Olive, Poplar and Ash wood as precursor for biochar production and application to compoistes.